Parallel Session 2A

Actions on Bridges

Leere Seite

Blank page

Page vide

ENV 1991 - Part 3 : Traffic loads on bridges
Calibration of road load models for road bridges

Aloïs BRULS, Dr. Engineer, Lecturer. University of Liège, Belgium
Aloïs Bruls, born 1941, received his civil engineering degree from the University of Liège in 1965. He is currently a research engineer with the Department of Bridge and Structural Engineering at the University of Liège and a consultant with the compagny Delta G.C. in Liège.

Pietro CROCE, Dr. Engineer, Researcher. University of Pisa. Italy.
Pietro Croce, born in 1957, got is PhD degree in 1989. He is researcher at the Department of Structural Engineering of the University of Pisa. He is involved in several research works concerning bridges, fatigue and structural reliability.

Luca SANPAOLESI, Professor of Structural Engineering, University of Pisa. Italy.
Luca Sanpaolesi, born in 1927, graduated in Civil Engineering at the Technical University of Pisa. At present he is Professor of Structural Engineering at the Pisa University and is involved in the studies of Eurocodes.

Gerhard SEDLACEK, Professor of steel structures, RWTH Aachen. Germany.
Gerhard Sedlacek, born 1939, Dipl.-Ing. TU Karlsruhe in 1964, Dr.- Ing. TU Berlin 1967, in Steel Construction Industry until 1976. He has been involved in various projects for the Eurocodes.

Summary

Part 3 of Eurocode 1 defines the traffic load models to be used for the design of bridges. The load models representing road traffic loads have been calibrated on traffics recorded in Europe in the eighties. This paper shows how the representative values of these loads have been determined.

1.   Introduction

The present paper concerns background studies about the calibration of the load models representing the actions induced by the road traffic [1]. Its content allows to outline, together with the topics discussed in [2], a complete description of the studies carried out in the definition of actions on road bridges. The models have been defined so that it is possible to obtain correct bridge design, following the requirements of the design codes, mainly EC 2-2 Concrete Bridges, EC 3-2 Steel Bridges, EC 4-2 Composite Bridges.

The aim of the calibration is to obtain load models which are able to reproduce as well as possible the effects induced by the road traffic, being at the same time very simple and easy to use. In order to do this, it has been necessary first of all to evaluate the so called «target values», representing the real traffic effects.

Taking into account the needs concerning ultimate and serviceability limit states checks as well as fatigue assessments, target values have been defined for a lot of load effects, regarding various influence lines and bridges spans, considering several traffic scenarios, several extrapolation methods and dynamic effects induced by different roughness of the pavements. In this paper, a wide set of comparisons between the target values and the EC 1-3 load model values is also reported for each case.

2. Extrapolation methods

The choice of the main load model and its calibration require preliminarly the knowledge of the effects induced by the real traffic on the bridge, in terms of their characteristic, infrequent and frequent values, which must be reproduced by the load model itself.

The procedure to be followed to evaluate these target values is not obvious. In fact, because the recorded traffic data concern flowing traffic on time intervals limited to few hours or to few days, it is necessary to study how to transfer these data to the whole life of the bridge, taking also into account the extreme traffic situations which can happen on one or on several lanes.

In a very general scheme, the procedure can be summarised as follows : the most representative traffic samples are considered to cross the bridge, in such a way that the histograms of the extreme values of the considered effects are determined, and subsequently, using a suitable extrapolation method, the values with prefixed return periods are evaluated.

Traffic samples, traffic situations, hazard scenarios, as well as set of influence lines considered in the calibration, are outlined in [2].

To evaluate both, the extreme values of axle and lorry loads and the extreme values of the traffic effects, basically three different extrapolation methods have been adopted, using respectively, the half-normal distribution, the Gumbel distribution and the Montecarlo simulation [3], which are shortly described in the following.

2.1. Half-normal distribution

The method is based on the hypothesis that the queue of the extreme values distribution of the stochastic variable x is gaussian, so that the upper part, for $x \geq x_o$, of the histogram of the effect induced by the real traffic can be fitted with a gaussian curve through a suitable choice of the parameters of the curve itself. Generally, the parameter x_o is close to the last mode of the histogram [8][9].

The value x_R, corresponding to the return period R, is given by $x_R = x_o + \sigma.Z_R$, being Z_R the upper α-fractile of the standardised normal variable $Z = (x-m)/\sigma$. In the present case $\alpha = (2.N_T)^{-1}$, where N_T is the total number of events during the period R.

2.2. Gumbel distribution

Under hypotheses similar to those illustrated in the previous point, the extreme values distribution can be represented using the Gumbel distribution (or extreme value I type distribution), which is completely described by the parameters u, representing the mode of the distribution, and α, depending on the scattering of the distribution.

The parameters of the Gumbel distribution can be obtained, starting from the histogram of the extreme values, as $u = m - 0,45.\sigma$ and $\alpha = (0.7797.\sigma)^{-1}$, where m and σ are, the mean and the standard deviation of the histogram. The value x_R is then given by $x_R = u + y.\alpha$ being $y = -\ln [-\ln(1 - R^{-1})]$ the reduced variable of the distribution.

2.3. Montecarlo simulation

The Montecarlo simulation is based on the automatic generation of a set of extreme traffic situations, starting from the recorded traffic data, so that it is possible to obtain the extreme value sample on which the extrapolation method is applied.

The sample can be generated in several ways, depending essentially on the number of applications of the method itself.
The most intuitive procedure consists in the application of the method several times. The lorries crossing the bridges are chosen from a suitable garage, i.e. a set of standard vehicles representing the most common real lorry schemes. Lorry types, axle loads, interaxle distances as well as intervehicle distances are obtained applying repeatedly the Montecarlo method, on the basis of the statistical parameters derived from the analysis of the recorded data.
Beside that, an alternative procedure, more complex but very efficient, has been adopted : in this one the aim of the Montecarlo simulation is to obtain, using the parameters of the extreme values distribution obtained with the recorded traffic data, a statistical sample of the effects. In this way the application of the Montecarlo method is limited only to the final steps on the procedure, in order to determined the input data for the calculation of the parameters of the Gumbel type distribution [4].

3.   Dynamic effects

Besides the extrapolated values, the determination of the target values requires the evaluation of the dynamic effects due to the interaction between the vehicles and the bridge.
In order to obtain the values of the dynamic load effects to be used for the calibration for serviceability limit states, for ultimate limit states as well as for fatigue assessments, special studies have been carried out by an ad hoc Working Group [5].

3.1.   Inherent dynamic increment

Because the recorded traffic data have been obtained by measurements from flowing traffic, they contain already dynamic increments, so that it is necessary to correct them with the inherent impact factor. The inherent impact factors for recorded traffics have been determined by computer programmes in which measurements are simulated assuming rigid ground with good surface roughness, and vehicle loads are represented as sequence of static actions. Regarding the extreme values of Auxerre data relevant for the ULS consideration, an inherent impact factor $\varphi_{inh}= 1.10$ has been found, while for loads belonging to the fractile ranges between 10 % and 90 %, relevant for SLS and fatigue, there is no significant difference between static and dynamic distribution, so that it results $\varphi_{inh} \cong 1.00$.

3.2. Impact factor

The dependence of the impact factors on the model parameters, like bridge type, static scheme, span, fundamental frequency, damping quality, dynamic characteristics of the vehicles, roadway roughness, vehicle speed and so on, has been preliminary investigated in order to determine the weight of each parameter.
Subsequently, using computer programmes, a lot of numerical simulations has been carried out for several bridge types and for various traffic scenarios, with medium or good roadway roughness, evaluating the corresponding global dynamic increments. Beside that the local dynamic effects as well as the timber effect due to a concentrated irregularity, 30 mm high and 500 mm wide, simulating uneven transition joint, lost board or ice slab, has been determined.

The results of each numerical simulation is a time history of the considered effect, from which the ratio between the extreme dynamic response and the extreme static response of the bridge can be determined. This ratio is commonly said physical impact factor $\varphi = max_{dyn}/max_{stat}$. The above defined physical factor refers to a particular loading situation and depends on such a variety of parameters that cannot be directly employed for load model calibration. In fact φ is usually high for light vehicles and low for heavy vehicles, while the target values depend mainly on the extreme values of the dynamic distribution.

For code purposes, the dynamic magnification can be taken into account directly, referring to the distribution of the dynamic effects, or, in an alternative way, increasing the static distribution by an impact factor φ_{cal} ratio between dynamic and static values corresponding to the same x-fractile $\varphi_{cal} = E_{dyn(x\text{-}fractile)}/E_{stat(x\text{-}fractile)}$.

Of course, φ_{cal} is purely conventional because the static and dynamic x-fractiles don't correspond necessarily to the same load condition. The characteristic values of the conventional impact factors φ_{cal} have been determined, using Auxerre data for flowing traffic, simulating a lot of influence lines, span lengths and pavement roughnesses occurring in actual bridges. The results are summarised in Figure 1.

The dynamic target values of the effects can be then computed, starting from the effect E_{stat}, obtained using the recorded traffic data together a suitable extrapolation method, as $E_{dyn} = E_{stat} \cdot \varphi_{cal} \cdot \varphi_{local}/\varphi_{inh}$, where φ_{local} represents the impact factor for local effects.
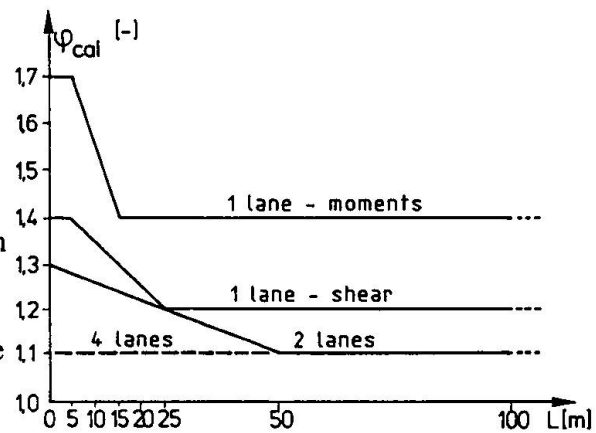

Fig. 1 Impact factors

3.3. Damage equivalent impact factor

The impact factor for fatigue design is defined as the ratio between the fatigue damage induced by the dynamic stress history and the fatigue damage induced by the static stress history. This definition leads to a damage equivalent impact factor φ_{fat} expressed by

$$\varphi_{fat} = \left[\sum n_{i,dyn} \left(\Delta E_{i,dyn} \right)^m \Big/ \sum n_{i,stat} \cdot \left(\Delta E_{i,stat} \right)^m \right]^{1/m}$$

where ΔE_i are the effect ranges and m is the slope of the S-N curve.

This definition allows to obtain an increased histogram, leading to the same damage as the original dynamic histogram, simply multiplying all the stress amplitudes of the static histogram by the constant impact factor φ_{fat}.

4. Safety factors γ_Q and reduction factor ψ_i

4.1   General

The safety elements for actions $F_{d1} = \gamma_{F1} \cdot F_{k1}$ and $F_{d1} = \gamma_{Fi} \cdot \Psi_i \cdot F_{ki}$ can only be determined by considering both,

the action side

and the resistance side

and the relevant limit states.

$$S_d = S (\gamma_{F1}. F_{k1}, \gamma_{Fi}. \psi_i. F_{ki}., a_{nom})$$

$$R_D = R (f_k, a_{nom})/\gamma_M$$

4.2. Procedure and results for γ_Q

The following procedure has been adopted to determine the magnitude of the safety factor $\gamma_F = \gamma_Q$ to be applied to traffic loads [6] :
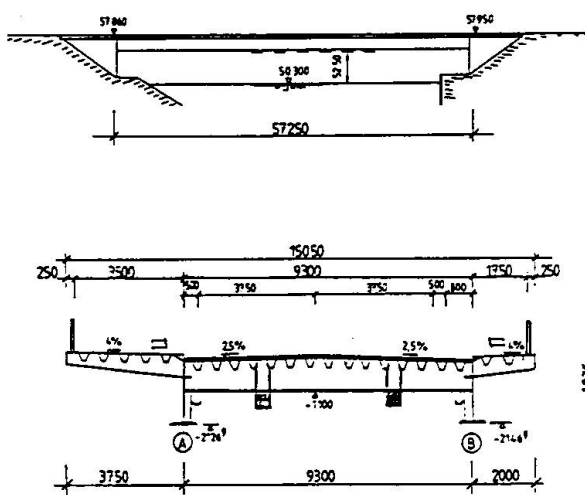

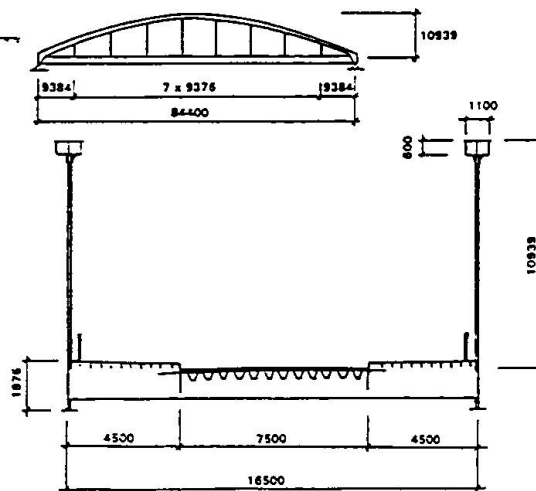
Fig. 2a. Single span bridge K 210   Fig. 2b. Tied arch bridge K 138

1.Two steel bridges were selected (Fig. 2a and 2b) for which the first order reliability method was used to determine the safety index β for various elements considering.
- bridges loaded by the Auxerre-traffic used to define the main load-model,
- the limit states constituted as follows :

ULS :   attainment of the first yielding ;

SLS :   attainment of a defection limit ;

Fatigue :   attainment of a required service life.

- all actions in combination with the traffic loads (selfweight, wind, temperature gradient) and all bridge properties relevant for the limit states described by statistical data independent on the bridges selected for the calibrations.

2. From the reliability studies the β-values as indicated in Figure 3 were determined, from which the following requirements for target β-values to be applied to parameter studies were taken :

$\beta = 6,00$ for   ULS and
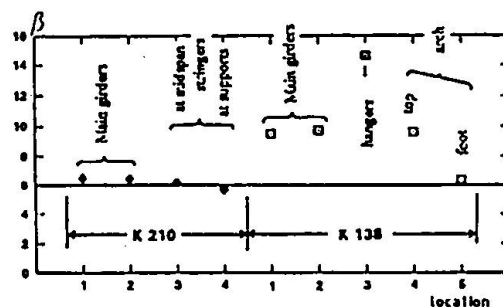
$\beta = 3,00$ for   SLS and fatigue.

Fig. 3 : β values for bridges elements.

3. For a set of representative bridge systems (single spans or continuous spans, one or several lanes) a probabilistic design was carried out using the same statistical parameters as used for the calibration described in 1 and 2. The probabilistic design resulted in the required section moduli $W_{required}$.

4. The required safety factor γ_Q to be applied to the Eurocode traffic load model was then determined by comparing the design values M_{Qd} from the probabilistic design,

$$M_{Qd} = f_y . W_{erf} / \gamma_M - M_g . \gamma_G$$

where f_y and $\gamma_M = 1,10$ were taken from Eurocode 3 and

M_g and $\gamma_G = 1,35$ were taken from Eurocode 1, with the action effect from the traffic load model LM,

$$M_{Qd} = \gamma_Q . M_Q^{LM}$$

This comparison implies that the combination rule is $\gamma_G .G + \gamma_Q. Q$.

Figure 4 gives the results of that comparison that yielded to the value $\gamma_Q = 1,35$ that was recommended to be applied to the European load model.
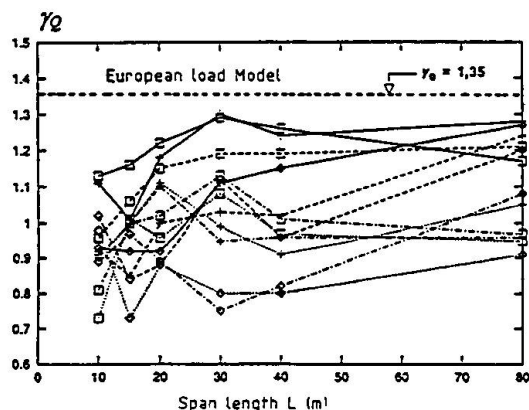

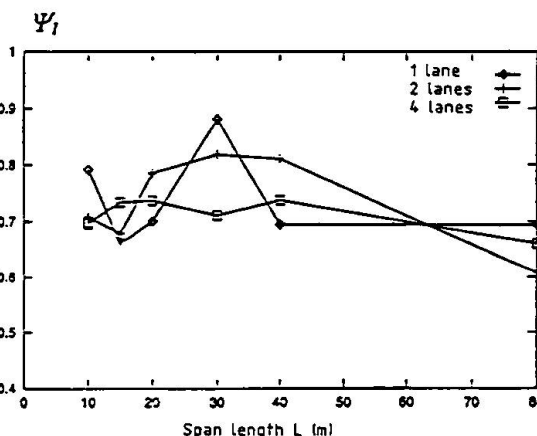Fig. 4 : γ_Q values for bridge elements   Fig. 5 : Ψ_l values for bridge elements

4.3.   Results for Ψ_1

For determining the reduction factor Ψ_1 for the serviceability limit state of deflection the same statistical parameters were used as for the parameter study for ultimate limit state design. Deflections are caused both by traffic loads and by temperature differences that were considered in combination.

The comparison was performed on the basis of the required second moment of area $I_{required}$ that was determined for the set of representative bridge systems by a probabilistic calculation on one side and by using the characteristic load models in Eurocode 1 with a reduction factor Ψ_1 on the other side. This comparison leads to

$$\psi_1 = M_{Qd\,serv} / M_{Qk}^{LM,\,ULS}$$

Figure 5 gives the results for the required ψ_1-values for single span bridges. The value adopted in EC 1-3 is $\psi_1 = 0,75$.

4.4.   Results for fatigue

A comparison of the required section moduli $W_{required}$ from the probabilistic fatigue calculation and from the fatigue loading model FLM 3 in EC 1-3 is given in Figure 6a for the main girder of a single span bridge with a span length of 20 m and in Figure 6b for a span length of 80 m. Apparently $\beta = 3.0$ is reached for smaller spans only, whereas the FLM-3 model must be modified for longer spans (see section 7.2)
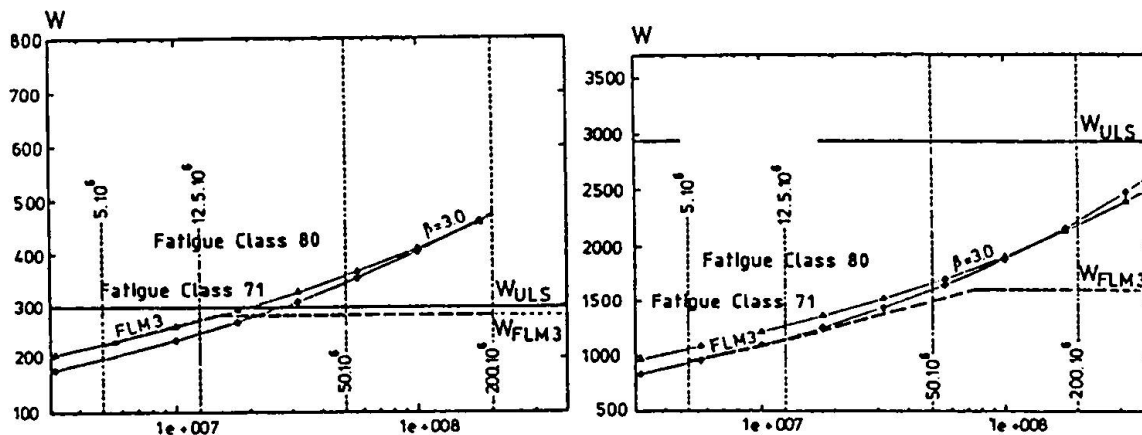

Fig. 6a. $W_{required}$ - Main girder, L = 20 m   Fig. 6b. $W_{requied}$ - Main girder, L = 80 m

5.   Characteristic loads

5.1.   Procedure of calibration

The characteristic loads have been defined for a return period of 1000 years. The importance of the choice of the return period is shown in section 6.2.

The characteristic loads model have been defined considering several traffic scenarios and influence lines [2], with reference to the Auxerre traffic, recorded on the motorway Paris-Lyon in France. The calibration has shown that two influence lines are determining : M_o, the bending moment at mid span of a simple supported beam and M_2 the bending moment on the central support of a beam with two spans [7]. The results given later for these two lines are sufficient to illustrate the whole calibration studies.

The members of the Project Team have proposed several traffic scenarios and several extrapolation methods. All the proposed target values have been compared on graphs giving a fictitious load Q' in function of the span length L : $Q' = k.M/L$ or $Q' = k.V$, where M is a bending moment,V is a shear force, and k is a factor depending on the type of load effect. On such a graph, a load effect produced by a constant load is represented by an horizontal straight line and a load effect produced by a constant uniform distributed load is represented by a slopping straight line.

The load effects produced by the load model should cover, as far as possible, all proposed target values, because all proposals have to be considered.

The development of the characteristic load models was carried out studying, first the general shape of the load model on lane 1, than the local loads on lane 1 and finally the load model on a carriage-way with several lanes.

5.2. General shape of the load model on lane 1

The target values, dynamic effect included, proposed by five members of the Project Team are reported on Figures similar as Figure 7 [7]. The Figures showed that for short spans (below 30 m. to 50 m.) free traffic produces higher moments than congested traffics for reason of the dynamic effect. The envelope of all results should be represented by a straight line, that will say that the load model producing the moments may be composed by a concentrated load and a constant uniform distributed load. Regarding all influence lines, the concentrated load is comprised between 450 to 720 kN, values close to the characteristic weight of a vehicle, and the distributed load is comprised between 21 to 28 kN/m, value close to the mean linear weight of the lorries running in jam.

The curve LM1, given on Figure 7 corresponds to the load model 1 prescribed in the EC, where the local load is equal to 600 kN and the distributed load is equal to 27 kN/m. This model gives too high values
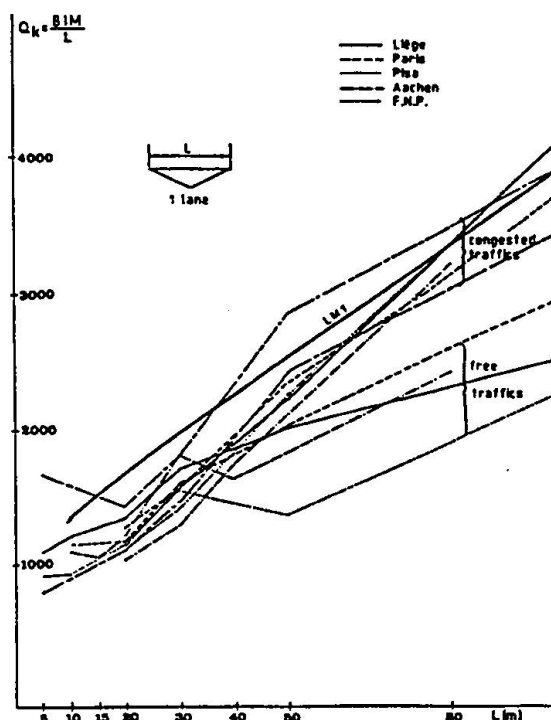

Fig. 7. Target values - M_o - 1 lane

for short spans and in some cases too low values for long spans. But, as for long spans a carriage-way comprises always more than on lane, this problem is to reconsider in section 5.4.

5.3. Local loads on lane 1

The position and the weight of the axles of actual lorries are relevant for local load effects. The extrapolation of the recorded loads available leads to characteristic loads, without any dynamic effect ; that are given in the table.

	characteristic loads (kN)		
	Min.	Max.	Auxerre traffic
simple axle	17	250	230
tandem axle	280	400	360
tridem axle	350	480	480
lorry	560	870	750

The heaviest vehicle is shown on Figures 8a and 8b. In one case, on Figure 8b, a tandem axle of 2 x 200 kN of an other vehicle produces the highest effect.The Figures compare the target values, dynamic effect included, with the values produced by three load models comprising respectively, 1, 2 or 3 axles.

The Figures show that the model with one axle of 600 kN (LMa1) gives too high values for short spans and is therefore not appropriate for the calculation of local effects. The model with 2 axles of 300 kN (LMa2), that corresponds to model 1 of the Eurocode 1.3., gives the best fit, even if the moments at midspan are too high for spans above 7 m. (up to 18 %, see Figure 8a) and the moments on support are too low for spans comprised between 4 and 9 m. (up to 10 %, see Figure 8b).
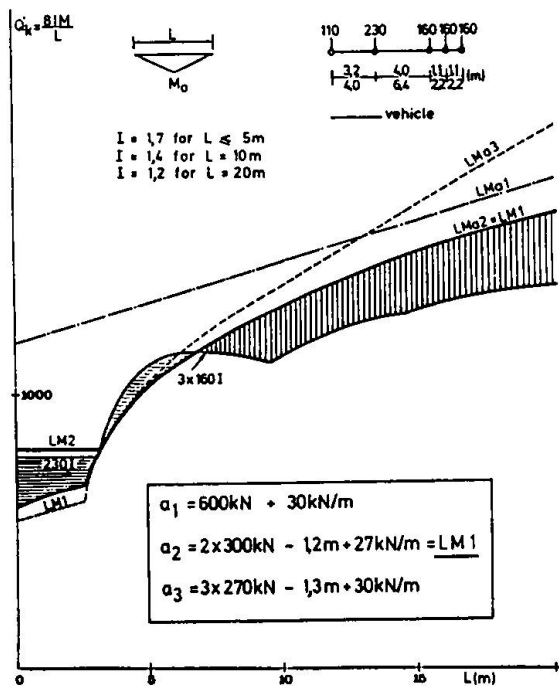
Fig. 8a . Target values - M_o - Local effects
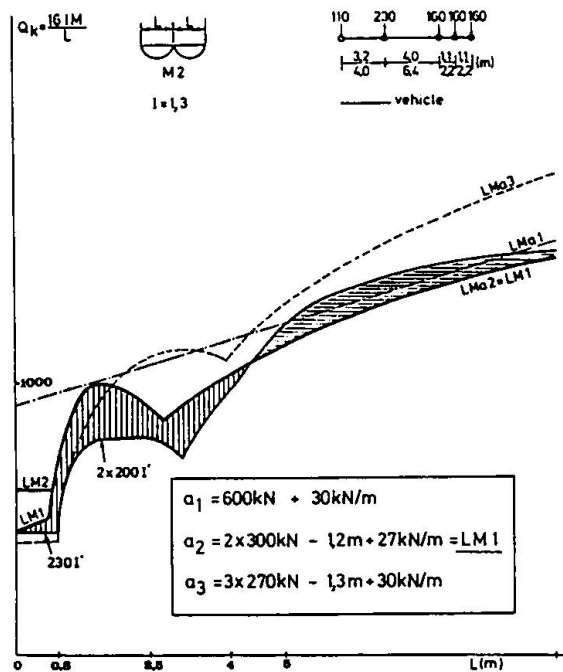
Fig. 8b. Target values - M_2 - Local effects
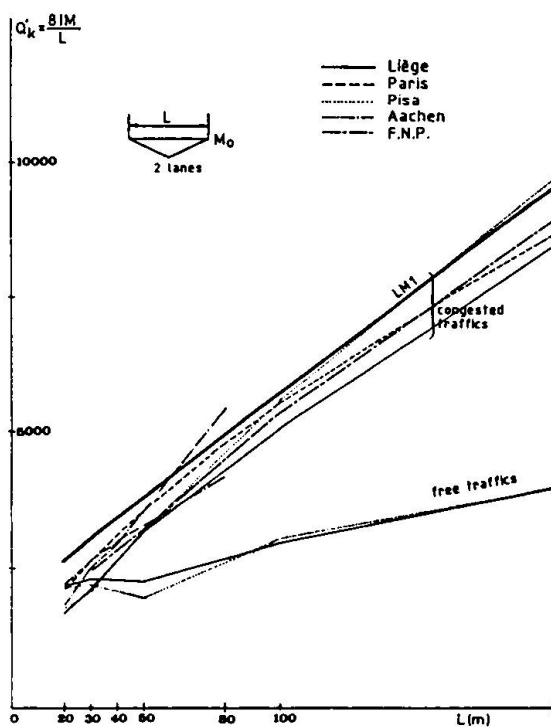
Fig. 9. Target values M_o - 2 lanes
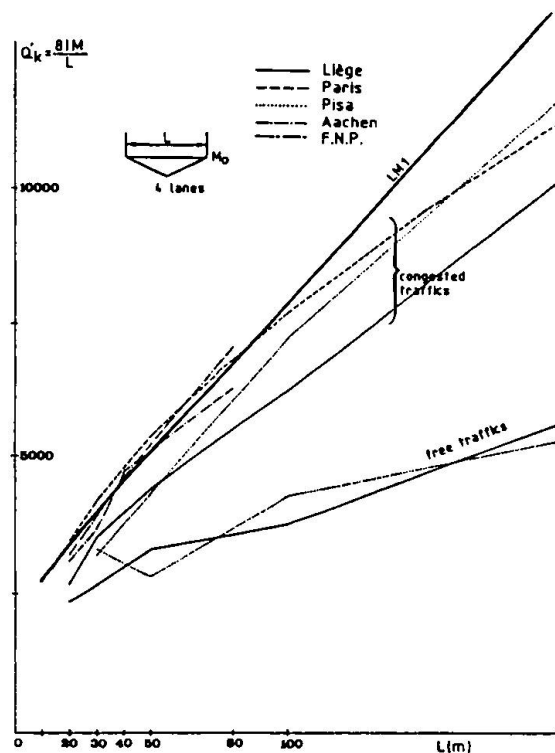
Fig. 10. Target values M_o - 4 lanes

As for short spans the model gives too low load effects, model 2, comprising one axle of 400 kN, has been introduced in the code. This single axle corresponds to the heaviest extrapolated axle load (250 kN), multiplied by a dynamic factor I = 1,6.

5.4. Load model on a carriage way with several lanes

Figure 9 shows that for a two lanes bridge, congested traffics are mainly to consider for the determination of the load model.

Figure 10 shows that for a four lanes bridge, LM1 is very close to the highest target values proposed, but the distributed load should be reduced for spans longer than 100 m., while in some cases the local load is too low.

The load model of EC 1-3 will cover all traffic scenarios envisaged if the distributed load on lane 2 (2,5 kN/m²) is increased and axle loads should be applied on each lane [7].

The distributed load could be reduced on large bridges, having four or more lanes and spans longer than 100 m, but 2,5 kN/m² seems an acceptable minimun.

5.5. Conclusions on characteristic load models

It has been shown here that the characteristic load models prescribed in EC 1-3 are a good compromise between simplicity and accuracy . The most relevant aspects concerning the application of theses models can be summarised as follow :
- no dynamic effect is to calculate, because this effect is included in the loads.
- a minimum uniform distributed load is applied on all the carriage way, apart lane 1 :

$$q_2 = q_3 = q_r = 2,5 \text{ kN/m}^2,$$

- a high uniform distributed load, corresponding to a jam of lorries is applied on one lane, 3 m wide : $q_1 = 9 \text{ kN/m}^2,$
- two axle loads are applied on a maximum of 3 lanes with each axle load equal respectively to
$$Q_1 = 300 \text{ kN}, \qquad Q_2 = 200 \text{ kN} \quad \text{and} \qquad Q_3 = 100 \text{ kN}.$$
- in order to avoid local weak points, one axle of 400 kN (LM2) is to consider alone, every where on the carriage way.

Figures 7 to 10 illustrate the accuracy of the model regarding all the traffic scenarios considered in the calibration, when the heaviest motorway traffic recorded in Europe and an average roughness of the pavement are considered. The code allows also reduction factors β if the expected traffic is not so heavy. Bisedes, when heavier traffics may occur, axle loads should to be considered on more than 3 lanes and high distributed loads on several lanes should be considered.

6. Infrequent and frequent loads

6.1. Definitions

The bridge design needs for the verification of serviceability limit states, the definition of loads that have return periods below 1000 years. For code purposes, the infrequent loads has been defined as having a return period of one year and considering a reduced dynamic effects, corresponding to a good roughness of the pavement.

The frequent loads have been defined as having a return period of one week and considering a good roughness of the pavement and free flowing traffics. The extreme traffic scenarios considered for determining the characteristic loads have not been envisaged here.

The infrequent and the frequent loads may be deduced from the characteristic loads. It has been demonstrated that the load distributions, as well as the load effect distributions, present two modes, and correspond to a Gaussian law for values above the 2nd mode x_0 [8] [9]. The value corresponding to a return period R is given by : $x_R = x_0 + \sigma \cdot z_R$ (see section 2.1). The ratio x_0/x_k corresponding to free flowing traffics is comprised between 0,3 and 0,5, while 0,7 may be reached for congested traffics. Here only 1 % of the total traffic volume is assumed to run in jam.

6.2.   Infrequent loads

For a return period of 1 year, $x_R/x_k = 0,9$ for free traffics and 0,92 for congested traffics. When a good roughness of the pavement is considered instead of an average roughness, the loads may be reduced by 10 %, so that finally, the infrequent loads in Eurocode are obtained by applying a factor $\Psi_1 = 0,8$ on the characteristic loads.

This means that the return period chosen for the definition of characteristic loads is not very important (section 5.1).

6.3.   Frequent loads

For a return period of one week and free traffic, $x_R/x_k = 0,82$. Here too, a good roughness of the pavement allows a reduction of the loads equal to 10 %. But, as the frequent loads result from free traffics only, the uniform distributed loads are always below 50 % of the congested traffic loads [9].

Finally, the frequent loads prescribed by the Eurocode are obtained by applying two different ψ_1 factors on the characteristics values of LM 1 et LM 2 :

$\psi_1 = 0,7$ for axle loads and

$\psi_1 = 0,40$ for distributed loads.

7.   Fatigue loads

7.1.   Introduction

The calibration of fatigue load models considers free flowing traffics on the slow lane, in fact :
- the fatigue damage concerns mainly short span elements, where dead load is low, and therefore the stress ranges are high,
- on short span elements, below 30 to 50 m, free traffic produces higher load effects than congested traffics (see section 5.2.),
- the highest fatigue damage occurs when the distances between lorries correspond to free traffic [10],
- the highest volume of the traffics runs flowing and not in jam,
- minimum 90 % of lorries are running on the slow lane.

The available data show that the number of lorries on the slow lane of highways is very high, and reaches 1000 to 8000 per day. That will say 25 to 200 million during a life time of 100 years. It results in local elements much more cycles than corresponding to the cut off limit

prescribed in EC 3 (100 million). In order to avoid fatigue damage in bridges submitted to high density traffic, all stress ranges have to be below the fatigue limit under constant amplitude. Therefore a fatigue frequent load has been defined, as a load producing a stress range $\Delta\sigma_f$, in such a way that 99 % of the total fatigue damage results from the stress ranges below $\Delta\sigma_f$. For the fatigue life assessment, an equivalent load has been defined as the centre of gravity of the damage distribution obtained applying the Miner rule [8] [10].

Starting from these considerations, 5 fatigue load models are defined in EC 1-3:

- FLM 1 defines frequent loads derived directly from the characteristic loads by applying two factors : 0,7 on the axle loads of model 1 or 2, and 0,3 on the uniform distributed load.

- FLM 2 defines frequent loads by a set of 5 lorries characterised by the weight, the position and the contact area of each axle, because FLM 1 is not accurate enough for short spans (Figure 11)

- FLM 3 defines a symmetrical vehicle usable for the fatigue life assessment, where the equivalent load of each axle is equal to 120 kN, dynamic effect included,

- FLM 4 defines equivalent loads for the same set of lorries given for FLM 2, allowing a more accurate fatigue assessment than FLM 3, for local effects,

- FLM 5 is not really a load model : a whole load spectrum should be used for a fatigue assessment by applying a cycle counting method and the Miner rule.

7.2.   Accuracy of the load models

The fatigue assessment has been performed by considering the free flowing Auxerre traffic recorded on the slow lane, and SN curves with 3 values of the slope, corresponding to m = 3, 5 and 9. In Figure 11 the ratio between $\Delta M_{fEC\,1}$, which are the effects produced by FLM 1, and ΔM_{fA}, which are the target effects produced by the Auxerre traffic, is given, depending on the span, for m = 3. The Figure shows that FLM 1 gives too high values for short spans (L < 20 m.), and too low values for one influence line (M2). The first problem is solved by FLM 2 (see Figure 12). The second problem should be solved by increasing the uniform distributed load, for example by accepting here the frequent load defined in section 6.3. FLM 1 and FLM 2 have to be on the safe side in all cases, because, if these models show that the fatigue life is limited, the final conclusion of the fatigue assessment results from the use of FLM 3 or FLM 4.

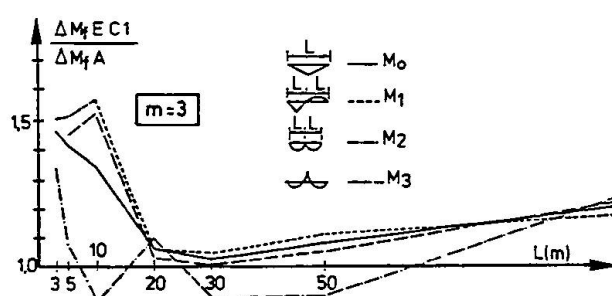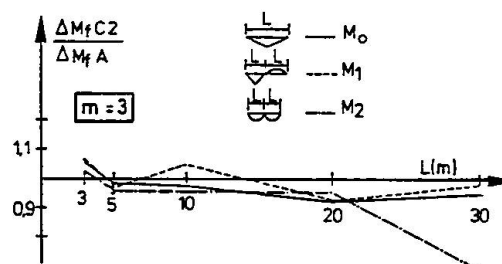*Fig. 11   FLM 1*   *Fig. 12   FLM 2*

Figure 13 gives the ratio between ΔM_{eEC}, which are load effects produced by FLM 3 and ΔM_{eL}, which are the equivalent load effects produced by the Auxerre traffic, where the equivalent number of cycles is given by : $n_e = k_1.k_2.n_L$, where

$k_1 = 2/3$ for Auxerre traffic,

$k_2 = 1$,   if < 10 m. ,

$k_2 = 0,6 + 1/0,25$ L, if $1,18$ m. $\leq$ L ≤ 10 m,

$k_2 = 4$,   if L $\leq 1,18$ m. ;

L is the span length. ;

n_L is the number of lorries.

The ratio is generally between 0,95 and 1,15, if the load effect on support M_2 is disregarded .

In order to solve the problem of M_2 when FLM 3 is used, it is necessary to consider a **second vehicle** 40 m. after the first. The second vehicle has the geometry of FLM 3, while the axle loads are multiplied by a factor 0,3 (see Fig. 14).

The need of a second vehicle, running 40 m. after the first, results from the analysis of the traffic and from the shape of the influence lines :

- the probability of the presence of 2 vehicles on a lane length longer then 40 m. is significant,

- the second vehicle increases the equivalent load effect in span (M_0, M_1, M_3) for spans longer than 80 m., and on support (M_2) for spans longer than 25 m. Practically, the second vehicle is only needed for the fatigue assessment of details where the influence line presents two contiguous areas of the same sign.
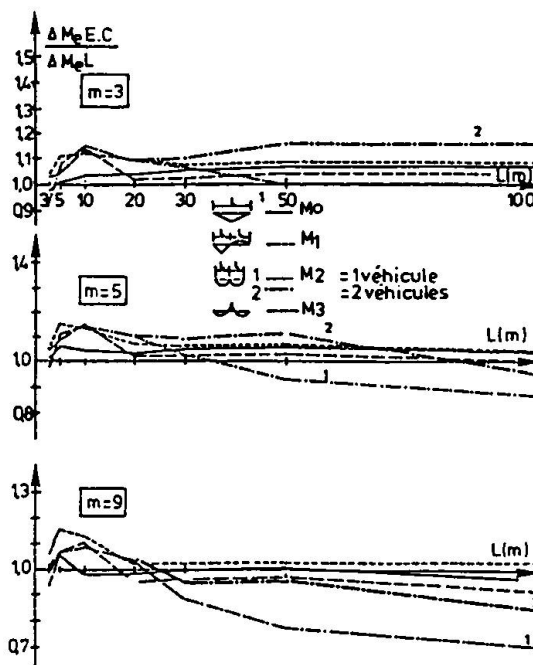

Fig. 13 FLM 2

In conclusion, the models prescribed in EC 1-3 result very accurate and independent on the slope of the SN curves defined by the factor m.
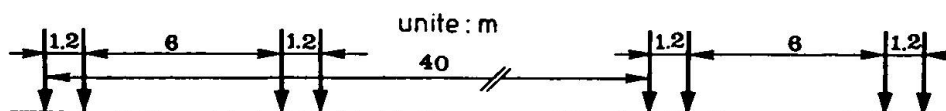

Fig. 14   F LM3 - modified.

7.3. Fatigue assessment using damage equivalent factor λ

Fatigue assessment can be also carried out, using the so called damage equivalent factor λ.

The basic idea of the λ factor method is to relate the damage induced by the stress spectrum to an equivalent stress range $\Delta\sigma_{eq}$ referring to 2×10^6 cycles, $\Delta\sigma_{eq} = \lambda.\phi_{fat} . \Delta\sigma_p$, where $\Delta\sigma_p$ is the maximum stress range induced by the fatigue load model $\Delta\sigma_p = (\sigma_{p.max} - \sigma_{p.min})$ and ϕ_{fat} is the damage equivalent impact factor.

Of course, the λ factor depends on the material by the slope m of the S-N curve.

When the fatigue assessment is based on FLM 3, the damage equivalent factor can be expressed as $\lambda = \lambda_1.\lambda_2.\lambda_3.\lambda_4$, where λ_1 depends on the shape and on the length of the influence line, i.e. on

traffic flow and the traffic composition, λ_3 is a factor depending on the design life of the bridge and λ_4 takes into account the multilane effect.

The numerical values of λ_i depend, as well as on the slope m, on the reference traffic used for the calibration and on the reference design life of the bridge LT_R. Said N_o the flow and Q_o the equivalent weight of the reference traffic, it is

$$\lambda_2 = k \cdot \frac{Q_{ml}}{Q_o} \cdot \left(\frac{N_1}{N_o}\right)^{\frac{1}{m}} , \text{ where k is a constant, } N_1 \text{ is the actual flow and}$$

$$Q_{ml} = \left(\sum_i n_i Q_i^m / \sum_i n_i\right)^{\frac{1}{m}}, \text{ the equivalent lorry weight for the considered lane,}$$

$$\lambda_3 = \left(LT / LT_R\right)^{\frac{1}{m}}, \text{ being LT the actual design life.}$$

To evaluate λ_4 it is necessary to take into account, as well as the effect of the lorries travelling alone on different lanes, the simultaneous transit of lorries on several lanes [11], so that

$$\lambda_4 = \left\{\frac{N_1^*}{N_1} + \sum_i \left[\frac{N_i^*}{N_1} \cdot \left(\frac{\eta_i}{\eta_1}\right)^m\right] + \sum \left[\frac{N_{comb}}{N_1} \cdot \left(\frac{\eta_{comb}}{\eta_1}\right)^m\right]\right\}^{\frac{1}{m}}, \text{ in which}$$

N_1 is the lorry flow on the main lane, η_i is the effect of the i-th lane, N_i^* is the flow of the individual lorries on the main lane, N_{comb} the flows and η_{comb} the effects of interacting lorries, and the second sum is extended to all the relevant combinations of several lorries.

7.4. Conclusions on fatigue assessment

The fatigue load models defined in E 1-3 allow a simple approach of the fatigue assessment using the SN curves of the detail to verify [12].

If a fatigue limit under constant amplitude is defined, as in the design code for steel structures EC 3, the use of the frequent load models FLM 1 or FLM 2 may allow a first quick conclusion concerning the existence, or not, of a fatigue damage.

The fatigue life may be calculated by using **FLM 3**, if two requirements are satisfied :

1. the SN curves are unlimited : the cut off limit defined in EC 3 have to be deleted,
2. two vehicles have to be considered with a spacing equal to 40 m.

FLM 2 and FLM 4 are more accurate only for the fatigue life assessment of local effects, occurring in concrete or orthotropic slabs.

It could be suggested to increase the values of FLM 1 up to the frequent values given in section 6.3.

8. Conclusions

Starting from a wide set of data obtained by in site measurements of road traffic loads, it has been possible to define scientifically the representative values needed for design of bridges.

The main load models given in the Eurocode 1-3 have been calibrated on a Continental European highway traffic. In order to take into account lighter traffics reduction factors are foreseen, while loads can been incresead when heavier traffics are expected.

The fatigue load models allow an engineer approach by checking first if fatigue damage is expected or not, and than by calculating the fatigue life.

The aim of the drafting panel of EC 1-3 was to propose models that are a good compromise between accuracy and simplicity, in spite of the complexity of the problem.

References

1. prENV 1991-3 Eurocode 1 : Basis of Design and Actions on Structures.
    Part 3 : Traffic Loads on Bridges. Final draft - August 1994.
2. A. BRULS, A. MATHIEU, J. CALGARO, M. PRAT
    ENV 1991 Part 3 : The main models of traffic loads on road bridges - Background studies. IABSE Colloquium Delft 1996.
3. B. JACOB, A. BRULS, A.FLINT, MAILLARD, G.MERZENICH, G. SEDLACEK.
    Eurocode on actions - Part 12 - Traffic Loads on Roads Bridges.
    Report of subgroup 8 : Methods for Prediction of the Extreme Vehicular Loads and Load Effects on Bridges - 1990.
4. P. CROCE, F. MARTINEZ, R. NICOTERA, M. PETRANGELI, L. SANPAOLESI,
    I modelli di carico dei ponti stradali nell'EC 1.
    C.T.A. Congress, Abano Terme, 1991.
5. G. SEDLACEK, A. ASTUDILLO, .A. BRULS, R. CANTIENI, S.DROSNER,
    M. EYMARD, A. FLINT, R. HOFFMEISTER, B. JACOB, G.MERZENICH,
    R. NICOTERA, M. PETRANGELI,
    - Eurocode on Actions - Part 12 - Traffic Loads on Road bridges.
    Report of subgroup 5 - Definition of dynamic impact factors. September 1991.
6. G. MERZENICH. Entwicklung eines europäischen Verkehrslatmodells für die Bemessung von Strassenbrücken.
    Doktor Arbeit- 1994 - Stahlbau - RWTH - Aachen.
7. A. BRULS. Eurocode on Actions - Traffic Loads on Road Bridges.
    Target values and proposed load model.Characteristic Load effect - Infrequent and frequent load effects. Working Draft of PT6 - 1992.
8. A. BRULS. Determination des actions pour le calcul des ponts-routes.
    IABSE Colloquium - Fatigue of Steel and Concrete Structure -
    Lausanne - 1982 - pp. 865 à 872.
9. A. BRULS, B. JACOB, G. SEDLACEK. Eurocode on Actions : Part 12 - Traffic loads on road Bridges. Report of W.G.2. : Traffic data of the European Countries. 1989.
10. A. BRULS. Résistance des ponts soumis au trafic routier -
    Modélisation des charges - Réévaluation des ouvrages.
    Thèse de doctorat.Université de Liège. Février 1995.
11. P. CROCE. Vehicle interactions and fatigue assessment of bridges.
    IABSE Colloquium Delft 1996.
12. A. BRULS. Evaluation of Existing Bridges under Actual Traffic
    IABSE Symposium. Extending the Lifespan of Structures.
    San Francisco 1995 - pp. 829 to 834.

Leere Seite

Blank page

Page vide

Comparative research to establish load factors for railway bridges

H.H. SNIJDER
Civil Engineer
Holland Railconsult and
Eindhoven University of
Technology
The Netherlands.

F.H. ROLF
Mechanical Engineer
Holland Railconsult
Utrecht
The Netherlands.

Frans Rolf, born in 1949, got his mechanical engineering degree at Twente University of Technology in 1974. He started his career as consultant for dynamics at the Netherlands Railways. In 1980 he became bridge engineer specialised in movable bridges. Since 1987 he was subsequently head of the bridge maintenance department, head of the steel design section and the civil works section of Netherlands Railways. Today he is senior account manager of Holland Railconsult.

Bert Snijder, born in 1959, got his civil engineering degree at Delft University of Technology in 1983. He started his career at TNO Bouw as research engineer in the field of stability and fatigue of steel structures. In 1989 he became design engineer specialised in fixed steel bridges at the Netherlands Railways. At present he is involved in the design of steel building structures for Holland Railconsult. Since 1993 he is part time professor of steel structures at Eindhoven University of Technology.

Summary

In this paper the results of a comparative research to establish load factors for railway bridges are presented. These results form the main input for section 6. part 3 of Eurocode 1 'Railway Loading' [1] for as far as partial factors are concerned. The research has been carried out by a working group of the subcommittee 'Bridges' of the UIC (Union Internationale des Chemins de fer). Aim of the research was to examine existing practices and codes. Based on these, a set of partial safety factors was proposed, to be applied to variable and permanent actions for structures carrying railway traffic.

1. Introduction

During development of European Design Codes there was need to establish safety factors for railway loading. The subcommittee 'Bridges' of UIC (Union International de Chemin de Fer) set up a working party 'Safety factors'. The results of this working party are presented in a report [2].

The rules for establishing Eurocodes say that the safety factors have to be based on probabilistic study. As very little data were available, the working party decided first to compare existing practices in the member countries with proposed Eurocodes and then tried to propose a set of partial safety factors on basis of those results.

2. Approach

It was quite clear from a brief survey of the five countries involved that just a comparison of used safety factors in the different codes would not be satisfactory.
The fact that the safety of the construction was sometimes covered by other figures than the safety factors made this impossible. Sometimes safety is implicitly available in the allowable stresses or in a higher traffic load.

The five codes (table 1) involved were the regulations used by the railways in:

Denmark	(DSB);
France	(SNCF);
Germany	(DB);
The Netherlands	(NS);
United Kingdom	(BR).

ACTION		PARTIAL SAFETY FACTORS				
		ADMINISTRATION				
		NS	SNCF	BR	DSB	DB
Permanent Action	Self Weight (Steel)	1.50	1.32	1.10	1.00	1.35
	Ballast	1.50	1.32x1.30	1.75	1.20	1.80
Variable Traffic Action	Load Model 71*	1.50	1.35	1.40	1.30	1.35

Table 1. Fundamental partial safety factors for loads.

This leads to the conclusion that for comparison the total effect of the code on a structure should be studied. So it was agreed that comparative calculations would be required.

Six steel bridges and three concrete bridges were chosen to cover the range of spans most commonly encountered. For steel bridges three bridges with ballasted track were considered and three with non ballasted track. Only simply supported structures were chosen and only the positions of maximum bending and maximum shear of the main structure were studied. The bridges listed in table 2 were involved in the study.

Name	Material	Type	Span	Track	Annex
SU	steel	girder	11.1	non ballasted	1 a
MU	steel	trough	29.4	„	1 b
LU	steel	truss	59.7	„	1 c
SB	steel	girder	11.1	ballasted	1 a
MB	steel	trough	29.4	„	1 b
LB	steel	truss	59.7	„	1 c
S	concrete	reinforced slab	5	„	2 a
M	concrete	reinforced slab	15	„	2 b
L	concrete	posttensioned boxgirder	42	„	2 c

Table 2. Bridges studied.

3. Utilisation factors

Each bridge of table 2 was calculated by using the five sets of regulations of the administrations involved and once by using the proposed Eurocodes. So for each bridge six calculations were made and in each calculation two utilisation factors (α) were established,

one for maximum bending and one for maximum shear. In case of truss bridges utilisation factors for maximum normal force were established.

$$\alpha_{code} = \frac{\text{effect of design loads according the code}}{\text{design value of resistance according the code}}$$

Only direct permanent and variable traffic action and strength criteria were considered. Aspects as stability and fatigue were neglected.

The results using the national codes were compared with those according to the proposed European codes by establishing a utilisation factor α^1 as given below:

$$\alpha^1 = \frac{\alpha_{admin}}{\alpha_{Eurocode}}$$

As the aim of the study was to establish a set of partial safety factors, the set of safety factors for Eurocode could be varied.
The calculations were carried out by using a set as given below:

γ_{G1} = 1.35   permanent action self weight
γ_{G2} = 1.80   permanent action ballast
γ_{Q} = 1.50   variable traffic action

By varying this set the α^1 value could be influenced and a best fit between national codes and the European code could be established. Two criteria, as given below, were used for this purpose:

$$\underline{1} \qquad A = \frac{\sum (\alpha' - 1.0)}{n}$$

$$\underline{2} \qquad B = \frac{\sqrt{\sum (\alpha' - 1.0)^2}}{n}$$

where n = number of calculations.

In practice, the value of criterion A proved the more sensitive as can be seen from table 3 for four sets of safety factors.

ACTION		PARTIAL SAFETY FACTOR			
Permanent Action	Self Weight (steel)	1.20	1.20	1.20	1.20
	Ballast	1.60	1.60	1.60	1.60
Variable Traffic Action	Load Model 71	1.50	1.35	1.40	1.30
CRITERION A		+0.112	+0.050	- 0.006	- 0.056
CRITERION B		+0.021	+0.017	+0.015	+0.016

Table. 3. Comparison of sensitivity of criterion A and B.

4. Load factors for steel bridges only

For the six steel bridges the calculation results are shown in table 4. It can be seen from this table that α^1 varies from 0.77 to 1.21. It is quite easy to understand that for $\alpha^1 = 1$ there is complete fit between the national code and Eurocode. This coincides with A or B = 0. As A is the more sensitive only A-values are considered for optimising.

Partial safety factors

$$\gamma_{g1} = 1,35 \quad \text{steel}$$
$$\gamma_{g2} = 1,80 \quad \text{ballast}$$
$$\gamma_{uic} = 1,50 \quad \text{live load}$$

bridge type	sectional forces	EC3 α_{EC}	DB α_{DB}	α'	NS α_{NS}	α'	DSB α_{DSB}	α'	SNCF α_{SNC}	α'	BR α_{BR}	α'	Tot	
SU	M	0,81	0,73	0,90	0,83	1,02	0,85	1,05	0,67	0,83	0,83	1,02	0,78	0,97
	Q	0,44	0,37	0,84	0,42	0,95	0,41	0,93	0,35	0,79	0,38	0,86	0,39	0,88
MU	M	0,47	0,44	0,94	0,51	1,08	0,50	1,06	0,41	0,87	0,57	1,21	0,49	1,03
	Q	0,27	0,25	0,92	0,30	1,11	0,30	1,11	0,25	0,92	0,25	0,92	0,27	1,00
LU	N5	0,62	0,56	0,90	0,70	1,13	0,62	1,00	0,51	0,82	0,57	0,92	0,59	0,96
	N7	0,77	0,69	0,90	0,87	1,13	0,77	1,00	0,63	0,82	0,71	0,92	0,73	0,95
	N8	0,51	0,45	0,88	0,58	1,14	0,51	1,00	0,41	0,80	0,51	1,00	0,49	0,96
SB	M	0,96	0,85	0,89	0,88	0,92	0,95	0,99	0,77	0,80	1,03	1,07	0,90	0,93
	Q	0,64	0,57	0,89	0,60	0,94	0,63	0,99	0,53	0,83	0,69	1,08	0,60	0,95
MB	M	0,69	0,62	0,90	0,63	0,91	0,66	0,96	0,55	0,80	0,81	1,18	0,65	0,95
	Q	0,42	0,38	0,90	0,38	0,90	0,40	0,95	0,29	0,69	0,37	0,88	0,36	0,86
LB	N5	0,89	0,79	0,89	0,88	0,99	0,85	0,95	0,69	0,77	0,87	0,98	0,82	0,91
	N7	1,11	0,98	0,88	1,09	0,98	1,06	0,95	0,86	0,77	1,07	0,96	1,01	0,91
	N8	0,73	0,64	0,88	0,73	1,00	0,69	0,95	0,56	0,77	0,77	1,05	0,68	0,93
Σ (x-1)/n	$\rightarrow$		-0,11		0,01		-0,01		-0,19		0,00		-0,058	
$\sqrt{\Sigma}$ (x-1)2/n	$\rightarrow$		0,03		0,02		0,01		0,05		0,03		0,014	

Table. 4. Resume of α-values for steel bridges.

For optimising the A-value the partial safety factors for self weight steel and ballast were fixed at 1.35 and 1.80. The safety factor for variable traffic action was varied. The value of the partial safety factor for ballast of 1.80 was made up from a self weight factor of 1.35 and a height factor of 1.33 (1.35 x 1.33 = 1.80). The self weight factor 1.35 is in line with values for permanent actions elsewhere in the Eurocodes.

The results of this analysis are shown in figure 1.
The dashed line indicates the optimum value for the safety factor for variable traffic action.
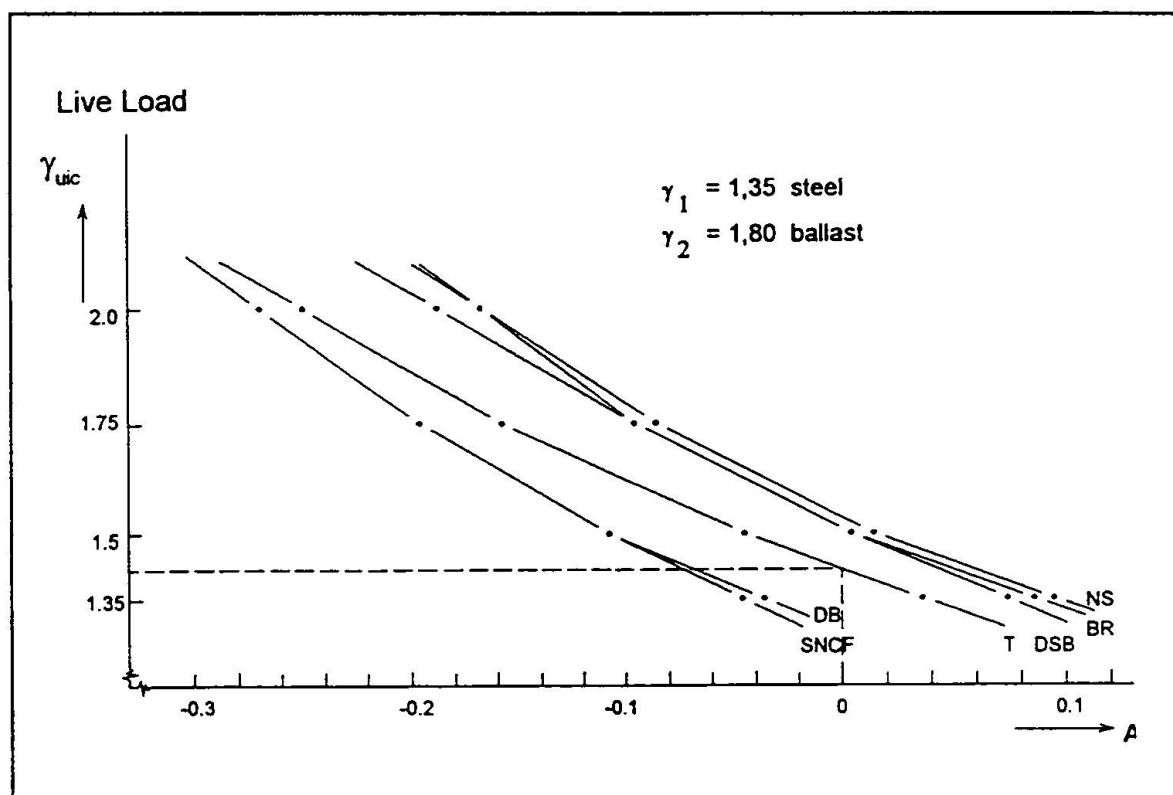
Figure. 1. Optimisation of criterion A with $\gamma_{dead\ load}= 1.35$.

It is interesting to note that the values of A derived from the codes of DB and SNCF are similar and always smaller than the values derived from the codes used by DSB, NS and BR. By T the mean values of the total amount of data are represented.

This means that in general DB and SNCF allow heavier traffic than DSB, BR and NS on the same construction. The proposed approach for this study will lead to a Eurocode that allows traffic that will lie between the two sets of administrations (DB and SNCF on the one hand DSB, BR and NS on the other).

The best fitting set found is:

$$\gamma_{G1} = 1.35$$
$$\gamma_{G2} = 1.80$$
$$\gamma_{Q} = 1.40$$

The difference between the values of γ_{G1} and γ_{Q} is very small. It seems unrealistic that the safety factor for self weight permanent actions and variable traffic action are so similar. Traffic actions are in general much less predictable than self weight actions. So a new optimum was investigated on basis of the following self weight factors:

$$\gamma_{G1} = 1.20 \text{ and}$$
$$\gamma_{G2} = 1.60.$$

The results are shown in figure 2.
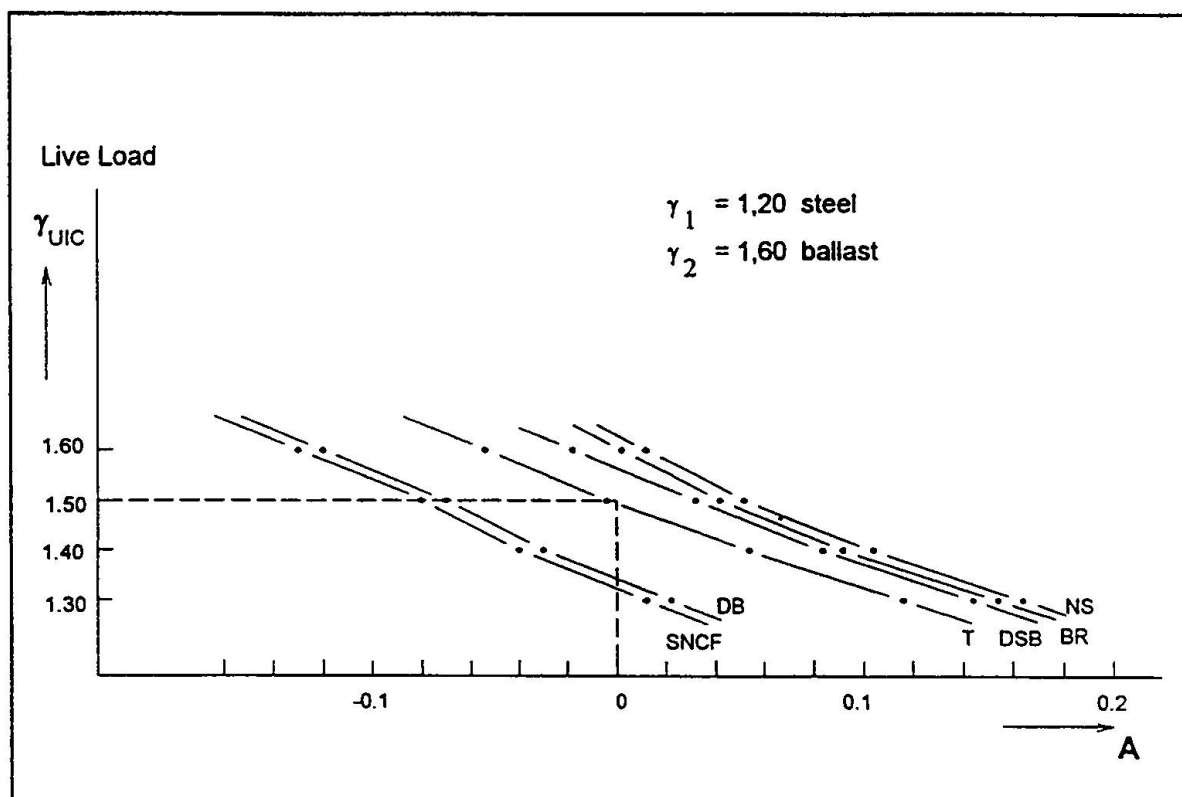
Figure. 2. Optimisation of criterion A with $\gamma_{dead\ load} = 1.20$.

The optimum set showed to be:

$$\gamma_{G1} = 1.20$$
$$\gamma_{G2} = 1.60$$
$$\gamma_{Q} = 1.50$$

for steel bridges.

5. Load factors for steel and concrete bridges

The approach as shown above for steel bridges showed to be more complicated for concrete structures . Due to the fact that the model of failure used in the national codes are not the same, the design verification of various national codes differed very much.

So for concrete bridges new α factors had to be defined. A list of 11 different factors was the result (see table 5).

	criterion of checking	limite state	DEFINITION OF α-VALUE	according to Eurocode
BENDING				
1	concrete	SLS	$\alpha_c = \max\sigma_c/(0.45f_{ck})$ (quasi-permanent) $\alpha_c = \max\sigma_c/(0.60f_{ck})$ (infrequent)	EC2/2 4.4.1.1 (2) EC2/2 4.4.1.1 (3)
2	reinforcement steel	SLS	$\alpha_s = \max\sigma_s/(0.8f_{yk})$ (infrequent)	EC2/2 4.4.1.1 (6)
3	prestressing steel	SLS	$\alpha_p = \max\sigma_{poo}/(0.65f_{pk})$ (quasi-permanent) $\alpha_p = \max\sigma_{po}/(0.75f_{pk})$ (infrequent)	EC2/2 4.4.1.1 (7) EC2/1 4.4.1.1 (7)
4	cross section (reinforced)	ULS	$\alpha_{cs} = M_{Sd}/M_{Rd}$	EC2/2 4.3.1
5	prestressing steel	ULS	$\alpha_p = M_{Sd}/M_{Rd}$ $\quad$ ($M_{Rd}: 0.9f_{pk}/\gamma_s$)	EC2/1 4.2.3.3.3
6	concrete (prestressed)	ULS	$\alpha_c = \max\sigma_c/(\alpha f_{cd})$	EC2/1 4.2.1.3.3
7	crack width (reinforced)	SLS	$\alpha_{crack} = \max\sigma_s/\sigma_{s(table\ 4.11.a\ or\ b)}$	EC2/2 4.4.2.3.3
8	decompresion (prestressed)	SLS	$\alpha_{p,\ decomp} = F_{p,min}/F_{p,exist}$ $\quad$ $F_{p,min}: s_{c1} = 0$ (infrequent)	EC2/2 4.4.2.1 (3)
9	deflection	SLS	$\alpha_f = f_{(\Phi UIC71)}/(1/1000)$	Ec1 3.4 (agreement based on a paper of discusion for PT7)
SHEAR				
10	struts	ULS	$\alpha_{c,strut} = V_{Sd(x=0)}/V_{Rd2}$	EC2/1 4.3.2.4.3 (stand.) EC2/1 4.3.2.4.4 (incl.)
11	steel + concrete	ULS	$\alpha_{s+c} = V_{Sd(x=0.5d)}/V_{Rd3}$	EC2/1 4.3.2.4.3 (stand.) EC2/1 4.3.2.4.4 (incl.)

Table. 5. Definition of α-value for concrete bridges.

As very few criteria were used in all national codes only criteria 4 and 5 were available for comparison.

A partial safety factor for prestress was introduced for the prestressed or post tensioned structures. This factor was assumed to be 1,00.

In the same way as for steel bridges, the optimum value for A could be found by varying the set of safety factors. To limit the amount of work 10 sets were investigated with γ-factors varying as follows:

γ_{G1} = 1,20; 1,35

γ_{G2} = 1,60; 1,78; 1,80

γ_{pr} = 1,00

γ_{Q} = 1,35; 1,40; 1,43; 1,45; 1,50

Out of these the most interesting sets are:

γ_{G1} = 1,20 $\quad$ 1,35

γ_{G2} = 1,80 $\quad$ 1,80

γ_{pr} = 1,00 $\quad$ 1,00

γ_{Q} = 1,50 $\quad$ 1,43

The results of these two sets are given in the tables 6 and 7.

Partial safety factors

γ_{g1} = 1,20   dead load
γ_{g2} = 1,80   ballast
γ_{uic} = 1,50   live load
γ_{pre} = 1,00   prestress

bridge type	criterium	EC α	DB α	DB α'	NS α	NS α'	DSB α	DSB α'	SNCF α	SNCF α'	BR α	BR α'	Tot (Σα)/n	(Σα/n)/α
steel														
SU	M	0,81	0,73	0,91	0,83	1,03	0,85	1,05	0,67	0,83	0,83	1,03	0,78	0,97
	Q	0,44	0,37	0,84	0,42	0,96	0,41	0,94	0,35	0,80	0,38	0,87	0,39	0,88
MU	M	0,46	0,44	0,96	0,51	1,11	0,50	1,09	0,41	0,90	0,57	1,25	0,49	1,06
	Q	0,26	0,25	0,95	0,30	1,14	0,30	1,14	0,25	0,95	0,25	0,95	0,27	1,03
LU	N5	0,60	0,56	0,94	0,70	1,17	0,62	1,04	0,51	0,85	0,57	0,95	0,59	0,99
	N7	0,74	0,69	0,93	0,87	1,17	0,77	1,04	0,63	0,85	0,71	0,96	0,73	0,99
	N8	0,49	0,45	0,91	0,58	1,18	0,51	1,04	0,41	0,83	0,51	1,04	0,49	1,00
Σ (x-1)/n	→		-0,08		0,11		0,05		-0,14		0,01			-0,012
√Σ (x-1)2/n	→		0,03		0,05		0,03		0,06		0,04			0,019
SB	M	0,95	0,85	0,89	0,88	0,92	0,95	1,00	0,77	0,81	1,03	1,08	0,90	0,94
	Q	0,63	0,57	0,90	0,60	0,95	0,63	1,00	0,53	0,84	0,69	1,09	0,60	0,96
MB	M	0,67	0,62	0,92	0,63	0,93	0,66	0,98	0,55	0,82	0,81	1,20	0,65	0,97
	Q	0,41	0,38	0,92	0,38	0,92	0,40	0,97	0,29	0,70	0,37	0,90	0,36	0,88
LB	N5	0,87	0,79	0,91	0,88	1,01	0,85	0,98	0,69	0,80	0,87	1,00	0,82	0,94
	N7	1,08	0,98	0,91	1,09	1,01	1,06	0,98	0,86	0,80	1,07	0,99	1,01	0,94
	N8	0,71	0,64	0,90	0,73	1,03	0,69	0,97	0,56	0,79	0,77	1,09	0,68	0,96
Σ (x-1)/n	→		-0,09		-0,03		-0,02		-0,21 C		0,05			-0,059
√Σ (x-1)2/n	→		0,03		0,02		0,01		0,08		0,04			0,020
Σ (x-1)/n	→		-0,09		0,04		0,02		-0,17		0,03			-0,035 •
√Σ (x-1)2/n	→		0,02		0,03		0,01		0,05		0,03			0,014
concrete														
S	4	0,58	0,53	0,91	0,52	0,89	0,55	0,94	0,60	1,03	0,72	1,24	0,58	1,00
M	4	0,82	0,81	0,99	0,81	0,99	0,85	1,04	0,90	1,10	0,91	1,12	0,86	1,05
L	5	0,77	0,86	1,12	0,85	1,11	0,83	1,08	0,76	0,99	0,78	1,02	0,82	1,06
Σ (x-1)/n	→		0,01		0,00		0,02		0,04		0,12			0,038 ••
√Σ (x-1)2/n	→		0,05		0,05		0,04		0,04		0,09			0,025 D =
total														
Σ (x-1)/n	→		-0,07		0,03		0,02		-0,14		0,04			-0,022
√Σ (x-1)2/n	→		0,02		0,02		0,01		0,04		0,03			0,012

MEAN(steel, concrete)   Σ(x-1)/n   A   0,001 A
MEAN(steel, concrete)   √Σ(x-1)2/n   B   0,019

A : 0.001
C : - 0.21
D : 0.073

Table. 6. Resume of α-values for steel and concrete bridges for the first set of γ-factors.

Partial safety factors

γ_{g1} = 1,35   dead load
γ_{g2} = 1,80   ballast
γ_{uic} = 1,43   live load
γ_{pre} = 1,00   prestress

bridge type	criterium	EC α	DB α	DB α'	NS α	NS α'	DSB α	DSB α'	SNCF α	SNCF α'	BR α	BR α'	Tot $(\Sigma\alpha/n)$	$(\Sigma\alpha/n)/\alpha$ $(\Sigma\alpha)/n$
steel														
SU	M	0,77	0,73	0,94	0,83	1,07	0,85	1,10	0,67	0,87	0,83	1,07	0,78	1,01
	Q	0,42	0,37	0,88	0,42	1,00	0,41	0,97	0,35	0,83	0,38	0,90	0,39	0,92
MU	M	0,45	0,44	0,97	0,51	1,12	0,50	1,10	0,41	0,90	0,57	1,26	0,49	1,07
	Q	0,26	0,25	0,96	0,30	1,15	0,30	1,15	0,25	0,96	0,25	0,96	0,27	1,03
LU	N5	0,60	0,56	0,93	0,70	1,17	0,62	1,03	0,51	0,85	0,57	0,95	0,59	0,99
	N7	0,75	0,69	0,93	0,87	1,17	0,77	1,03	0,63	0,85	0,71	0,95	0,73	0,99
	N8	0,49	0,45	0,91	0,58	1,17	0,51	1,03	0,41	0,83	0,51	1,03	0,49	1,00
Σ (x-1)/n	→		-0,07		0,12		0,06		-0,13		0,02			0,000
$\sqrt{\Sigma}$ (x-1)2/n	→		0,03		0,05		0,03		0,05		0,04			0,019
SB	M	0,93	0,85	0,92	0,88	0,95	0,95	1,02	0,77	0,83	1,03	1,11	0,90	0,96
	Q	0,62	0,57	0,92	0,60	0,97	0,63	1,02	0,53	0,86	0,69	1,12	0,60	0,98
MB	M	0,67	0,62	0,92	0,63	0,94	0,66	0,98	0,55	0,82	0,81	1,21	0,65	0,97
	Q	0,41	0,38	0,93	0,38	0,93	0,40	0,97	0,29	0,71	0,37	0,90	0,36	0,89
LB	N5	0,87	0,79	0,91	0,88	1,01	0,85	0,97	0,69	0,79	0,87	1,00	0,82	0,94
	N7	1,09	0,98	0,90	1,09	1,00	1,06	0,98	0,86	0,79	1,07	0,99	1,01	0,93
	N8	0,71	0,64	0,90	0,73	1,02	0,69	0,97	0,56	0,78	0,77	1,08	0,68	0,95
Σ (x-1)/n	→		-0,09		-0,03		-0,01		-0,20 C		0,06			-0,054
$\sqrt{\Sigma}$ (x-1)2/n	→		0,03		0,02		0,01		0,08		0,04			0,019
Σ (x-1)/n	→		-0,08		0,05		0,02		-0,17		0,04			-0,027 ♦
$\sqrt{\Sigma}$ (x-1)2/n	→		0,02		0,03		0,02		0,05		0,03			0,013
concrete														
S	4	0,57	0,53	0,93	0,52	0,92	0,55	0,97	0,60	1,06	0,72	1,27	0,58	1,03
M	4	0,83	0,81	0,98	0,81	0,98	0,85	1,02	0,90	1,08	0,91	1,10	0,86	1,03
L	5	0,80	0,86	1,08	0,85	1,07	0,83	1,04	0,76	0,95	0,78	0,98	0,82	1,02
Σ (x-1)/n	→		0,00		-0,01		0,01		0,03		0,11			0,028 ♦
$\sqrt{\Sigma}$ (x-1)2/n	→		0,04		0,04		0,02		0,04		0,09			0,023 D
total														
Σ (x-1)/n	→		-0,06		0,04		0,02		-0,13		0,05			-0,017
$\sqrt{\Sigma}$ (x-1)2/n	→		0,02		0,02		0,01		0,04		0,03			0,012

MEAN(steel, concrete) Σ(x-1)/n   **A**   0.000 A
MEAN(steel, concrete) $\sqrt{\Sigma}$(x-1)2/n   **B**   0,018

A : 0.000
C : - 0.20
D : 0.055

Table. 7. Resume of α-values for steel and concrete bridges for the second set of γ-factors.

As the comparing values A and B were no longer decisive for this situation two new criteria were formulated:

$$C = \frac{\Sigma (\alpha' - 1.0)}{n_{adm}}$$

the maximum deviation from zero of the national value where n_{adm} = number of calculations carried out using national code for a particular material.

$$D = \left| \frac{\Sigma (\alpha' - 1.0)}{n_c} - \frac{\Sigma (\alpha' - 1.0)}{n_s} \right|$$

the minimum deviation from zero between steel and concrete results where
n_c = number of calculations for concrete
n_s = number of calculations for steel.

Table 8 shows the different values for the criteria A, C and D as obtained for a number of sets of safety factors.

ACTION		PARTIAL SAFETY FACTORS			
		Set 1	Set 2	Set 3	Set 4
Permanent Action	Self Weight	1.20	1.35	1.35	1.35
	Ballast	1.80	1.80	1.80	1.80
	Prestress	1.00	1.00	1.00	1.00
Variable Traffic Action	Load Model 71	1.50	1.43	1.40	1.45
CRITERION A		+0.001	+0.000	-0.013	0.008
CRITERION C		-0.21	-0.20	-0.19	-0.21
CRITERION D		+0.073	+0.055	+0.052	0.056

Table. 8.   Values obtained for criteria A, C and D.

Sets 2 to 4 give almost the same results. Subcommittee bridges of UIC decided to adopt set number 4 having practical figures and being on the safe side compared to the second set:

γ_{G1} = 1.35
γ_{G2} = 1.80
γ_{pr} = 1.00
γ_{Q} = 1.45

This set has also been included in part 3 of Eurocode 1 [1].

6.   Conclusions

On basis of the research executed by this working party the following can be concluded.

A set of safety factors for railway loading was found which gives very good compatability with the bridge design commonly used in Western Europe.

Chosing a self-weight factor in accordance with earlier Eurocodes leads to a life-load factor which is only slightly higher than the self-weight factor.

7.   Recommendations

On basis of the work done by the working party the following recommendations can be made.

A probabilistic research to justify the proposed safety factors is needed.
During this research special attention should be paid to the self-weight factor of the bridges.

Execution of more comparative calculations and exchange of the results between the railway organisations will be of great help to evaluate the draft codes during the ENV period.

More research should be done on composite bridges.

8.   Acknowledgement

The authors wish to express their gratitude to all those who contributed to this work. To Mr. Tschumi, chairman of the UIC subcommittee 'bridges' who initiated the work of the working party. To Mr. Hermansen of DSB, Mr. Voignier and Mr. Bousquet of SNCF, Mr. Stier, Mrs. Crail and Mr. Pfeifer of DB, Mr. Brouwer of NS and to Mr. Wigley and Mr. Gohil of BR who did most of the work as members of the working party and the ad-hoc group on concrete bridges.

9.   References

[1]   ENV 1991-3, Eurocode 1: Basis of design and actions on structures,
       Part 3: Traffic loads on bridges, CEN/TC250/SC1

[2]   UIC working party - Safety factors - Final Report, May 1994.

Annex 1

steel bridges

11.106 m span (unballasted)
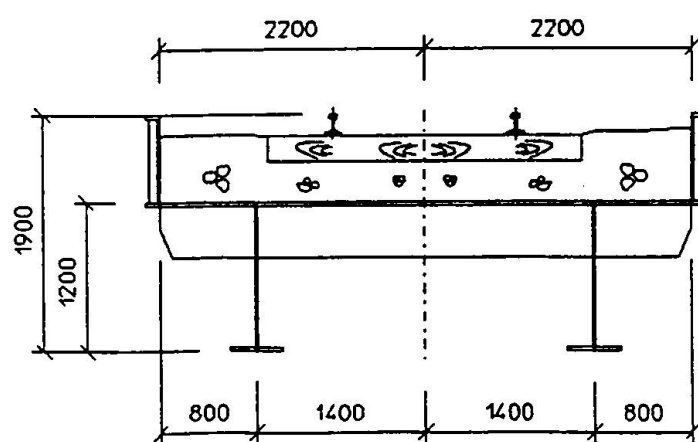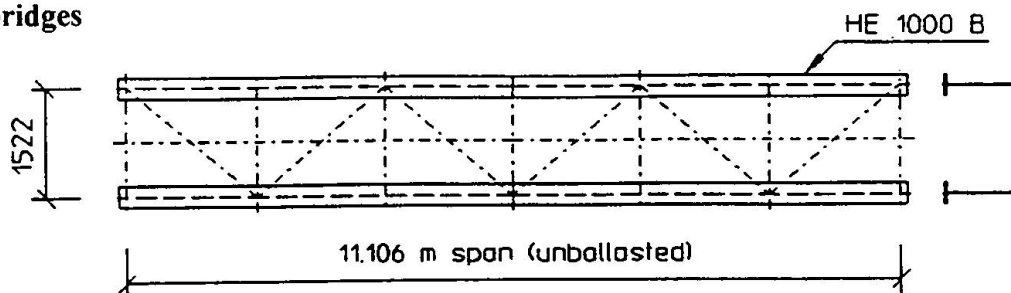
11106 m span typical section for a ballasted bridge

a
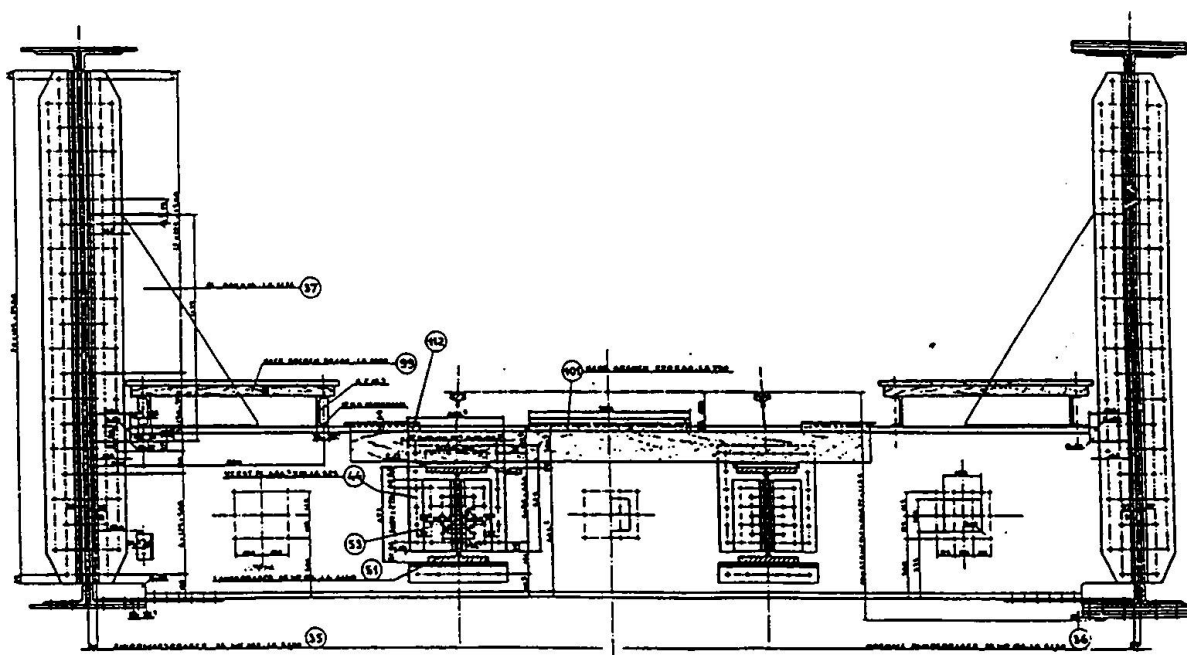
b

29.4 m span ballasted + unballasted
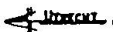
59.73 m span ballasted + unballasted

Annex 2

concrete bridges

5 m span typical section

a

load resisting reinforced concrete section

dead load

15 m span typical section

b

support

span

c

typical section 42 m span
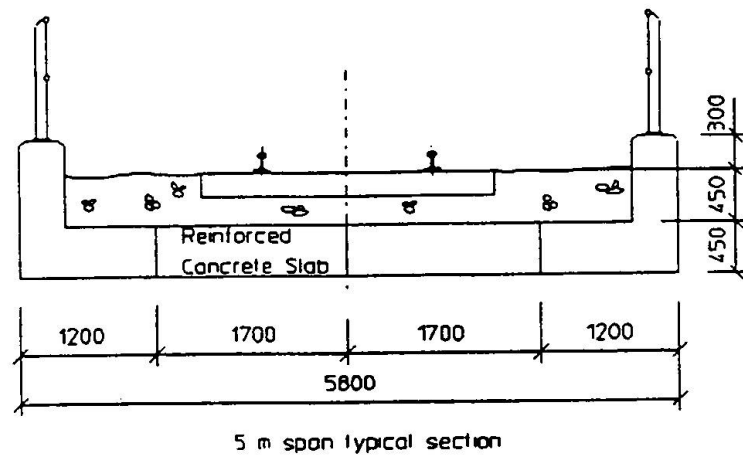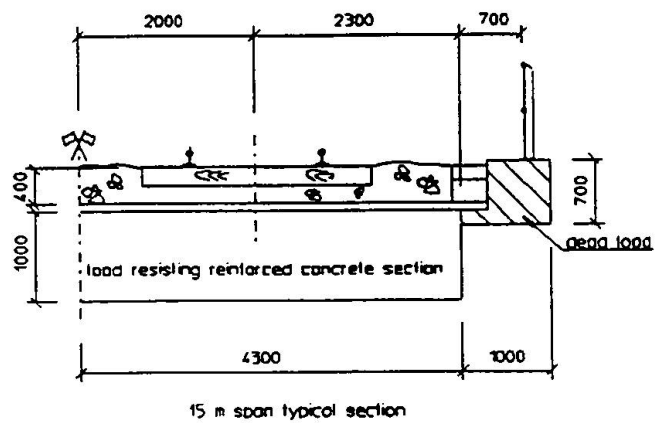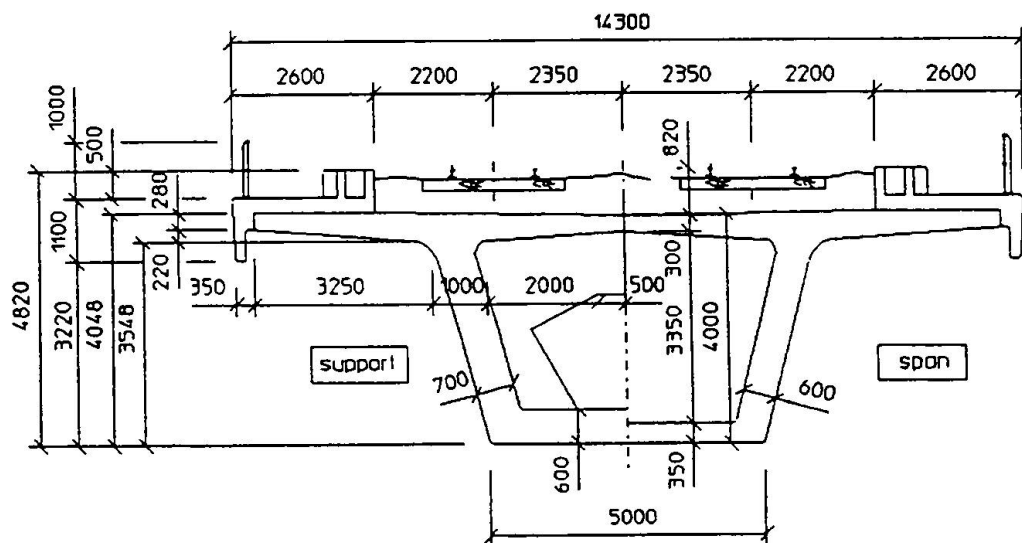
Extreme Traffic Loads on Road Bridges and
Target Values of their Effects for Code Calibration

Anthony R. FLINT
Consultant
Flint & Neill
Partnership
14 Hobart Place
London, UK

Dr. Flint graduated from Imperial College and obtained the degree of PhD at the University of Bristol. Following an early career in structural engineering research and teaching he formed the Partnership in 1958. He has been engaged in design and assessment of large bridges and in the development of Codes of Practice for bridgeworks and of Eurocode 1 part 3.

A graduate of Ecole Polytechnique and Ecole Nationale des Ponts et Chaussées, started work as a research engineer at the SETRA. Since 1982 with the LCPC, first as head of the "Structural Behaviour and Safety" section and now in the Scientific and Technical Division. He has been engaged in the committee preparing the Eurocode 1.3.

Bernard JACOB
Civil Engineer
Laboratoire Central
des Ponts et
Chaussées
Paris, France

Summary

The paper describes some of the preliminary statistical analysis of traffic data from heavily trafficked European highways which led to the derivation of vehicular loading models in Eurocode 1 part 3. The studies indicated reasonable compatibility between extrapolations to extreme loads and load effects using diverse methods despite differences in modelling and assumptions. The dominance of the effects of congested traffic for medium and long spans indicated the need for better data on traffic jam characteristics.

1.   Introduction

The comparison and the calibration of conventional traffic load models proposed for the Eurocode 1 part 3 [1], required a complete set of target values of both axle and vehicular loads, and load effects on representative influence lines and surfaces. A large representative selection of spans and bridge elements was defined providing more than 800 influence lines and surfaces. A complete survey of European traffic data, recorded by Weigh-In-Motion (WIM) systems in D, E, F, I and UK, provided weeks of full traffic measurements vehicle by vehicle over the main motorways and highways [2]. Among these traffic records, the most aggressive for bridges according to the loads an the intensity were selected.

The studies described below primarily made use of comprehensive data from the A6 motorway at Auxerre, collected over a representative week. Those undertaken by different organisations were conducted independently and as a result employed a variety of methods and assumptions [3].

2. Return period and fractile

The occurrence of lorries on a bridge may be described by a stationary time series X_1, X_2, ...,X_n, the ith lorry having a gross weight X_i. It is additionally assumed that one event occurs at each time unit, counted by i, and that the X_i are independent and identically distributed (iid), with a cumulative distribution function (CDF) F. The return period R_x of a specified value x of X_i is defined as :

$$R_x = E[N_x] \text{, where } N_x = \inf \{n / X_1 < x, X_2 < x, ...,X_{n-1} < x, X_n \geq x\}. \tag{1a}$$

It is easy to show that : $R_x = (1 - F(x))^{-1}$, for $F(x) < 1$. (1b)

If the time series is replaced by a stationary time random process $(X_t)_{t \in R+}$, we have :

$$R_x = E[T_x], \text{ where } T_x = \inf \{t / X_u < x, \forall u < t, \text{ and } X_t \geq x\}. \tag{1c}$$

For any $\alpha < 1$, the α-upper fractile x_α of X_t is derived from : $\alpha = 1 - F(x_\alpha)$. (1d)

The maximum $Y_N = \text{Max}_{0 < i \leq N} (X_i)$, if N is the expected number of lorries passing during a reference time period T, representing the expected lifetime of a structure. Because the X_i are iid, the CDF of Y_N is $F(x)^N$. If y_α is the α-upper fractile of Y_N, it is possible to show that for N and $T \to +\infty$:

$$R = R_{y_\alpha} \cong \frac{-T}{Ln(1-\alpha)} \cong \frac{T}{\alpha} \qquad \text{if } 0 < \alpha << 1. \tag{1e}$$

This relationship is independent of the value of y_α and of the density of X. For example, if T=50 years and α=0.05, we get R=975$\cong$1000 yrs.

3.   Extreme Axle and Lorry Loads

The objective was to compute the probability distribution function (PDF), mean value, standard deviation and the single, double and triple axle loads, gross weights and weights per unit length with given return periods, from the experimental histograms of these variables measured over a week and the traffic flow. Three methods were employed :

3.1   Method 1: Half-normal distribution

With this method it was assumed that the upper tails of the distributions of the local extrema of the variables have a Gaussian shape [4]. Half-normal PDF's were fitted to the part of the histogram for $x \geq x_0$, where x_0 is chosen in order to minimise the mean square error in a Henry's diagram.

The standard Gaussian PDF was adopted with a standardised variable z : z = (x - m)/σ , where the mean m and the standard deviation σ were fitted on the Henry's diagram, for $x \geq x_0$. The value with a return period R is given by $x_R = x_0 + \sigma.Z_R$, with Z_R being the α-upper fractile of Z for α=1/2N_τ. N_τ is the total number of events in a histogram for the period R, computed from the total number N_S in the measured histogram by $N_\tau = N_S.R/D$ (D= period of measurement).

3.2   Method 2: Multimodal Gumbel distributions

A bimodal (or a trimodal) Gumbel PDF was fitted to the experimental data [5]; each distribution was obtained by a linear regression on a sub-population of the whole histogram. The conditional PDF of the maximum load of N axles, axles groups or vehicles was computed. The α-upper fractile x_α of these maxima is given by :

$$1 - (1 - p)^N = \alpha \qquad \text{and} \qquad x_\alpha = F_Y^{-1}(\alpha) \tag{2}$$

where p is the proportion of the distribution considered and F_Y the fitted CDF of this distribution.

3.3   Method 3: Multimodal Gaussian distributions

A trimodal Gaussian PDF was fitted by a least mean square method and the α-fractile of this distribution computed [5].

3.4   Method of the asymptotic extreme distributions

As for method 1 it was assumed that the upper tails of the load PDF's have a Gaussian form [6]. The asymptotic distributions of the maxima were derived as Gumbel PDF's with the parameters [7] :

$$a_n = \frac{\sqrt{2Ln(n)}}{\sigma} \qquad \text{and} \qquad u_n = m + \sigma \left(\sqrt{2Ln(n)} - \frac{Ln(Ln(n)) + Ln(4\Pi)}{\sqrt{2Ln(n)}} \right) \tag{3}$$

in which m and σ are the parameters of the normal distribution governing the maximum, and n=p.N, where p is the proportion of this distribution in the whole distribution of the considered load and N the total number of loads. This method provides a full PDF of the maximum instead of only a fractile, and defines explicitly the variation of this maximum with n.

3.5   Comparisons and conclusions

Table 1 shows predictions obtained by the methods for single axle, double axle and triple axle and gross vehicle weights for different return periods. The results show very consistent trends. The biggest differences between the predictions appears not to be due to the methods, but rather to the actual parameters of the distributions used to match the tails of the data histograms.

Methods 2 and 3 give high extreme lorry weight predictions since they are based upon the distribution of the uppermost mode of the best fit curve to the Type 4 vehicle data. Predictions based on the entire data sample become dominated by the large numbers of Type 3 vehicles, whose upper mode has less variance than Type 4. In several cases, the best fitting set of distributions contains one which has a relatively low mode and total proportion, but whose high variance leads to its dominating the extreme values. In these cases only the uppermost mode was used.

R	Item	Method 1	Method 2	Method 3	Method 4
20 weeks	Axle	224 *	226	234	252
	Double	356 *	353	348	332
	Triple	469 *	436	439	442
	Lorry	737 *	711 +	736 +	690
			728 ++	750 ++	
20 years	Axle	236 **	249	249	273
	Double	380 **	394	376	355
	Triple	504 **	459	474	479
	Lorry	782 **	775 +	758 +	736
			819 ++	800 ++	
2000 years	Axle	245 ***	278	264	295
	Double	397 ***	442	403	379
	Triple	527 ***	487	508	517
	Lorry	811 ***	850 +	787 +	782
			925 ++	900 ++	

R = return period, * R=50 weeks   ** R=50 years   *** R=1000 years
Based on distribution for : $^+$ = Type 3 vehicles, $^{++}$ = Type 4 vehicles.

Table 1. Comparison of the Extrapolated Maximum Loads (kN).

4.   Extreme Total Load on a Lane Length

The maxima of the total load (or the uniformly distributed load : UDL) on a lane length were computed by various methods for various lengths from 5 to 200 m, for a return period R. The traffic used was again that in a slow lane of Auxerre.

4.1   Method 1: Half-normal distribution

The method described in 3.1 was applied to the histograms of the local extrema of the total loads. The traffic was randomly generated by the use of its characteristic parameters and measured inter-vehicle spacing, and a Gaussian distribution was fitted on the local extrema histogram, for free traffic (case (a)). Congested traffic with cars (case (b)) and without cars (case (c)) were also considered. In the case (b), the proportion of lorries was taken equal to 25%. In both jam cases (b) and (c), the spacing between vehicles (from axle to axle) was taken as 5 m. It was assumed that 1% of the vehicles would be involved in jams occupying the chosen lane length.

4.2   Method 2 : Monte-Carlo simulation

The Monte-Carlo method was used to create artificially and randomly composed jammed traffic with 5 m inter-vehicle spacing for simulation purposes [8] and the parameters of Gumbel distributions were derived.

The 'garages' used in random generation were derived for Auxerre traffic, with and without cars with eight classes of vehicle each with a derived distribution of gross weight, proportions of weight on each axle and axle spacings.

For each span length, 50 sequences of 1000 simulations were performed, the Gumbel distributions being derived from the maximum values found in each of the 50 simulation sequences. It was assumed that such maxima were annual extremes from 4 traffic jams per working day.

4.3   Method 3 : Analytical modified Poisson model

This model [6] also adopted a bimodal gross weight distribution, with two Gaussian modes, and was applied to flowing traffic with measured vehicle spacings and to congested traffic with and without cars.

The analytical convolution of the flow process and the gross weight distribution led to the expression of the total load density $f_Q(x)$ on lane length L :

$$f_Q(x) = P(N=0)\delta_0 + \Sigma_{n>0} P(N=n) \Sigma_{i=0,..n} C_n^i p^i (1-p)^{n-i} g(m_{ni},\sigma_{ni},x) \qquad (4)$$

where : δ_0 is the Dirac distribution in 0,
             p is the proportion of vehicles in the second mode,
             g is the Gaussian standardised distribution,
             $m_{ni}= i m_1 + (n-i) m_2$ and $\sigma_{ni}^2 = i \sigma_1^2 + (n-i) \sigma_2^2$,
             $m_1, \sigma_1, m_2, \sigma_2$ are the parameters of the two modes of the gross weight
                        distribution.

Flowing traffic flow and vehicle weight distributions were described by a modified Poisson process, in which the lengths of the vehicles (taken constant) were introduced in order to avoid overlapping. The exponential law of the times of arrival was shifted to the right of $\tau_0 = L_0/S$, L_0 (10 m $\leq L_0 \leq$ 15 m) being the mean length of the vehicles plus the minimum spacing and S the mean speed.

This model is briefly defined by :

-       the distribution of the inter-vehicle time intervals :

        $P(\Delta t=t)= \mu e^{-\mu(t-\tau_0)}$, $\mu= \phi / (1-\phi \tau_0)$, with $\phi=$ traffic flow rate,

-       and the deduced cumulative distribution of the total number of vehicles on
        the length L :

        $P(N\leq n)= P(\Sigma_{i=1,...,n+1} \Delta t_i > \tau)$, with $\tau= L/S$.

The α-upper fractile of Q was obtained by solving numerically the equation :

$$1 - F_Q(x) = 1 - (1-\alpha)^{1/N_T} \cong \alpha / N_T \qquad (5)$$

where N_T is the total number of vehicles expected in T ($N_T= \phi T$).

For congested traffic, $f_Q(x)$ becomes a binomial distribution if : $P(N=n)= \delta_{n,k}$, where $k=[L/L_o]$ is the mean number of vehicles on the lane length L, in case of jam.

The number of independent load configurations considered was : $[N'_T/k]$, with N'_T the total number of vehicles involved in a jam on L during T, such that each vehicle belongs only to one configuration.

4.4   Method 4: Simulation and extrapolation from real traffic

Method 3 was also used for providing *extrapolation coefficients* [6] from a reference period T of 1 week to those of 1 month, 1 year, 50 and 500 years. The modified Poisson model gives the 5%-fractiles of the total load Q for different periods T, noted Q(T), and the extrapolation coefficient is defined by : Q(T)/Q(1 week).

The traffic recorded during a week was passed over the influence lines of the total load by the simulation program CASTOR-LCPC [9], and the maximum values obtained for each length L were magnified by the corresponding extrapolation factor for each T or R.

Congested traffic was also simulated by compressing the spacings between measured vehicles (with or without cars), and passing the traffic over the same influence lines. The 5% upper-fractiles of the maximum total loads for the target value calculations were derived, the number of load cases with standing traffic on the lane length taken into account being assumed to represent those which would occur during 100 years.

4.5   Method 5 : Jams simulation program

Another Monte-Carlo simulation program was used to generate traffic jams and to compute bridge load effects [10], based on the Auxerre data. Vehicle weights were modelled by bi- or tri-Gaussian distributions.

Traffic jam rates were based upon UK studies showing breakdown rates of 60 incidents per million vehicle kilometres (I/m veh.km) for HGV, and 30 (I/m veh.km) for light vehicles. The accident rate was 4 I/m veh.km in the simulation, with 26% of accidents blocking more than one traffic lane.

The assumed flow in vehicles per hour above which congestion will occur were :

Blockage	Number of lanes per carriageway			
	1	2	3	4
No blockage	1500	3700	5500	7400
1 lane blocked	0	1300	2700	4300
2 lanes blocked		0	1200	2600

The flow rate was taken to be 1200 vph for 10 hours, 5 days per week, on a two lane carriageway, and vehicle spaces in traffic jams were assumed to be log-normally distributed, with :   mean($\log_e$(space))=0.647, and standard deviation of $\log_e$(space))=0.578.

These data were used to model the build up, passage and depletion of vehicles in queues past obstructions. Vehicle kilometres per incident were found by inverting the incident rate to give the mean separation between successive obstructions during any desired return period for a particular flow rate.

Successive jam location points were chosen, spaced according to the return period and flow rate until the jam initiation point has not arrived at the bridge, the effect of the traffic on the bridge influence line being calculated for each and the maximum in each return period recorded. These maxima were then used to derive extreme value distributions. The 10^{-6} fractile values were taken to have a 2000 years return period.

The program also modelled flowing traffic by using the same vehicle types and flow rates as for jammed traffic using variable inter-vehicle spacing and without light vehicles.

4.6 Comparisons and discussion

The 50 years return maxima for different traffic scenarios calculated by the above methods are illustrated in Figure 1. The congested traffic results dominated for most spans and discrepancies between these for the various methods are mainly due to differences in assumptions concerning vehicle length and spacing and in jam frequency.

Maximum of the total load

(a) flowing traffic, (b) congested traffic with cars, (c) congested traffic without car
m1 = half-normal distribution, m2 = Monte-Carlo simulation, m3 = analytical
Poisson, m4 = simulation + extrapolation by m3, m5 = jam simulation.
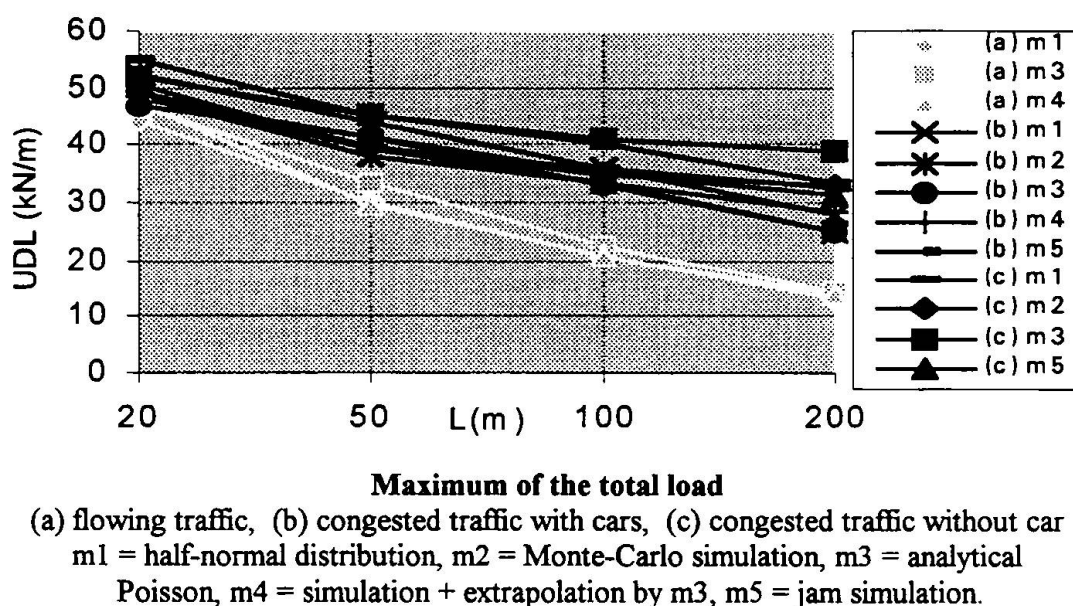
Fig. 1. Comparison of the extrapolation methods for flowing and congested traffic.

5. Extreme Load Effects

Extreme values of bending moments in a simple supported bridge at midspan for various span lengths and bending moments of two continuous bridges (Pont à Mousson and La Nive) were derived by five methods. Methods 1, 2, 4 and 5 were broadly as described in 4. above applied to the relevant influence lines.

Method 3 was based on the crude assumption that the load effect is a Gaussian stationary process X(t). For this Rice's formula gives the level crossing distribution, with the Gaussian density :

$$p(x) = \frac{1}{2\Pi} \frac{\sigma_{\dot{x}}}{\sigma_x} \exp\left(-\frac{(x-\bar{x})^2}{2\sigma_x^2}\right) = k . \exp \exp\left(-\frac{(x-m)^2}{2\sigma^2}\right)$$ (6)

k, m and σ are fitted on the level crossing histogram of the load effect computed by simulation (CASTOR-LCPC) for a traffic record over a time period τ. Then for a reference period T and an α-upper fractile : p(a)= ατ/T , which gives :

$$a = m \pm \sigma\sqrt{2\ln(kT / a\tau)}$$ (+ if a>0, - if a<0).   (7)

Table 2 shows results for the continuous bridges, by methods 1 and 3 for flowing traffic and by methods 4 and 5 for congested traffic. Figure 2 illustrates the results for simply supported spans for 50 years return values.

Bridge	Moment	Flowing traffic		Congested traffic	
		Method 1	Method 3	Method 4	Method 5
Pont à Mousson	positive	9740	9800	10460	11037
	negative	-3060	-3960	-3954	-3540
La Nive	positive	-	46.6	43.3	47.9
	negative	-	-42.0	-27.4	-28.1

Table 2. Comparison of the 5%-fractiles of the extreme bending moment of real bridges (kN.m).
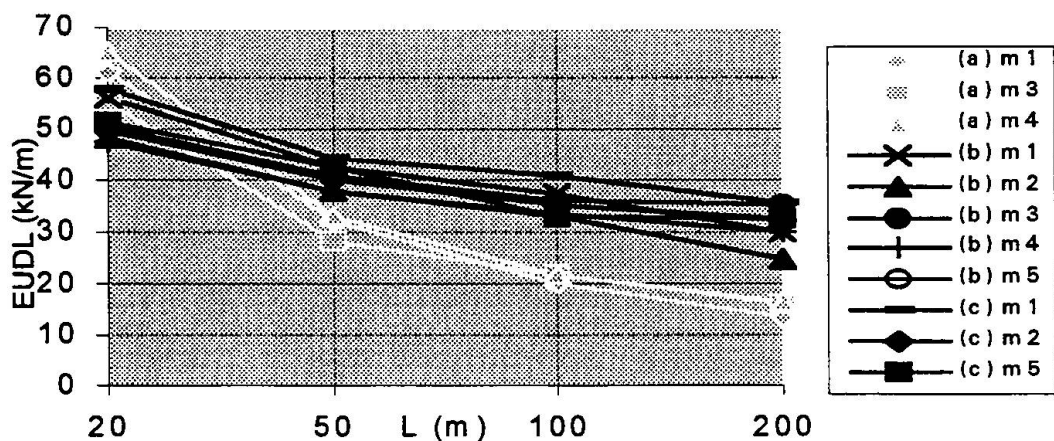
Maximum of the simply supported span bending moment
(a) flowing traffic, (b) congested traffic with cars, (c) congested traffic
m1 = half normal distribution, m2 = Monte-Carlo simulation, m3'= Rice's formula, m4 = simulation + extrapolation by Poisson, m5 = jam simulation.

Fig. 2. Comparison of the extrapolation methods for flowing and congested traffic.

6.   Conclusions

The results obtained by the different extrapolation methods were generally in reasonably close agreement. Having in mind that the return periods for the characteristic values of loads and load effects are far in excess of the period of records used, it was concluded that any of the methods could be applied. Those described in 3.4 and 4.3 were used in European traffic samples and 800 influence surfaces to provide target values for calibration of candidate loading models for the Eurocode 1 part 3. It was evident that the congested traffic scenarios dominate the maxima for loaded lengths in excess 50 m. However in the subsequent development of the loading model dynamic magnifiers were applied to the flowing traffic effects for the lower lengths and this altered the transition.

Acknowledgements

References

[1] Eurocode 1 part 3, *Traffic loads on road bridges - Assessment of various load models*, draft July 1994, revised May 1995, 82 p.

[2] Jacob B. and al., *Traffic data of the European countries*, Report of the WG 2, Eurocode 1 part 3, March 1989.

[3] Jacob B. and al., *Methods for the Prediction of Extreme Loads and Load Effects on Bridges*, Report of the WG 8, Eurocode 1 part 3, August 1991.

Jacob B., Maillard J.B., *Probabilistic Extrapolations and Maximum Load Effect Prediction for Bridge Code Calibration*, Proceedings of ICASP'6, Mexico, 1991, pp. 865-71.

[4] Bruls A., *Détermination des actions pour le calcul des ponts-routes*, IABSE Colloquium on Fatigue of Steel and Concrete Structures, Lausanne, 1982.

[5] Flint & Neill Partnership, *Vehicular Bridge Loading*, Report on Preliminary Study of Vehicle Weight Records taken at Auxerre (France, highway A6 1986), n°72-0004 Issue A, 21st September 1989.

[6] Jacob B., Maillard J.B., Gorse J.F., *Probabilistic Traffic Load Model and Extreme Loads on a Bridge*, ICOSSAR'89 Proceedings, San Francisco, 1989.

[7] Cramer H., *Mathematical Methods of Statistics*, Princeton University Press, 1946.

[8] Bez R., *Modélisation des charges dues au trafic routier*, Thèse n°793, EPFL Lausanne 1989.

[9] Eymard R., Jacob B., *Un nouveau logiciel : le programme CASTOR pour le Calcul des Actions et des Sollicitations du Trafic dans les Ouvrages Routiers*, Bull. liaison des LPC, n°164, pp 64-77, novembre-décembre 1989.

[10] Flint & Neill Partnership, *Interim Design Standard - Long Span Bridge Loading*, TRRL, Contractor Report 16, 1989.

Leere Seite

Blank page

Page vide

Calibration of bridge fatigue loads
under real traffic conditions

Bernard JACOB
Civil Engineer
Laboratoire Central
des Ponts et
Chaussées
Paris, France

A graduate of Ecole
Polytechnique and
Ecole Nationale des
Ponts et Chaussées,
started work as a
research engineer at the
SETRA. Since 1982
with the LCPC, first as
head of the "Structural
Behaviour and Safety"
section and now in the
Scientific and Technical
Division.

A graduate of Ecole
Polytechnique and
Ecole Nationale des
Ponts et Chaussées,
started work as a
research engineer at the
SETRA. Now vice-head
of the Large Bridge
Division at the SETRA.

Thierry KRETZ
Civil Engineer
Service Technique
des Routes et
Autoroutes
Paris, France

Summary

This paper explains how the conventional fatigue load model n°3 of the Eurocode 1.3 is calibrated versus real measured traffic loads, by comparison of their respective load effects and fatigue damages on an extensive sample of influence surfaces of representative bridges. The calibration procedure is developed for one slow traffic lane and then for several slow traffic lanes. The final calibration and application rules of the Eurocode model are presented, with respect of most relevant parameters to be taken into account.

1. Conventional Fatigue Load Models

The Eurocode 1 part 3 [1] contains conventional load models for the assessment of characteristic values of loads. A special chapter of this document deals with the fatigue loads, to be used for fatigue checking of sensitive details in bridges. In the most recent existing national codes [2,3,4] or in specific recommendations as it is the case in France [5,6,7], similar or simpler fatigue load models were already elaborated; but the calibration of some of these models were not based on rigorous scientific bases. The expert panel of the Eurocode 1.3 worked for 3 years (1988-90) and collected the up-to-date knowledge and tools to elaborate and calibrate the proposed fatigue load models. Further works [5,8] were then carried out in France by the LCPC and the SETRA to complete and make more operational this common work and to prepare the final draft of the document.

The fatigue load models proposed in [1] are mainly devoted to the steel bridges or the steel parts of the composite bridges, which are the most sensitive to fatigue. Five models are defined, n°1 to 5, for various purposes. Models 1 and 2 are a bit « pessimistic » and allow some quick and simple checking to identify the details exposed to fatigue damage. Model 3 is a standard model to be used for most common checking, and will be described in detail in this paper. Models 4 and 5 are more sophisticated and allow full damage calculation using the Palmgreen-Miner law and the S-N resistance curves. Model 4 consists in a set of five lorries

(as model 2), but with different axle loads; the proportion of each lorry type depends on the traffic characteristics of the considered road. Model 5, which may only be used if specified in the project requirements, uses a full traffic record, e.g. a sample of many thousands of lorries weighed in motion on a road, and applied by a specific computer software (such as CASTOR-LCPC [9]) on the influence surfaces of the bridge to assess the stress variations and then to compute the fatigue damage. Extrapolation may be carried out to investigate deeper the issue of the structural lifetime.

Model 3 consists of 4 axles, each of them loaded at 120 kN, and grouped in two tandem as shown in figure 1.
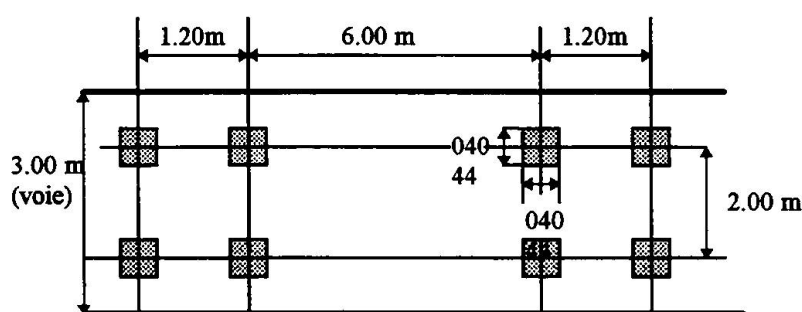
Fig. 1. Model 3 for fatigue load (Eurocode 1.3).

2. Calibration for one traffic lane

The procedure is the same than that used in the French recommendations, described in [5,6]. Only one stress cycle is considered for a given detail during the lorry crossing. Its amplitude is the maximal stress variation. The lorry mass is then calibrated to produce the same damage after 2 millions of crossings as the damage of one hundred years of real traffic. The traffic damage for the detail considered is computed by the CASTOR-LCPC software [9], from any traffic record of the existing LCPC's database « PESAGE » [10]. The detail is represented by an influence surface or two influence lines (one longitudinal and one transversal). The « rain-flow » histogram of the stress variations is computed and used for the damage or lifetime calculation with the Miner law and the relevant S-N curve.

Nine composite bridges with main span lengths from 20 to 102 m have been selected as representative of the existing bridges. The span widths are between 5.5 and 16 m. 64 details have been analysed, sensitive to the longitudinal bending moment. Two traffics were applied, recorded on the A6 motorway near Auxerre (one of the most aggressive in Europe) and on the National road RN23 near Angers. All the details were assumed to be in class 36, in a conservative way and to obtain a more accurate calibration. The S-N curve with two slopes and a truncating at 10^8 cycles was used.

The number of crossings of the 4-axle lorry (model 3), loaded at 30 t to get stress amplitudes in the same range as with the real traffics - e.g. in the slope -1/5 of the S-N curve -, providing a damage equal to 1 was computed for each detail. A graph plotting the results is shown in the figure 2. Each point corresponds to a detail, with the abscissa x equal to the logarithm of the lifetime (in years) computed by CASTOR-LCPC and the ordinate y equal to the logarithm of

the number of crossings (in millions) of the lorry. The damage is 1 after y millions of crossings. A linear regression is made on the points and the accuracy of the simple calibration is evaluated by the correlation coefficient (1 in the ideal case). The correlation coefficient is 0.97 with the A6 traffic and 0.954 with the RN23 traffic. The acceptable number of lorry crossings N_{100} (in millions) for an expected lifetime of 100 years is the ordinate of the regression strait line at x=2 (100 years), increased by one standard deviation.

The next step replaces this criteria on the number of crossings by a weighing coefficient c on the lorry mass. The number of crossings is fixed at 2.10^6 and the lorry mass is 4 x 120 kN (model 3). The coefficient c is derived from another coefficient c_{30} applied to the 30 t lorry to give the same damage, after 100 years or 10^8 crossings, than the real traffic:

$$c = c_{30} \times \frac{30 \times 9.81}{4 \times 120} \times \left(\frac{100}{5}\right)^{\frac{1}{5}} \times \left(\frac{5}{2}\right)^{\frac{1}{3}} = 1.515 \times c_{30} \tag{1}$$

with : $N_{100} \times \Delta\sigma_{30}^5 = 10^8 \times (c_{30} \times \Delta\sigma_{30})^5$

and $\Delta\sigma_{30}$ is the stress amplitude induced by the 30 t lorry.

Finally the coefficient c is 2.20 for the A6 traffic (heavily trafficked motorway) and 1.40 for the RN23 (national road). The average coefficient c=1.80 is taken into account for a heavily trafficked road or an average trafficked motorway.
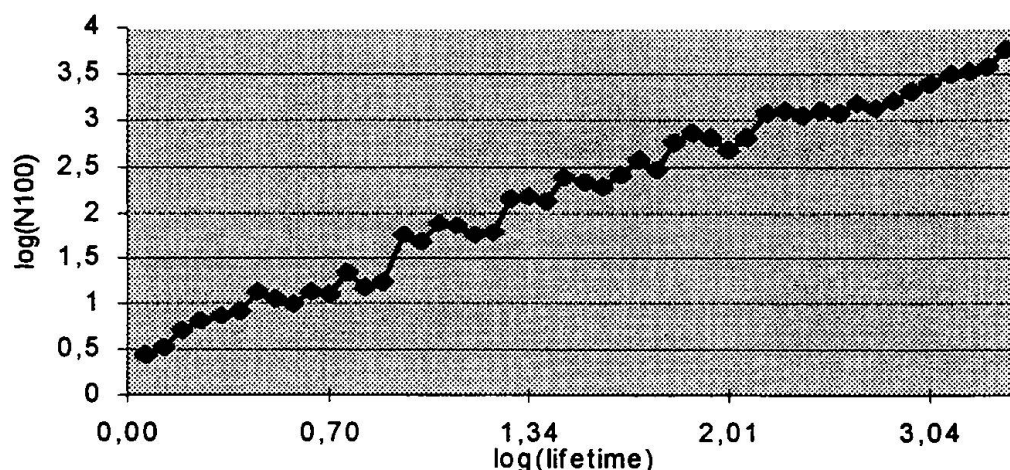
Fig. 2. Calibration of model n°3: number of millions of crossing versus lifetime (in log)

3.   Calibration for several slow traffic lanes

Generally a bridge supports at least two slow traffic lanes heavily loaded. The effects of all theses slow lanes must then be added for fatigue assessment. A procedure was proposed in [8]. We briefly present the case of two slow lanes in opposite directions.

The total damage D may be written, because of the linearity of the Miner's law, as:

$D = D_1 + D_2 + D_3$, where indices 1 and 2 correspond to the lane 1 or 2 only loaded, and indices 3 corresponds to both lanes loaded (vehicles passing each other).

In most bridge details, the stress cycle amplitudes under real traffic are in the area of the S-N curve with a slope $-1/5$. Then the damages may be written:

$$D_i = \alpha \ (1 - p/100) \ \Delta\sigma_i^5 \quad \text{for i=1 or 2, and} \quad D_3 = \alpha \ p \ (\Delta\sigma_1 + \Delta\sigma_2)^5/100 \tag{2}$$

where $\Delta\sigma_i$ is the stress cycle amplitude when the lorry crosses on lane i, and p is the percentage of « equivalent passing cases ».

From Eq. 2, and assuming that p/100 is rather small, we get at the first order:

$$p \approx 100 \ (D - D_1 - D_2)/(\ D_1^{1/5} + D_2^{1/5})^5 \tag{3}$$

and the total damage becomes:

$$D = \alpha \left((1 - \frac{p}{100}).\Delta\sigma_1^5 + (1 - \frac{p}{100}).\Delta\sigma_2^5 + \frac{p}{100}(\Delta\sigma_1 + \Delta\sigma_2)^5 \right) = \alpha \ \Delta\sigma_{tot}^5 \tag{4a}$$

with :

$$\Delta\sigma_{tot} = \left((1 - \frac{p}{100}).\Delta\sigma_1^5 + (1 - \frac{p}{100}).\Delta\sigma_2^5 + \frac{p}{100}(\Delta\sigma_1 + \Delta\sigma_2)^5 \right)^{\frac{1}{5}} \tag{4b}$$

Eq.4a and 4b include the percentage of « equivalent passing cases » p, which depends on two main parameters: the length of the influence line and the traffic density. p will be calculated in the following section.

4. Sensitivity to the influence line

4.1 Simple supported span

4.1.1 Mathematical Model
We will calculate theoretically the percentage p, for a box girder simple supported span of length L, with two slow traffic lanes in opposite directions. In this case, the transverse influence line is constant (equal to 1) and the longitudinal influence line is triangular. Then the effect of vehicle passing may be significant.

An simple idealised traffic model is built for our purpose, with the following assumptions, and the results were validated with real traffic records and the CASTOR-LCPC software:
- all the lorries are identical, with a mass P concentrated,
- all the lorries are at uniform spacing and travelling at constant speed v,
- all the passing situations have the same probability of occurrence,
- the traffic characteristics are the same in both directions.

q is the traffic density on one lane (in veh/sec). If a lorry enters the span in direction 1 at time t_1, and takes $T = L/v$ to cross the span, we have a passing case if another lorry travelling in direction 2 enters the span at t_2, with $t_1 - T/2 < t_2 < t + T/2$. The figure 3 indicates the stress cycle amplitude $\Delta\sigma_{max}$ in this passing case, with respect of the time interval $(t_2 - t_1)$:
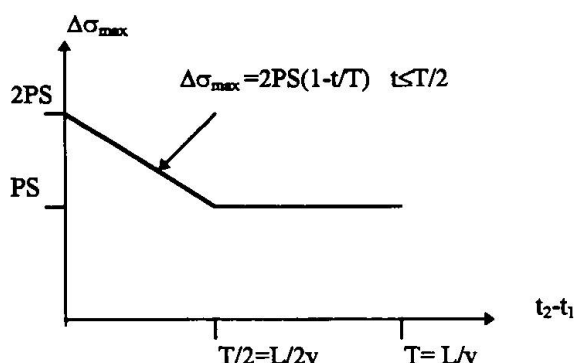
Fig. 3. Stress cycle amplitude for a passing case.

Then the damage due to a passing case is, per second:

$$D_3 = \alpha \times 2q \int_0^{\frac{T}{2}} \left(2PS \times \left(1 - \frac{t}{T}\right)\right)^5 \times q\, dt$$

$$D_3 = \alpha \times 2q \times q \times (2PS)^5 \times \frac{T}{6}\left[1 - \left(1 - \frac{1}{2}\right)^6\right] = \alpha \times q \times (2PS)^5 \times \frac{63}{64}\frac{qT}{3} \tag{5}$$

and the percentage p is given by:

$$\frac{p}{100} = \frac{63}{64}\frac{qT}{3} = \frac{63}{64}\frac{q \times L}{3v} \tag{6}$$

and p is proportional to the span length L and the traffic density q.
For example, with the realistic data:
v=20 m/sec, L=60 m, q=10^8 veh/100 yrs = 0.0317 veh/sec, we have : p = 3.1%. An exact calculation with the A6 traffic by CASTOR-LCPC gives p = 2.3% (see 4.1.2).

4.1.2   Calibration with CASTOR-LCPC

With this software and the data of the A6 traffic recorded on all the four traffic lanes during one week in 1986 (we only use here the slow lanes 1 and 4), the damages D_1, D_2 and D are calculated for simple supported spans of various lengths from 3 to 132 m (neglecting the calibration factor α mentioned above). Eq.3 gives the percentages p for each L, and the very good proportionality is shown on figure 4, with an empirical linear relation:

$$p = 0.7 + 0.027\,L \tag{7}$$

which is adopted for a heavily trafficked motorway;
with the RN23 traffic, Eq.7 is slightly modified into :

$$p = 0.5 + 0.012\,L \tag{7a}$$

which is adopted for a common highway;
finally for a heavily trafficked highway or a common motorway, an intermediate relation is:

$$p = 0.6 + 0.020\,L \tag{7b}$$
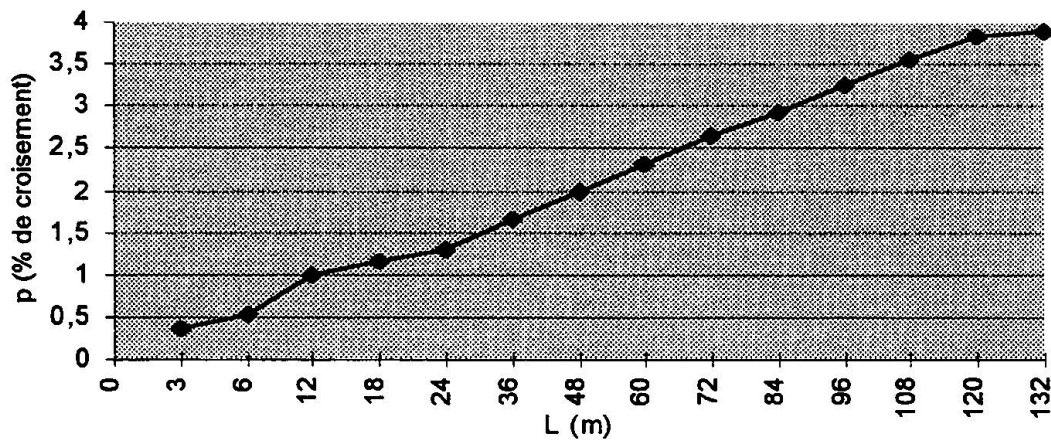
Fig. 4. Variation of p with L (CASTOR-LCPC, traffic A6).

4.1.3   Consequence of the passing cases

In our case the lorry induces the same stress amplitude if travelling on each lane, then the total stress amplitude for two independent crossings (on each lane) is:

$$\Delta\sigma_{tot} = \left(\Delta\sigma_1^5 + \Delta\sigma_2^5\right)^{1/5} = \left(\Delta\sigma_1^5 + \Delta\sigma_1^5\right)^{1/5} = 2^{1/5} \Delta\sigma_1 = 1{,}1487 \ \Delta\sigma_1 \tag{8a}$$

but for a passing case, with L=60 m and p=2.32 :

$$\Delta\sigma_{tot} = \left(\left(1-\frac{p}{100}\right)\Delta\sigma_1^5 + \left(1-\frac{p}{100}\right)\Delta\sigma_2^5 + \frac{p}{100}\left(\Delta\sigma_1 + \Delta\sigma_2\right)^5\right)^{\frac{1}{5}}$$

$$\Delta\sigma_{tot} = \left(2\Delta\sigma_1^5 + \frac{30p}{100}\Delta\sigma_1^5\right)^{\frac{1}{5}} = \left(2{,}696\right)^{1/5} \Delta\sigma_1 = 1{,}22\Delta\sigma_1 \tag{8b}$$

Then the passing case induces an increase of 6% in the total stress amplitude, or an increase of more than 30% in the damage.

4.1.4   Checking the calibration of the fatigue load model

The damage calculations for these triangular influence lines of various lengths also allowed the calibration of the weighing coefficients c_{30} and c applied to the conventional lorry mass (Eq.1). With the same notations as in section 2, if D_1 is the damage computed (neglecting the coefficient α) by CASTOR-LCPC under the traffic loads of the lane 1 of the A6 motorway, during a period T (in years), e.g. the sum of the stress cycle amplitudes to the power 5, then we have:

$$D_1 = \frac{T}{100} \times 10^8 \times \left(c_{30} \times \Delta\sigma_{30}\right)^5 \quad \Rightarrow \quad c_{30} = \frac{D_1^{1/5}}{\Delta\sigma_{30}} \times \left(\frac{10^{-6}}{T}\right)^{\frac{1}{5}} \tag{9}$$

and c is obtained by the Eq.1.

For the triangular influence lines (with a peak value of 2.5 t/m²), from L=3 m to 132 m, the coefficient c remains very constant around 2.40, with a minimum at 2.32 and a maximum at 2.64. It proves that the conventional lorry, properly calibrated, gives a good picture of the real traffic, independent of the span length. The gap of 8% with the announced value c=2.20 is due

to the fact that the truncating threshold of the S-N curve was neglected here. Nevertheless, the values for the short spans (under 35 m) are slightly higher than the average. This phenomenon shows that the lorry is not aggressive enough for the short influence lines for two reasons:
- the counting method underestimate the number of cycles for influence lines shorter than the lorry length; in such a case it would be necessary to consider one cycle for each axle group, e.g. two cycles per lorry;
- the lorry silhouette is not representative of the real heavy vehicles.

Therefore an amplification coefficient λ was introduced for the short influence lines (0.5 to 40 m), defined by: $\lambda = \dfrac{c}{2.40}$, where the values of c were calculated for all the values of L, by steps of 0.5, 1 and 2 m. Figure 5 shows the variations of λ with L. An analytical approximation was found for λ as a function of L:

$$L \le 3{,}0\,m \qquad \lambda = 1{,}20$$
$$3{,}0\text{ m} < L \le 15\,m \qquad \lambda = 1 + \frac{(L-9)^2}{300} \tag{10}$$
$$5\text{ m} < L \le 35\,m \qquad \lambda = 1{,}21 - \frac{6 \times L}{1000}$$

For L under 2.40 m, the lorry axles act individually on the span, and therefore the coefficient of 1.20 correspond to 2.5 cycles per crossing.
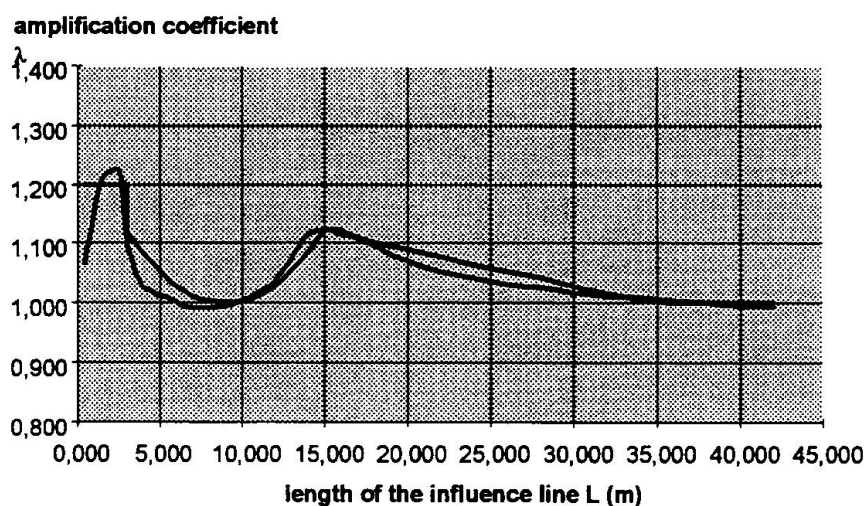
Fig. 5. Amplification coefficient λ for short influence lines (calculated and approx. Eq.10).

4.2   Bridge influence lines

Eq.7 for the calculation of p as a function of L is now simply extended to any type of influence line for real bridges. This rule is tested for 6 existing multiple-span (2 to 5) bridges and 3 to 5 sections per bridge. The span lengths are between 24 and 102 m.

In Eq.7, the length L is now replaced by L_{cal} defined by:
- the span length if the considered section is not on a pier,
- the sum of the two adjacent span lengths if the section is on a pier.

Using these values L_{cal} for each section in Eq.7, p_{cal} are obtained and compared to the p_{ex} directly calculated by CASTOR-LCPC and the real traffic. The fit between both is good as shown in the figure 6, with only one case of underestimation (-0.8% for L_{cal}=79 m) on the unsafe side, and a maximum overestimation of 1.94% for the largest L_{cal} on the safe side. The errors made on $\Delta\sigma_{tot}$ are respectively -1.7% and +3.6%, which justify the simple rule proposed.
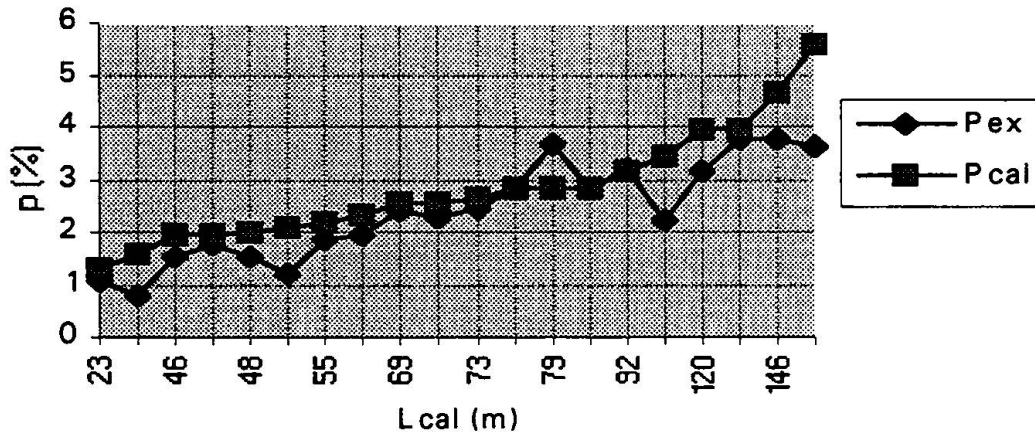
Fig. 6. Comparison of the exact and calculated (Eq.7) values of p for real bridges.

5. Final calibration of the fatigue model (EC 1.3)

The model 3 (lorry) for fatigue of the Eurocode 3.1 given in figure 1 is finally calibrated by a load coefficient λ_e such as 2.10^6 crossings of this calibrated lorry induce the same damage than the real traffic during the reference period of 100 years. λ_e accounts for various parameters related to the traffic and bridge characteristics, and is written as:

$$\lambda_e = \lambda_1 . \lambda_2 . \lambda_3 . \lambda_4 \tag{11}$$

where λ_1 accounts for the influence line length and is given by Eq.10,

                 λ_2 accounts for the traffic volume and content,

                 λ_3 accounts for the expected bridge lifetime,

                 λ_4 accounts for the effect of several traffic lanes.

$\lambda_2 = 2.20$ for a heavily trafficked motorway (such as A6 near Auxerre),

$\lambda_2 = 1.80$ for a common motorway or a heavily trafficked highway,

$\lambda_2 = 1.40$ for a common highway (such as RN23 near Angers);

$\lambda_3 = (DV/100)^{1/5}$ if DV is the expected bridge lifetime (in years);

Finally, for two slow traffic lanes (but this may be generalised), λ_4 is given by:

$$\lambda_4 = \left[\left(1 - \frac{p}{100}\right) + (1 - \frac{p}{100})\left(\frac{\Delta\sigma_2}{\Delta\sigma_1}\right)^5 + \frac{p}{100}\left(1 + \frac{\Delta\sigma_2}{\Delta\sigma_1}\right)^5 \right]^{\frac{1}{5}} \tag{12}$$

where p is calculated from Eq.7, 7a or 7b, in which L is the value L_{cal} defined in 4.2.

In conclusion, operational rules are given which allow a unique and simple conventional fatigue load model to be applied, after calibration by the proposed factors, to any type of bridge and detail, and to be adapted to various traffic conditions and expected lifetimes.

References

[1] Eurocode 1 part 3, *Traffic loads on road bridges - Assessment of various load models*, draft July 1994, revised May 1995, 82 p.

[2] BS 5400 Part 2, Steel, Concrete and Composite Bridges - IRLS: *Interim Revised Loading System*, London, British Standards Institution, 1986.

[3] DIN 1072, *Strassen- und Wegbrücken - Lastannahmen*, Berlin, Beuth Verlag, 1985.

[4] SIA 160, *Actions sur les structures porteuses*, Zürich, Société suisse des ingénieurs et des architectes, 1989.

[5] Kretz T., Jacob B., *Convoi de fatigue pour les ponts routes mixtes*, Revue Construction Métallique, n°1, 1991.

[6] Kretz T., Raoul J., *Vérification à la fatigue des ponts routes en ossature mixte*, Bull. Ouvrages d'art n°15, SETRA, 1993.

[7] METT, SETRA, CTICM, SNCF, *Ponts métalliques et mixtes - Résistance à la fatigue - Guide de conception et de justification*, to be published in 1996.

[8] Kretz T., *Convoi de fatigue sur ouvrages métalliques. Etude des croisements et d'autres effets secondaires*, Revue Construction Métallique, n°3, 1995.

[9] Eymard R., Jacob B., *Le logiciel CASTOR-LCPC pour le Calcul des Actions et Sollicitations du Trafic sur les Ouvrages Routiers*, Bull. liaison des LPC, n°164, pp. 64-77, 1989.

[10] Crémona C., Jacob B., *Une base de données d'enregistrements de trafics: un outil d'aide à la conception et à la gestion des ouvrages routiers*, Pre-Proceedings of the 1st European Conference on WIM, Zürich, pp. 379-86, March 1995.

Leere Seite

Blank page

Page vide

Vehicle interactions and fatigue assessment of bridges

Pietro CROCE
Dr. Engineer, Researcher
University of Pisa
Pisa, Italy

Pietro Croce, born in 1957, got PhD
degree in 1989. He is Researcher at the
Department of Structural Engineering
of the University of Pisa. He has been
member as invited expert of the PT6
for the preparation of ENV 1991 - 3.
At present, he is involved in several
research works concerning bridges,
fatigue and structural reliability.

Summary

Fatigue damage of bridge details is often increased in consequence of vehicle interactions. The paper deals in a very general way with the problem of vehicle interactions. Interactions due to simultaneity are solved in the framework of the queueing theory, while time independent interactions are taken into account on the basis of rainflow or reservoir method concepts. Two numerical examples illustrate the practical application of the procedure.

1.   Introduction

The fatigue assessment of bridges requires the knowledge, for each detail sensitive to fatigue, of the stress history $\sigma(t)$, representing the relationship between the time t and the stress σ induced by the vehicles crossing the bridge.

In ENV 1991 - 3 [1] five fatigue load models are given: models 1 and 2 are intended to be used whether the fatigue life is unlimited and constant stress amplitude fatigue limit is given, models 3 and 4 are intended to be used for fatigue life assessment with reference to S-N curves given in design Eurocodes, while model 5, using actual traffic data, is the most general one.

In general, for fatigue verifications, fatigue model 2 gives more accurate results than fatigue model 1 as well as fatigue model 4 gives more accurate results than fatigue model 3, provided that the simultaneous presence of several lorries on the bridge can be neglected. On the contrary, when the interaction of several lorries is relevant, fatigue models 2, 3 and 4, and, if the recorded data refer only to individual vehicles, fatigue model 5 as well, can be used only if supplemented by additional data. Clearly, the field of application of these fatigue models could be sensibly enlarged through the definition of general methods allowing to take into account the simultaneous presence of several vehicles on the same lane and/or on several lanes.

In the present paper the interaction between several vehicles is solved theoretically in the framework of the queueing theory, considering the bridge as a service system, with or without waiting queue, and the stochastic processes as Markov processes, so that the number of lorries crossing the bridge simultaneously can be determined.

The case of several vehicles simultaneously present on the same lane is solved first, considering the bridge as a single channel system with waiting queue, in which the waiting time, depending on the number of requests in queue, and the number of requests in queue itself are limited; subsequently, the case of vehicles simultaneously present in several lanes is solved in an

analogous way considering the bridge as a multiple channel system without waiting queue. Applying these procedures, a modified load spectrum, lonely vehicles spectrum, depending on traffic flow and on dimensions of the influence surface is obtained, whose members are single vehicles and vehicle convoys travelling alone, in such a way that the complete stress history can be considered as a random assembly of the individual stress histories induced by each member of this load spectrum. Finally, a general procedure for the evaluation of the stress spectrum is given, starting from the individual stress histories and using the reservoir or the rainflow method, taking into account the possibility that maximum and minimum stresses are induced by different individual members of the load spectrum.

Two numerical examples show the practical application of the method.

2.   Simultaneous transit of several lorries

Let the load spectrum consisting in a set of q types of lorries and be N_{ij} the annual flow of the i-th vehicle of the on the j-th lane. The total flow on the j-th lane is then $N_j = \sum_{i=1}^{q} N_{ij}$.

When the characteristic length L of the influence line increases, the simultaneous presence of several lorries on the same and/or in several lanes must be taken into account. Under the hypotheses that the vehicle flow follows a Poisson distribution and that the transit time Θ on L is exponentially distributed, the stochastic processes can be represented as Markov processes [2], the bridge can be then considered as a service system and the problem of the simultaneous transit of several lorries can be solved applying of the queueing theory [3], [4].

2.1.   Simultaneous transit of lorries on the same lane

In order to evaluate the probability P_n that n lorries are simultaneously travelling on L, the bridge can be considered as a single channel system with waiting queue, in which the waiting time, depending on the number of requests in queue, and the number of the request in the queue itself are limited. In fact, because there is a minimum value for the time interval T_s between two consecutive lorries, the waiting time for the i-th vehicle in queue is given by

$T_i = \Theta - i \cdot T_s$ and the number of requests in queue is limited to $w = int\left(\Theta \cdot T_s^{-1}\right) - 1$.

Under the assumption that each T_i is distributed with an exponential law whose parameter is $\varphi_i = T_i^{-1}$, the problem can be solved in a closed form (see [3] and [4]). The probability P_n to have n vehicles on the lane, i.e. n-1 requests in queue, is then given by

$$P_n = \left(\frac{\delta}{\alpha}\right)^n \cdot \left\{1 + \frac{\delta}{\alpha} + \sum_{i=2}^{w}\left[\delta^i \cdot \left(\alpha \cdot \prod_{s=1}^{i-1}\left(\alpha + \sum_{j=1}^{s}\varphi_j\right)\right)^{-1}\right]\right\}^{-1} \text{, for n=0, 1, or by}$$

$$P_n = \left\{\frac{\delta^n}{\alpha} \cdot \left[\prod_{s=1}^{n-1}\left(\alpha + \sum_{j=1}^{s}\varphi_j\right)\right]^{-1}\right\} \cdot \left\{1 + \frac{\delta}{\alpha} + \sum_{i=2}^{w}\left[\delta^i \cdot \left(\alpha \cdot \prod_{s=1}^{i-1}\left(\alpha + \sum_{j=1}^{s}\varphi_j\right)\right)^{-1}\right]\right\}^{-1} \text{, for 2≤n≤w,}$$

where δ represents the lorry flow density and $\alpha = \Theta^{-1}$. The annual number of interactions between n vehicles $i_1, .., i_n$ on the j-th lane can be then obtained substituting these formulae in

the general expression $N_{(i_1, i_2, \ldots, i_n), j} = \dfrac{P_n}{1 - P_0} \cdot \dfrac{N_j}{n} \cdot \dfrac{\prod\limits_{k=1}^{n} N_{i_k j}}{\sum\limits_{q^n} \left(\prod\limits_{s=1}^{n} N_{i_{t_s} j} \right)}$, where $\sum\limits_{q^n}$ indicates the

sum over all the possible choices with repetitions of n elements between a collection of q.

In the practice, the problem is reduced to the simultaneous presence of two lorries r and t, so

that it is $P_0 = \left[1 + \dfrac{\delta}{\alpha} \cdot \left(1 + \dfrac{\delta}{\alpha + \varphi_1} \right) \right]^{-1}$, $P_2 = \dfrac{\delta^2}{\alpha \cdot (\alpha + \varphi_1)} \cdot \left[1 + \dfrac{\delta}{\alpha} \cdot \left(1 + \dfrac{\delta}{\alpha + \varphi_1} \right) \right]^{-1}$ and the

annual number of interactions results $N_{(r, t), j} = \dfrac{N_{rj} \cdot N_{tj} \cdot \delta}{(\delta + \alpha + \varphi_1) \cdot \sum\limits_{q^2} \left(\prod\limits_{s=1}^{2} N_{i_{t_s} j} \right)} \cdot \dfrac{N_j}{2}$. When a

single vehicle model is given this formula simplifies further in $N_{(1, 1), j} = \dfrac{N_j \cdot \delta}{2 \cdot (\delta + \alpha + \varphi_1)}$.

2.2. Simultaneous transit of lorries on several lanes

Under the aforesaid hypotheses, the simultaneous transit of lorries on several lanes can be solved in an analogous way considering the bridge as a multiple channel system without waiting queue where new requests are refused if all channels are occupied. The probability P_k to have simultaneously vehicles on k lanes, i.e. k occupied channels, can be then obtained

solving a system of the Erlang type [3], [4], [5] so that it is $P_k = \dfrac{\mu^k}{\alpha^k \cdot k!} \cdot \left(\sum\limits_{i=0}^{m} \dfrac{\mu^i}{\alpha^i \cdot i!} \right)^{-1}$,

$0 \leq k \leq m$, being μ the density of the total flow N^* and $\alpha = \Theta^{-1}$. Substituting in the general

formula $N_{i_1 h_1, i_2 h_2, \ldots, i_k h_k} = \dfrac{P_k}{1 - P_0} \cdot \left(\prod\limits_{j=1}^{k} \dfrac{N_{i_j h_j}}{N_{h_j}} \right) \cdot \dfrac{N^*}{k} \cdot \dfrac{\prod\limits_{j=1}^{k} N_{h_j}}{\sum\limits_{\binom{m}{k}} \left(\prod\limits_{s=1}^{k} N_{h_{t_s}} \right)}$, where $\sum\limits_{\binom{m}{k}}$ is the

sum over all the possible choices of k elements between a collection of m, it is possible to derive the annual number of interactions of k lorries, i_1 on the h_1-th lane, ..., i_k on the h_k-th

lane, $N_{i_1 h_1, i_2 h_2, \ldots, i_k h_k} = \dfrac{\dfrac{\mu^k}{\alpha^k \cdot k!}}{\sum\limits_{j=1}^{m} \dfrac{\mu^j}{\alpha^j \cdot j!}} \cdot \left(\prod\limits_{j=1}^{k} \dfrac{N_{i_j h_j}}{N_{h_j}} \right) \cdot \dfrac{N^*}{k} \cdot \dfrac{\prod\limits_{j=1}^{k} N_{h_j}}{\sum\limits_{\binom{m}{k}} \left(\prod\limits_{s=1}^{k} N_{h_{t_s}} \right)}$. As said before, often

only the case of two lorries r and t simultaneously present on h-th and j-th lanes is relevant, so

that it is $P_2 = \dfrac{\mu^2}{2 \cdot \alpha^2} \cdot \left(\sum\limits_{i=0}^{2} \dfrac{\mu^i}{\alpha^i \cdot i!} \right)^{-1}$ and $N_{r h, t j} = \dfrac{N_{rh} \cdot N_{tj}}{N_h \cdot N_j} \cdot \dfrac{\mu^2}{2 \cdot \alpha^2} \cdot \left(\sum\limits_{i=1}^{2} \dfrac{\mu^i}{\alpha^i \cdot i!} \right)^{-1} \cdot \dfrac{N_h + N_j}{2}$,

or, simply, when a single vehicle is considered, $N_{h, j} = \dfrac{\mu^2}{2 \cdot \alpha^2} \cdot \left(\sum\limits_{i=1}^{2} \dfrac{\mu^i}{\alpha^i \cdot i!} \right)^{-1} \cdot \dfrac{N_h + N_j}{2}$.

2.3. Evaluation of the time independent load spectrum

In conclusion, using the procedures described in points 2.1. and 2.2., it is possible to obtain a suitably modified load spectrum, the *lonely vehicles spectrum* (l. v. s.), whose components are individual vehicles and vehicle convoys travelling alone on the bridge.

Generally, the evaluation of the l. v. s. requires the application of both procedures: the simultaneous presence of several lorries on the same lane is considered first, so that it is possible to obtain for each lane a new load spectrum, formed by individual vehicles and vehicle convoys travelling alone on the lane, to be used to solve the multilane case.

3. Time independent interactions

When the l. v. s. is known, it is possible to consider the complete stress history as a random assembly of the individual stress histories induced by each member of the l. v. s. itself. But, unfortunately, as it is well known, the stress spectrum depends on the cycle counting method and cannot be determined, in general, as a pure and simple sum of the individual stress spectra. In fact, it can happen that the maximum and minimum stresses are induced by different members of the l. v. s., so that it is necessary to consider time independent interactions too. When the reservoir or the rainflow methods are employed, the problem can be solved in the general case [3], [4]. The demonstration of the procedure is out of the scope of the present paper and it will be reported only the main results.

Using reservoir or rainflow counting methods it can be proved that two individual stress histories σ_{A_i} and σ_{A_j} interact if and only if $\max \sigma_{A_i} \leq \max \sigma_{A_j}$ and $\min \sigma_{A_i} \leq \min \sigma_{A_j}$ or $\max \sigma_{A_i} \geq \max \sigma_{A_j}$ and $\min \sigma_{A_i} \geq \min \sigma_{A_j}$. If the couples of interacting histories are sorted in such a way that the corresponding $\Delta\sigma_{max}$ are in descending order , it is possible to evaluate the number of the combined stress histories as well as the residual numbers of each individual stress history in a very simple recursive way.

In general, an individual stress history can interact with several others, so that the number of combined stress histories N_{cij}, obtained as h-th combination of the stress history σ_{A_i} and as k-th combination of the stress history σ_{A_j} is given by $N_{cij} = \dfrac{^{(h-1)}N_i \cdot ^{(k-1)}N_j}{^{(h-1)}N_i + ^{(k-1)}N_j}$, where $^{(h-1)}N_i$

and $^{(k-1)}N_j$ are the number of the individual stress histories σ_{A_i} and σ_{A_j} not yet combined and being $^{(0)}N_i = N_{A_i}$ and $^{(0)}N_j = N_{A_j}$ the number of repetitions of σ_{A_i} and σ_{A_j} induced by the l.v.s.. The actual number of the individual stress history σ_{A_i} which don't combines with other stress histories is given by $^{(p)}N_i = ^{(0)}N_i - \sum\limits_{k \neq i} \left(N_{ik} + N_{ki} \right)$, being the sum extended to all the stress histories σ_{A_k} which are able to combine with σ_{A_i} itself.

In this way it is possible to derive, in conclusion, a new modified load spectrum whose

members, represented by the original individual vehicles, by the vehicle convoys determined according to point 2. and by their time independent combinations, are interaction free, so that it can be defined as interaction-free vehicle spectrum (i. v. s.).

4. Numerical examples

In order to illustrate some practical applications of the formulae derived before, two simple exercises are developed in the following. The first one concerns the evaluation of the maximum length of a single lane for which the presence of several lorries can be disregarded, while the second one shows how the λ-factors for the multilane effect can be calibrated, in view of the fatigue assessment of steel bridges, using fatigue model 3 of ENV 1991 - 3. In the exercises a slope of the S-N curve m=5 is considered, while the flow rates are evaluated assuming 280 working days per year.

4.1. Evaluation of the critical length of one single lane

Let L the span of a simple supported beam, it is required to evaluate, for the bending moment at midspan, the value of L for which the interactions on a single lane become significant. Numerical calculations are developed referring to fatigue model 3 (single vehicle model) of ENV 1991 - 3, considering four different annual flows: $N_1=2.5\times10^5$; $N_2=5.0\times10^5$; $N_3=1.0\times10^6$; $N_4=2.0\times10^6$.

Let v=13.889 m/sec the lorry speed and $T_s=1.5$ sec the intervehicle interval; the annual numbers of interacting vehicles, determined using the formulae of point 2.1., depending on the annual flow and on the span L, are summarized in table 1.

Using these results and taking into account the relative positions of the two lorries along the lane, the equivalent stress range $\Delta\sigma_{eq}$ has been found.

The ratios $\lambda^*=\Delta\sigma_{eq}/\Delta\sigma_1$, being $\Delta\sigma_1$ the equivalent stress range determined disregarding interactions, are reported in table 2 (for L=40 m and L=50 m it results $\lambda^*\approx1$).

	N_1	N_2	N_3	N_4
L=40 m	1190	4729	18566	71605
L=50 m	1690	6670	25987	98813
L=60 m	2165	8515	32940	123618
L=75 m	2858	11177	42796	157689
L=100 m	3978	15423	58110	208240

Table 1 - Number of interactions (1 lane)

	N_1	N_2	N_3	N_4
L=60 m	1.002	1.004	1.007	1.013
L=75 m	1.007	1.014	1.027	1.047
L=100 m	1.013	1.025	1.045	1.076

Table 2 - λ^* values (1 lane)

The results, which appear in good agreement with the numerical simulations, show that the critical length is generally equal to 100 m, unless for high flows, when it reduces to 75 m.

4.2. Calibration of λ-factor for multilane effect

The formulae derived in point 2.2. are used to show how to calibrate of the λ-factor for the multilane effect of fatigue load model 3 [1].

In this case as well, reference is made to the bending moment at midspan of a simple supported

beam. Varying parameters are the span L and the vehicle flow, $N_1=2.5\times10^5$; $N_2=5.0\times10^5$; $N_3=1.0\times10^6$; $N_4=2.0\times10^6$, which is considered to be the same on each lane.

The annual number of interactions, found with v=13.889 m/sec, is reported in table 3.

	N_1	N_2	N_3	N_4
L=10 m	1846	7331	28901	112358
L=20 m	3666	14450	56179	212764
L=30 m	5458	21367	81966	303028
L=50 m	8967	34626	129532	458712
L=75 m	13213	50200	182480	617280
L=100 m	17312	64766	229356	746264
L=150 m	25100	91240	308640	943390
L=200 m	32383	114678	373132	1086953

Table 3 - *Interacting vehicles (2 lanes)*

	N_1	N_2	N_3	N_4
L=10 m	1.156	1.162	1.174	1.197
L=20 m	1.162	1.174	1.197	1.234
L=30 m	1.168	1.186	1.217	1.264
L=50 m	1.180	1.207	1.250	1.310
L=75 m	1.194	1.230	1.283	1.351
L=100 m	1.207	1.250	1.310	1.381
L=150 m	1.230	1.283	1.351	1.423
L=200 m	1.250	1.310	1.381	1.450

Table 4 - *λ-factors (2 lanes)*

Taking into account the interactions as well as all the relative positions of the two lorries, the equivalent stress ranges $\Delta\sigma_{eq}$ have been determined under the assumption that the lanes have the same influence. Being $\Delta\sigma_1$ the equivalent stress range induced by one lane flow only, the required λ-factors, reported in table 4, are given by $\Delta\sigma_{eq}/\Delta\sigma_1$. The reference value for λ, which corresponds to zero interactions, is 1.149.

The results demonstrate that λ is a quasi-linear function of $\Theta \cdot N$, which can be expressed as

$$\lambda = 1.149 \cdot \left(1.03 + 0.01 \cdot \frac{L \cdot N}{v \cdot 10^6}\right), \text{ where L is in m and v in m/sec.}$$

5. Conclusions

The interaction between the vehicles belonging to a load spectrum is solved in general way, taking into account all types of interactions, depending or not on the time. The solutions given in sequence in the paper allow to attain, through a step by step procedure, to an interaction-free vehicle spectrum (i. v. s.), formed by vehicles or vehicle convoys which cannot interact. The solutions of two simple but important problems show the practical application of the methods outlined in the paper.

References

[1] ENV 1991 - Basis of design and actions on structures - Part 3: Traffic load on bridges.

[2] Parzen E., *Stochastic Processes*, Holden-Day, San Francisco, 1982.

[3] Croce P., *Fatigue in Orthotropic Steel Bridge Decks*, Ph. D. Thesis, Pisa, 1989 (*in italian*).

[4] Croce P., Load Interactions and Fatigue Damage, *La Ricerca ed i Ricercatori della Facoltà di Ingegneria*, Pisa, 1995 (*in italian*).

[5] Ventsel E.S., *Probability theory*, MIR, Moscow, 1983.

Representative values of thermal effects
for concrete bridges in EC1, Part 2.5

Gert KöNIG
Prof. Dr.-Ing. Dr.-Ing. e.h.
Institut für Massivbau, THD
Darmstadt, Germany

Gert König, born 1934, got his civil engineering degree in 1960, got his doctor degree in 1966, since 1975 he is professor in the facility of civil engineering at the Technical University of Darmstadt. He got honorary degree of doctor (Dr.-Ing. e.h.) in 1992.

Dimitry SUKHOV
Dr.-Ing.
Institut für Massivbau, THD
Darmstadt, Germany

Dimitry Sukhov, born 1959, got his civil engineering degree in 1982, got his doctor degree in 1986, since 1991 he is researcher in the facility of civil engineering at the Technical University of Darmstadt.

Summary

The influence of the environmental conditions on the thermal effects in concrete bridges is considered. The representative values of thermal effects (the uniform temperature component and the linear temperature differences) are determined by means of the representative values of climatic actions (incoming solar radiation and shade air temperature), which are obtained with the help of statistical analysis and the theory of extremes.

1. Introduction

According to the system of Eurocodes characteristic value of an action is its main representative value. For thermal actions the characteristic value is taken as the value having a return period of 50 years.

According to [1] - [3] three design situations have to be considered for the serviceability limit state (SLS) and three corresponding representative values of actions have to be determined:

- infrequent (return period of occurrence is one year)
- frequent (return period of occurrence is two weeks)
- quasi-permanent.

These representative values can be obtained with the help of reduction coefficients Ψ, which - multiplied by the characteristic value, lead to the level of action with the given return period.

$$\Delta T_1' = \Psi_1' \cdot \Delta T_K \qquad \text{(infrequent value of thermal effect)},$$

$$\Delta T_1 \;=\; \Psi_1 \cdot \Delta T_K \qquad \text{(frequent value of thermal effect),}$$

$$\Delta T_2 \;=\; \Psi_2 \cdot \Delta T_K \qquad \text{(quasi-permanent value of thermal effect),}$$

where ΔT_K - characteristic value of thermal effect.

2.   Thermal effects in the bridge deck

The environmental conditions which have the greatest influence on the temperature of a bridge are shade air temperature, and radiation (incoming total solar radiation (TSR)). Wind speed may also play an important role; this may be reflected in the value of the heat transfer coefficient used for an analysis and entered not directly as a parameter.

These environmental conditions cause a non-linear temperature profile through the depth of the bridge deck. This distribution is active in producing strains of varying magnitude. It can be subdivided into three parts:

- *Bridge effective temperature range* T_N (or an uniform temperature component $\Delta T_N = T_N - T_0$, where T_0 is the datum temperature: effective bridge temperature at the time that the structure is restrained). This is the range of temperature which is used to determine the amount of movement due to expansion and contraction that the bridge must be able to accommodate and the uniform axial strains (and hence forces) induced in the structure due to restraint at bearing positions.

- *Linear temperature differences* ΔT_M. This is a linearly varying part of temperature profile through the depth of the bridge deck which is active in producing curvatures and strains of varying magnitude (and hence moments) where appropriate restraints are present.

- *Non-linear temperature distribution* ΔT_E. This is a non-linear part of temperature profile through the depth of the bridge deck which causes internal, non-linear selfequilibrating stresses which produce no net load effect on the structural element.

For concrete bridges, the uniform temperature component and the linear temperature differences play an important role. The non-linear temperature distribution may be not taken into account.

For positive differential temperature profile (only this profile is considered) the values of the temperature effects outlined above are dependent on differing environmental processes. For linear temperature differences, incoming total solar radiation (TSR) is the dominant variable rather than shade air temperature range. On the contrary, shade air temperature has the main influence on the effective bridge temperature.

Therefore, it is possible to consider the extreme values of effective bridge temperature as a function of the extreme values of shade air temperature range and average values of incoming total solar radiation (TSR), while the extreme values of linear temperature differences can be considered as a function of extreme values of TSR and average ranges of shade air temperature.

Large positive temperature difference profiles may occur within a structure during a day with high solar radiation, and a large range of shade air temperature. These conditions typically occur in the Middle Europe during the months of June, July or August. Thus, period of observations from 1st June till 31st August is considered.

3. Temperature profile through the depth of the bridge deck

The calculation of temperature distribution through bridge decks has been considered by numerous authors (see for example [4] - [8]). It was shown in [4], [5] that for concrete bridge decks, heat flow through the depth of a concrete deck can be considered to be effectively one-dimensional because of a large thermal inertia and relatively low diffusivity of concrete. Therefore, the temperature difference distribution for concrete decks can be derived using the iterative, one-dimensional heat flow model. Based on these investigations the computer program [9] was developed. The finite difference equations are solved at 50 mm increments through the entire depth of a bridge deck and at 15 minutes time increments during one day (24 hours).

The program uses the following data as input:

1. Solar radiation
   - The time of sunrise.
   - The duration of the solar day i.e. the number of hours of sunlight for the day considered.
   - The total daily value for TSR.

2. Temperature
   - The daily maximum shade air temperature.
   - The daily minimum shade air temperature.
   - The time at which the maximum value occurs.
   - The time at which the minimum value occurs.
   - The bridge effective temperature at starting time (at 08:00 a.m.).

3. Geometrical characteristics of bridge cross section
   (heights of all parts of the concrete deck).

4. Thermal and material properties of concrete deck
   - The coefficient of absorptivity
   - The coefficient of emissivity
   - The heat transfer coefficient of the surface
   - Thermal conductivity
   - The specific heat
   - Density

In order to begin calculations, the initial temperature in the bridge, which is unknown, must be defined. To overcome this, a start time must be chosen at which the temperature distribution through the section is considered to be the most uniform. For the climate of Middle Europe , it has been shown in [4, 5] that during the summer, this condition exists when the bridge reaches

it's minimum effective temperature, which, for concrete decks occurs typically at 08:00 a.m..
Therefore, a one-day calculation cycle begins at eight o'clock in the morning.

For wind conditions of Middle Europe the heat transfer coefficient of the upper surface
appears to be equal to 19 - 23 W/m^2 and the one of the lower surface is equal to 9 W/m^2.

According to [4] - [6] there is no significant benefit derived from allowing for slight difference
in the thermal properties of surfacing to those of concrete and therefore for concrete decks, the
surfacing is simply modelled as an additional thickness of concrete. All results are calculated
for surfacing 50 mm. The influence of other surfacing on linear temperature differences is also
investigated (see below Chapter 7).

Three groups of bridge cross sections are considered as the most useful in praxis (they are
shown in Annex A):

box girder
- type 1.0 (bridge Lucka), total depth 1.95 m
- type 1.1, total depth 2.0 m
- type 1.2, total depth 3.3 m
- type 1.3, total depth 4.7 m

T-beam
- type 2.1, total depth 1.2 m
- type 2.2, total depth 1.8 m
- type 2.3, total depth 2.4 m

slab
- type 3.1, total depth 0.6 m
- type 3.2, total depth 0.9 m
- type 3.3, total depth 1.2 m

For each type of cross section the upper width is 14.2 m with the exception of type 1.0 (bridge
Lucka in Thüringen, Germany), which has an upper width of 9.12 m. The bridge Lucka is
considered because of available experimental data which are used for comparison of results.

4.   Statistical analysis of thermal effects

Statistical analysis of thermal effects has been performed by some authors. In [10] available
data was the experimental ones of bridge Lucka. This data was recorded for the period 1984-
1985. Then three-day maxima of thermal effects were taken to establish the sample of
independent events. This is because of shade air temperature and solar radiation have a three-
day period of independence. Then representative values (see Chapter 1 above) of thermal
effects have been calculated.

The theoretical investigation for bridge Lucka also was performed in [11] - [12]. The climatic
data from Middle Germany (meteorological station Giessen) was used. The values of thermal
effects were obtained by means of program [9] for each day from 1st June till 31st August for

ten years period 1981 -1990. Then three-day maxima of thermal effects were determined and the representative values and coefficients Ψ (see above) were obtained with the help of statistical analysis and extreme values theory. The comparison with [10] gave a good coincidence, that shows that the using of program [9] is reasonable for concrete bridges.

It was reported that the results of 1982 are very close to results for all ten years 1981 - 1990. It was the reason for using only the climatic data of 1982 for all other cross sections (types 1.1 -3.3, see Chapter 3 above). In [11] - [12] the representative values of thermal effects for these types of cross section were calculated. Although this method gives very good results, it needs plenty of work and time because the program [9] calculates temperature profile only for one day, but for statistical analysis it is necessary to obtain the temperature profiles for some hundreds, even thousands of days.

5.   Statistical analysis of environmental conditions

Shade air temperature and solar radiation are the non-stationary stochastic processes. However, it appears, that during three summer months, these processes may be considered as the stationary ones.

The climatic data for the period of 1981 - 1990 is available from meteorological station Giessen (Hessen, Germany). This station is in the middle of Germany and Europe and can be considered as a representative place for Middle Europe. The data is:

- hourly values of solar radiation,
- hourly values of shade air temperature.

First of all the daily maximum and daily minimum of shade air temperature, and daily value of total solar radiation are obtained for all days during the months of June, July, and August for the above mentioned period. Then two different procedures for two different thermal effects can be used.

5.1   Linear temperature differences

Because for linear temperature differences incoming total solar radiation (TSR) is the dominant variable, only for total solar radiation the maximum for each three days is taken. For shade air temperature range (maximum and minimum of daily shade air temperature) only associated values are taken, i.e. maximum and minimum of shade air temperature which are observed on the same day in which the maximum of TSR occurs. Three days is a minimal interval of independent random events (TSR and shade air temperature). Thus, 30 values per summer are obtained for maximum of TSR and associated shade air temperature range, and 300 values are available for 10 years. According to [9] some supplementary input parameters need to be calculated for summer months (mean values):

- The time at which the daily maximum of shade air temperature occurs   15:00 p.m.
- The time at which the daily minimum of shade air temperature occurs   04:00 a.m.
- The time of sunrise   04:00 a.m.
- The duration of solar day   16 hours

Then parameters of random sample for maximum TSR and for associated shade air temperature range can be calculated (for period 1981 -1990):

- three-day maximum of TSR: mean value M(R)   = 5831.8 W/m²
                                     standard deviation s(R)   = 1368.5 W/m²

- associated values of shade air temperature range:
          mean value of maximum shade air temperature $M(T_{max})_{ass}$ = 23.7 °C
          mean value of minimum shade air temperature $M(T_{min})_{ass}$ = 11.9 °C

Almost the same values are obtained for year 1982 (see [11]). Only for the standard deviation of TSR the value (1165.3 W/m²) is a little different. This data is used for the types 1.1 - 3.3, so that results can be compared with results obtained by the „exact" method in [11] (see Chapter 4 above).

The probability distribution function of the three-day maximum of TSR can be assumed to fit a type III extreme value distribution (for the maximum). This distribution is limited in the tail to an upper cut-off value of x_0, because solar radiation has a physical upper limit (for Middle Germany this value is equal to 10150 W/m²):

$$F_X(x) = \exp \{ - [(x_0 - x) / (x_0 - u)]^c \}$$ (1)

where: c,u - the parameters of the distribution, which connect with mean value M_X and standard deviation σ:

$$M_X = x_0 - (x_0 - u) \Gamma(1 + 1/c)$$ (2a)

$$\sigma^2 = (x_0 - u)^2 [\Gamma(1 + 2/c) - \Gamma^2(1 + 1/c)]$$ (2b)

where: Γ - Gamma function.

Knowing the parameter c, u, x_0 and using the inverse probability distribution function

$$x = \Phi(P) = x_0 - (x_0 - u) [- Ln (P)]^{1/c},   P = [0,1]$$ (3)

it is possible to calculate fractile values for different return periods of the random variable R (three-day maximum of TSR).

For ultimate limit states (ULS) the return period is 50 years. Corresponding probability of not exceeding of the fractile value of action is (30 three-day intervals per year):

$$P = 1 - 1 / (30 \times 50) = 0.999333$$

For serviceability limit states (SLS) it is necessary to determine three different values of action (see Chapter 1):

- infrequent value   (return period 1 year),

- frequent value   (return period 2 weeks),
- quasi-permanent value   (return period seems to be assumed as 6 days, because available
                          statistical data of TSR is three-day maxima).

For these three situations the fractile values are calculated with the following probabilities of
not being exceeded:

T_{return} = 1 year: $P = 1 - 1 / 30 = 0.966667$,   (4a)

T_{return} = 2 weeks: $P = 1 - 1 / 4.67 = 0.785867$,   (4b)

T_{return} = 6 days: $P = 0.5$.   (4c)

With the help of (3) the representative values of TSR can be obtained:

Characteristic value R_K =   9557.6 W/m^2

Infrequent value R_1' =   8327.3 W/m^2

Frequent value R_1 =   6955.6 W/m^2

Quasi-permanent value R_2 =   5828.1 W/m^2

5.2   Bridge effective temperature

For bridge effective temperature the shade air temperature range is the dominant variable,
therefore three-day maxima of shade air temperature range are determined. For TSR only
associated values are taken, i.e. the value of TSR which is observed on the day in which the
maximum of shade air temperature range occurs. Thus, 30 values per summer are available for
the maximum value of shade air temperature range and the associated value of TSR, so that
300 values are available for 10 years. The supplementary input parameters are the same as in
Chapter 5.1 (see above).

The parameters of random sample for maximum shade air temperature range and for associated
value of TSR are (for period 1981 -1990):

- three-day maximum of shade air temperature range:

    mean value M(T):   - maximum shade air temperature = 24.8 ^{0}C
                             - minimum shade air temperature = 12.7 ^{0}C

    standard deviation s(T): - maximum shade air temperature =   4.3 ^{0}C
                             - minimum shade air temperature =   2.8 ^{0}C

- associated value of TSR:

                             - mean value $M(R)_{ass}$ = 5417.0 W/m^2

Almost the same values are obtained for 1982 (see [12]). This data is used for cross sections types 1.1 - 3.3 which results can be compared with results obtained by the „exact" method in [12] (see Chapter 4 above).

The probability distribution function of the three-day maximum of shade air temperature range can be assumed to fit a type III extreme value distribution (see above Chapter 5.1, eq. (1), (2a), (2b)). The upper cut-off value of x_0 for Middle Germany is equal to 40.0 ^{0}C for maximum shade air temperature and the one for minimum shade air temperature is equal to 30.0 ^{0}C.

With the help of the eq. (3), (4a) - (4c) the representative values of shade air temperature range are determined:

Characteristic value: - maximum $T_{K(max)}$ = 37.3 ^{0}C
                        - minimum $T_{K(min)}$ = 23.2 ^{0}C

Infrequent value: - maximum $T_{K(max)}$ = 32.8 ^{0}C
                        - minimum $T_{K(min)}$ = 18.4 ^{0}C

Frequent value: - maximum $T_{K(max)}$ = 28.2 ^{0}C
                        - minimum $T_{K(min)}$ = 14.8 ^{0}C

Quasi-permanent value: - maximum $T_{K(max)}$ = 24.7 ^{0}C
                        - minimum $T_{K(min)}$ = 12.4 ^{0}C

6. Calculation of representative values of thermal effects

6.1 Linear temperature differences

To obtain the representative values of linear temperature differences it is necessary to perform the calculations with the help of the program [9] only for 4 different design situations (characteristic, infrequent, frequent, quasi-permanent) using appropriate values of TSR and associated mean values of other input parameters.

A very high value of linear temperature differences occurs usually in a day with a very high total solar radiation and average range of shade air temperature, following one or two not very warm days. Program [9] uses a one-day cycle, therefore, the initial mean temperature of the bridge (see Chapter 3) in a given day can be considered as the final temperature of the previous day. Because two previous days were not very warm the initial temperature in the given day can be supposed to be close to the air temperature at the same time, i.e. at 08:00 a.m.. This value is close to the daily minimum air temperature and can be estimated as 12.0 ^{0}C (see Chapter 5.1) for the calculation of the characteristic value of linear temperature differences. Because other representative values (infrequent, frequent, and quasi-permanent) are smaller than the characteristic one, the two previous days need to be not so cold for these situations. It means that the mean bridge temperature is greater than the temperature of the surrounding air at 08:00 a.m. in a given day, and the initial effective bridge temperature can be derived by running the bridge model for the particular set of environmental conditions of interest for a

period of 2 - 3 days. The starting initial mean bridge temperature can be assumed again as 12 °C.

The calculations are performed for 10 types of bridge cross sections (types 1.0. - 3.3.) and results are shown in Table 1 (ΔT_M in °C).

Depth (m)	ΔT_{MK}	$\Delta T_{M1}'$ Ψ_1'	ΔT_{M1} Ψ_1	ΔT_{M2} Ψ_2

Box girder

1.95 (Lucka)	11.4	9.3 0.82	7.4 0.65	5.8 0.51
2.0	11.5	9.4 0.82	7.4 0.64	6.0 0.52
3.3	10.3	8.3 0.81	6.5 0.63	5.2 0.50
4.7	9.6	7.6 0.79	5.9 0.62	4.7 0.49

T-girder

1.2	19.0	14.8 0.78	11.7 0.62	9.5 0.50
1.8	16.0	12.2 0.76	9.5 0.59	7.7 0.48
2.4	14.1	10.6 0.75	8.2 0.58	6.5 0.46

Slab

0.6	18.0	15.2 0.84	12.5 0.69	10.4 0.58
0.9	13.8	11.6 0.84	9.5 0.69	7.8 0.57
1.2	10.8	9.1 0.84	7.3 0.68	6.0 0.56

Table 1. Representative values of linear temperature differences.

ΔT_{MK}, $\Delta T_{M1}'$, ΔT_{M1}, ΔT_{M2} are characteristic, infrequent, frequent, and quasi-permanent values of the linear temperature differences.

The comparison with the results in [11] obtained by the statistical analysis of linear temperature differences shows a very good coincidence. For characteristic situation the values from Table 1

are a little smaller (but the difference is only 0.5 - 2.5 %), for other representative situations the results are practically identical.

Reduction coefficients Ψ are determined as:

$\Psi_1' = \Delta T_{M1}'/\Delta T_{MK}$ for infrequent value of the action,

$\Psi_1 = \Delta T_{M1}/\Delta T_{MK}$ for frequent value of the action,

$\Psi_2 = \Delta T_{M2}/\Delta T_{MK}$ for quasi-permanent value of the action.

Values of these coefficients are shown also in Table 1.

Considering all results in Table 1 it is possible to propose the following values for the reduction coefficients Ψ:

Ψ_1' = 0.8
Ψ_1 = 0.6
Ψ_2 = 0.5

The same values are in [11].

6.2   Effective bridge temperature

To obtain the representative values of effective bridge temperature it is necessary to perform the calculations with the help of the program [9] only for 4 different design situations (characteristic, infrequent, frequent, quasi-permanent) using appropriate values of shade air temperature range and associated mean values of other input parameters.

A very high value of effective bridge temperature occurs usually in a day with a very high range of shade air temperature and average total solar radiation, following one, two or three very warm days with very warm nights. Because of the thermal inertia the mean bridge temperature rises during these days and, therefore, the starting mean bridge temperature is very high at 08:00 a.m. in a day considered. Analysis undertaken in [12] showed that this value can be assumed as $T_{rep,max} - 3\ ^0C$ (where $T_{rep,max}$ - the representative value for the situation of interest).

The calculations are performed for 10 types of bridge cross sections (types 1.0. - 3.3.) and results are shown in Table 2 (ΔT_N in ^0C).

ΔT_{NK} , $\Delta T_{N1}'$, ΔT_{N1} , ΔT_{N2} are characteristic, infrequent, frequent, and quasi-permanent values of the uniform temperature component.

The comparison with [12] shows that for characteristic situation the values are almost the same for box girders and a little smaller for T-girders and slabs (0.5 - 4.0 %), for other representative situations the values from Table 2 are a littler higher (on the safe side) for box girders and slabs (2 - 8 %) and very close for T-girders.

Depth (m)	ΔT_{NK}	$\Delta T_{N1}'$ Ψ_1'	ΔT_{N1} Ψ_1	ΔT_{N2} Ψ_2

Box girder

Depth (m)	ΔT_{NK}	$\Delta T_{N1}'$ Ψ_1'	ΔT_{N1} Ψ_1	ΔT_{N2} Ψ_2
1.95 (Lucka)	26.6	22.0 *0.82*	17.5 *0.65*	14.1 *0.53*
2.0	27.9	23.5 *0.84*	19.2 *0.68*	16.0 *0.57*
3.3	27.4	23.0 *0.84*	18.7 *0.63*	15.4 *0.56*
4.7	26.9	22.6 *0.84*	18.3 *0.68*	15.0 *0.56*

T-girder

Depth (m)	ΔT_{NK}	$\Delta T_{N1}'$ Ψ_1'	ΔT_{N1} Ψ_1	ΔT_{N2} Ψ_2
1.2	28.5	24.1 *0.84*	19.8 *0.69*	16.6 *0.58*
1.8	27.8	23.4 *0.84*	19.1 *0.68*	16.0 *0.57*
2.4	27.3	22.9 *0.83*	18.6 *0.68*	15.4 *0.56*

Slab

Depth (m)	ΔT_{NK}	$\Delta T_{N1}'$ Ψ_1'	ΔT_{N1} Ψ_1	ΔT_{N2} Ψ_2
0.6	27.6	22.2 *0.80*	18.8 *0.68*	15.6 *0.56*
0.9	26.5	22.1 *0.83*	17.8 *0.67*	14.5 *0.55*
1.2	25.9	21.6 *0.83*	17.3 *0.66*	14.0 *0.54*

Table 2. Representative values of the uniform temperature component
$$\Delta T_N = T_N - 10\ ^0C.$$

Reduction coefficients Ψ are determined as:

$\Psi_1' = \Delta T_{N1}'/\Delta T_{NK}$ for infrequent value of the action,

$\Psi_1 = \Delta T_{N1}/\Delta T_{NK}$ for frequent value of the action,

$\Psi_2 = \Delta T_{N2}/\Delta T_{NK}$ for quasi-permanent value of the action.

Values of these coefficients are shown also in Table 2.

In [12] coefficients Ψ calculated with the help of statistical analysis of uniform temperature component are proposed as:

$\Psi_1' = 0.8$
$\Psi_1 = 0.6$
$\Psi_2 = 0.5$

7. Influence of surfacing on the values of linear temperature differences

All results given above are obtained for surfacing of 50 mm. The variation of the thickness of surfacing affects only on linear temperature differences. For other values of thickness the procedure given above can be also used and conversion factor k may be proposed:

surface thickness (mm)	factor k
0	1.5
50	1.0
100	0.7
150	0.5

Table 3. Influence of surface thickness.

For other values of thickness factor k can be found by interpolation.

Thus, all representative values of linear temperature differences from Table 1 must be multiplied by factor k if the surfacing is other than 50 mm.

8. Conclusions

The statistical analysis of extreme values of environmental conditions (incoming total solar radiation and shade air temperature) is performed. According to the philosophy of Eurocodes four design situations and correspondingly four representative values of thermal effects in bridges are defined. The thermal effects in a concrete bridge deck can be derived from the difference temperature profile through the depth of the deck. The representative values of thermal effects (linear temperature differences and uniform temperature component) may be obtained using directly the appropriate representative values of environmental conditions. These latter ones are calculated with extreme values theory using extreme value distribution type III. The reduction coefficients Ψ and surfacing factors k are also obtained. This procedure can be used for different climatic zones. The results based on meteorological data from central Germany are performed for typical bridge cross sections and can be considered as valid for the middle of Europe.

The characteristic values of linear temperature differences and values of surfacing factor are incorporated in Eurocode 1, Part 2.5 „Thermal Actions". The values of coefficients Ψ are included in Eurocode 1, Part 3 „Traffic Loads on Bridges".

References

[1]   Eurocode 1, Part 1 „Basis of Design", 1994

[2]   Eurocode 1, Part 3 „Traffic Loads on Bridges", 1994

[3]   Eurocode 2, Part 2 „Design of Concrete Structures - Concrete Bridges", 1995

[4]   M. Emerson, The calculation of the distribution of temperature in bridges, *TRRL Report LR561*, Crowthorne, 1973 (Road Research Laboratory).

[5]   M. Jones, Bridge temperature calculated by a computer program, *TRRL Report LR702*, Crowthorne, 1976 (Road Research Laboratory).

[6]   M. Emerson, Temperature differences in bridges: basis of design requirements, *TRRL Report LR765*, Crowthorne, 1977 (Road Research Laboratory).

[7]   HRA, König-Heunisch, Mangerig, Background report: thermal effects on road and railway bridges, *Federal Ministry of Traffic*, Germany, FE-No. 15. 194 R 90 G.

[8]   F. Branco, P. Mendes, Thermal actions for concrete bridge design, *Journal of Structural Engineering*, Volume 119, No. 8, 1993.

[9]   A. Harris, Program THERM (Temperature difference profiles through highway bridge decks), *Flint & Neill Partnership*, 1992

[10]   B. Frenzel, Beitrag zur Ermittlung der repräsentativen Werte des linearen Temperatur-unterschiedes an Betonbrücken und Überprüfung ihrer Einpassung in die Kombinations-regeln des EC 2, Teil 2, *Kombinationsregeln für Brückenlasten*, HAB Weimar, October 1994

[11]   D. Sukhov, Two methods for determination of linear temperature differences in concrete bridges with the help of statistical analysis, *Darmstadt Concrete*, Vol. 9, 1994, p. 193-210.

[12]   D. Sukhov, Representative values of the uniform temperature component in concrete bridges, *Darmstadt Concrete*, Vol. 10, 1995, p. 193-214.
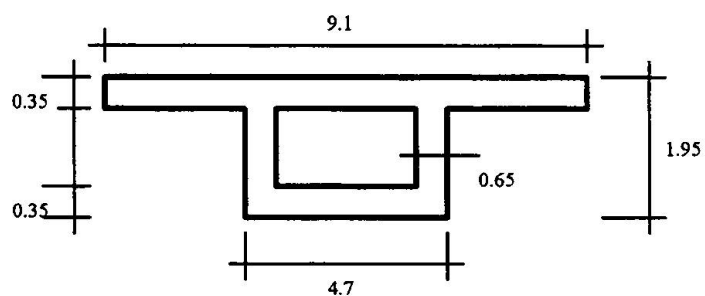
ANNEX A

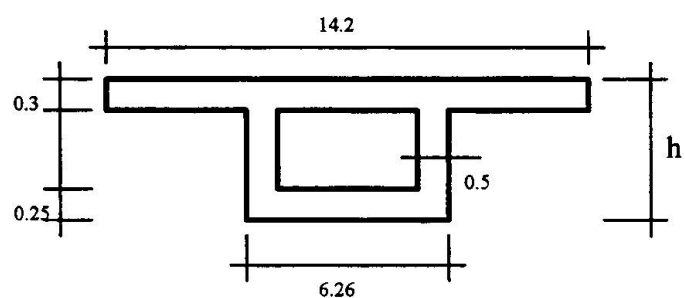**Bridge Cross Sections**

Box Girder   Type 1.0
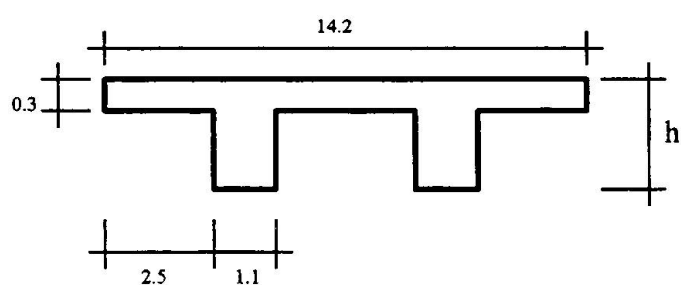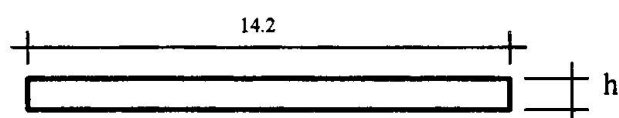

Type 1.1 (h=2.0 m), Type 1.2 (h=3.3 m), Type 1.3 (h=4.7 m)

T-girder   Type 2.1 (h=1.2 m), Type 2.2 (h=1.8 m), Type 2.3 (h=2.4 m)

Slab   Type 3.1 (h=0.6 m), Type 3.2 (h=1.2 m), Type 3.3 (h=1.8 m)

Research on the Transversal Thermal Behaviour of

a Prestressed Concrete Box Girder Bridge in Italy

Maurizio FROLI

*Research Engineer,
Istituto di Scienza
delle Costruzioni,
University of Pisa,
Italy*

Gabriele NATI

*Design Engineer,
Ferrocemento S.p.A.
Rome,
Italy*

Marco ORLANDINI

*Design Engineer,
Ferrocemento S.p.A.
Rome,
Italy*

Riccardo BARSOTTI

*PhD Student of
Structural
Engineering,
University of Pisa,
Italy*

Summary

This paper contains a contribution to the knowledge of transversal thermal actions on bridges, still under discussion in the Project Team of EC1, Part 2.6, based on three consecutive years of in-situ monitoring of the Casilina bridge. A simplified data-processing approach for the evaluation of the transversal thermal actions and stresses is exposed.

1. Introduction

Movements and stresses induced in modern bridge configurations by thermal fields of climatic origin have been recognized for many years to be relevant to the serviceability and the integrity of these structures and of the category of integral bridges in particular [1].

A certain number of damages which has occurred in the past on both concrete [2],[3] and steel bridges [4], has attracted the attention of many research and design structural Engineers on this type of problems, all over the world.

It was generally agreed that a prerequisite for the evaluation of thermal effects in bridges was a accurate evaluation of the time and space temperature distributions resulting from the transient heat exchanges between the bridge surface and its environment.

A considerable number of theoretical and experimental researches performed during the last ten years by structural Engineers have demonstrated that realistic and a complete set of information on the thermal behaviour of a bridge can only be obtained by a combined and interactive use of both refined transient F.E.M. or F.D.M. analysis and continuous field measurements of the principal climatic variables and of the temperatures in a good, but necessarily limited, number of points within some cross-sections of the monitored bridge [5],[6],[7],[8].

It is known that non-linear, time dependent temperature fields arise under the influence of changes in solar and thermal radiation, wind speed and shade air temperature, and that both longitudinal (or global) and transversal (or local) stresses and deformations are induced in box girder bridges by these temperature changes (see for example ref.[5]).

It is also known that in the plane of a boxed cross section, which can be schematized as a closed frame of unit width, transverse bending moments and axial efforts are due to the restrained thermal movements of the component walls of the frame.

Nevertheless, for the sake of clarity, these basic notions will be shortly recalled in the following points.

1.1 Global thermal actions of a temperature field

Let us consider a rectilinear girder bridge with a cross section of constant height. It has been theoretically [7] and experimentally [8] found that for such a bridge the temperature distribution of climatic origin is at any instant non-linear and does not depend on the z abscissa taken along the bridge longitudinal axis.

Let $T(x,y,t^*)$ be the non-linear temperature field acting at a t^* instant over a homogeneous box section of a girder bridge (Fig.1). The field can be decomposed into the following quantities that may be called the global effective parameters of the temperature field.

1) Global mean temperature $T_m = \frac{1}{A}\iint_A T(x,y,t^*)dA$ [°C].

2) Global linear gradient along y axis $DT_y = \frac{1}{J_x}\iint_A T(x,y,t^*)ydA$ [°C/m].

3) Global linear gradient along x axis $DT_x = \frac{1}{J_y}\iint_A T(x,y,t^*)xdA$ [°C/m].

In the preceding expressions A is the area of the cross section and J_x, J_y are respectively its principal central moments of inertia.
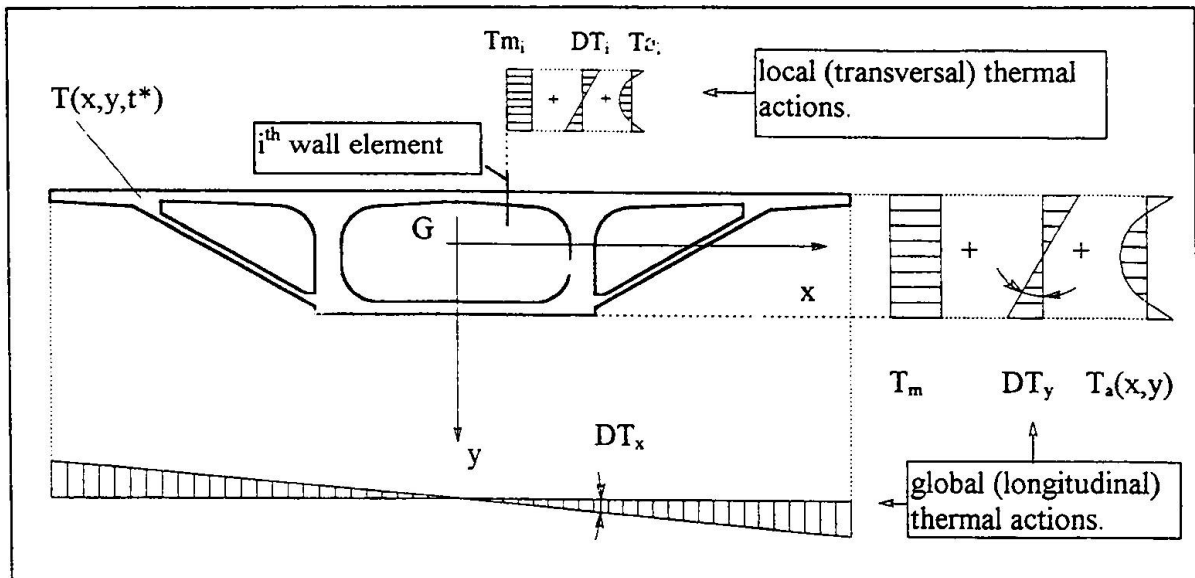
Fig.1. Decomposition of a temperature field into global (longitudinal) thermal actions and local (transverse) thermal actions.

T_m is responsible for the axial uniform movements of the bridge while DT_y, DT_x are respectively responsible for the cross sections rotation around its x (horizontal) and y (vertical) central principal axis of inertia.

The differences between the global effective parameters at a t^* instant and those at the instant t_0 of restraint of the structure (initial instant) may be called global (or longitudinal) thermal actions because they concern the whole cross section of the bridge.

If the movements induced by the global thermal actions are not freely allowed, axial forces and bending moments arise which are usually calculated by schematizing the girder bridge as a continuous beam. The associated stresses have been called secondary thermal stresses (**M.J.N. Priestley** [9]) because they may be present only in statically indeterminate structures.

The remaining self-compensated non-linear part of the temperature field

$$4) \qquad T_a = T(x,y,t) - \left[T_m + xDT_x + yDT_y \right],$$

produces axial displacements and rotation of the end cross sections which are meanly equal to zero and thus are not able to cause any axial force or bending moment even if the structure is statically not determinate.

On the other hand, when cross-sections can be supposed to remain plane (Saint-Venant's bodies), at a sufficient distance from the ends axial stresses arise which are proportional to expression (4) and are sometimes called residual stresses or, better, primary thermal stresses [9] because they do not depend on the restraint of the structure but only on the non linearity of the temperature field.

1.2 Local thermal actions of a temperature field

Modern girder bridges often have boxed cross sections. In addition to global thermal actions, and hence global thermal effects, local temperature distributions over the thickness of each wall element of the section must also be considered due to the closed frame transversal behaviour of the box sections.

If $T_i(s, t^*)$ is the local temperature distribution across the thickness S_i of the ith wall element at the instant t^*, it can be decomposed in the same way used for the global quantities into the following effective local parameters of the temperature distribution.

5) Local mean temperature $\qquad T_{m_i} = \frac{1}{S_i} \int_S T(s,t^*)ds.$

6) Local linear gradient $\qquad DT_i = \frac{12}{S_i^3} \int_S T(s,t^*)sds,$ with: $(-S_i/2 \le s \le + S_i/2)$

In each ith wall element, the differences between the local effective parameters at a t^* instant and those acting at the initial restraint instant of the element are called local (transversal) thermal actions because they act on the cross section regarded as a closed plane frame of unit width.

The remaining self-compensated non-linear part of the temperature distribution across the thickness of the ith wall element

$$7) \qquad T_{a_i} = T_i(s,t^*) - \left[T_{m_i} + sDT_i \right],$$

induces tension and compression stresses in the thickness of the element that are self-equilibrating and independent of the end restraint of the wall element.

Concrete box girder bridges may experience heavy cracking due to longitudinal thermal actions, like in the case of the Market Viaduct [3], but also crack damages due to transversal thermal actions, like in the case of the Jagtbrücke [2].

In spite of this, transversal thermal actions have been quite disregarded by researchers and the level of available knowledge and experience about this topic is nowaday much lower to that reached on longitudinal thermal actions.

For this reason, an attempt has been made to offer the first insight into this problem by illustrating a simplified procedure used to evaluate the magnitude and time variations of transversal thermal actions from the great number of experimental data recorded from the

Casilina bridge. Further research will be devoted in the future for the assessment of the statistical properties of such transversal action distribution.

2. Field monitoring of Casilina bridge

The Casilina bridge is a prestressed segmental box girder bridge of the motorway Fiano Romano-San Cesareo, near Rome. The static scheme is that of a continuous beam (whose longitudinal axis almost coincides with the North-South direction) with three intermediate spans of 50 m and two end spans of 30 and 40 m. The cross-section has a three cellular trapezoidal form with a constant height of 240 cm and a 130 mm thick asphalt pavement The construction was carried out post-tensioning precast segments erected in balanced cantilever from the piers.

The shrinkage, creep and thermal behaviour of the bridge was extensively monitored within the framework of the research programme named E.V.E.R. (Effetti Viscosità E Ritiro).
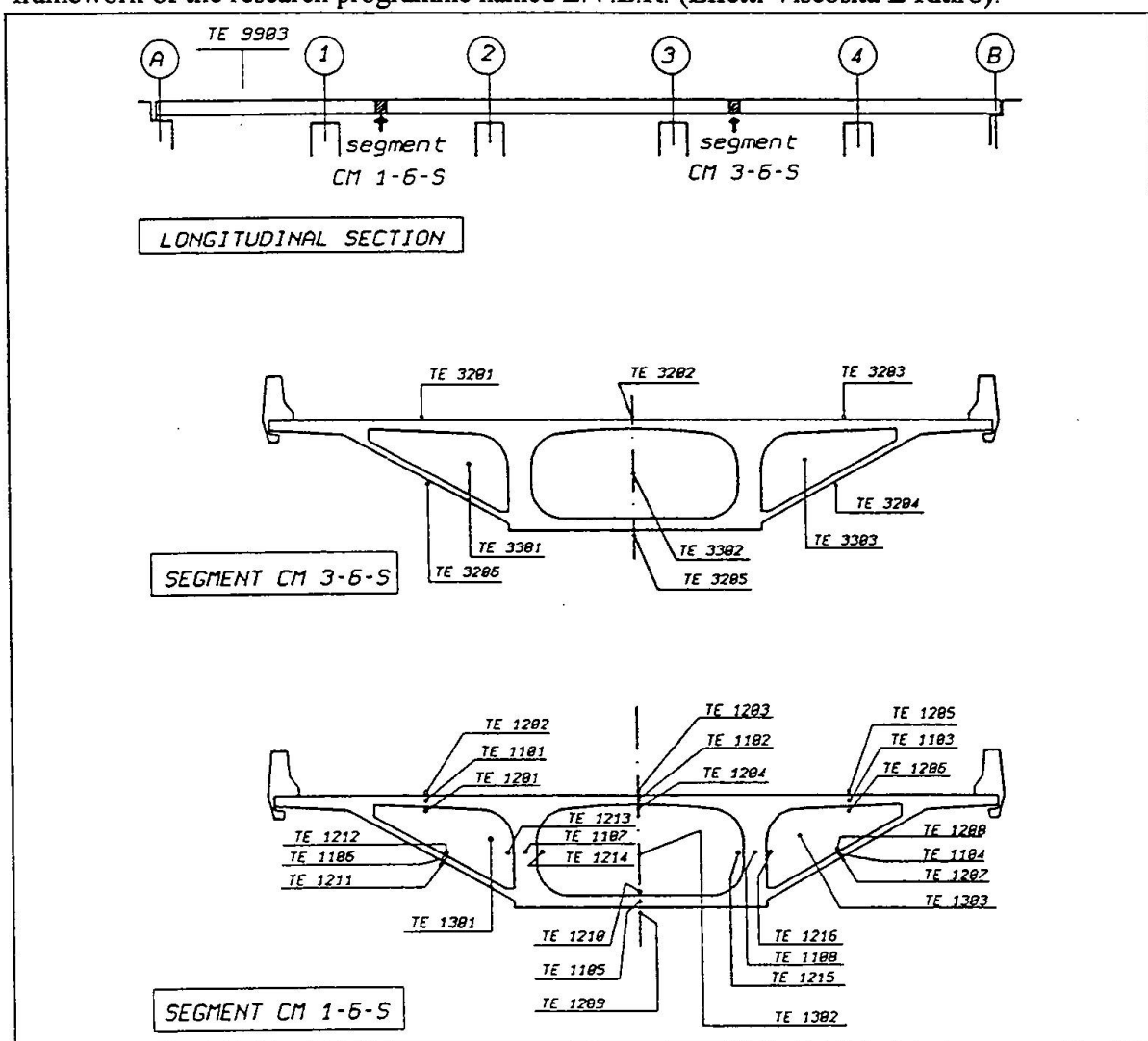

Fig. 2. Longitudinal and cross sections of the bridge with the location of the thermistors.

Measurements were executed every hour from 18.00 a.m. of 2nd April 1987 until 10.00 a.m. of 7th August 1987 and every two hours from that instant until 14.00 p.m of 31st July 1990 when

the programme was stopped. Referring only to the thermal aspect of the campaign, some around 600.000 data were collected in this period. The instrumentation used, as well as the data measurement, storage and transmission techniques have been already described in reference [8]. Therefore it shall be here only briefly recalled, with reference to figure 2, that segments C.M 1.6.S and C.M 3.6.S were equipped with respectively 24 and 6 embedded thermistors and that ambient air temperature was measured in 6 points inside the box cells. Shade air temperature has been recorded several meters above the bridge deck surface.

All the measures have been systematically submitted to a numerical procedure of validation in order to define their reliability and, when possible, to reconstruct some missing data [8].

2.1. Evaluation of global thermal actions

The global effective parameters of a temperature field can be exactly calculated with relations (1) to (3) only when the function $T(x,y,t^*)$ is completely known all over the cross section. It is evident that by direct measurement the temperature field can be known only in a limited number of points and that, in order to calculate the global effective parameters, simplifying assumptions on the form of the temperature field have to be introduced. An alternative and more precise method is to develop a F.E.M. heat transfer model of the bridge where the boundary conditions reproduce with sufficient accuracy the time-histories of the climatic variables of the surrounding environment. The soundness of the numerical model must be checked, and if necessary fitted back, by comparison with the experimental data. Once the calculated time distributions of the temperatures in the measurement points fit satisfactorily the measured distribution, than the numerical outputs can be used at any instant to accurately calculate the effective parameters.

This kind of interactive analysis was carried on the Casilina bridge; a detailed description of which may be found in reference [8].

The absolute value and the sign of global thermal actions are generally very difficult to evaluate because the thermal fields at the initial instants are not known and also because it is sometimes even very difficult to establish exactly which were the initial instants when the restraint operations lasted some days. Since the monitoring of the thermal rensponse of the Casilina bridge included also the construction phases, it was in this case possible to individuate, within a rather small range of uncertainty, the global effective parameters at the times when the different spans were joined together, and hence the global thermal actions acting on the bridge [11].

2.2. Evaluation of local thermal actions

The evaluation of the local thermal actions may be carried out in a simpler way than that needed for global thermal actions due to the relative small and almost uniform thickness of the wall elements. Indeed, it has been found [8] that, at sufficient distance from the ends, the local temperature field is almost uniform along the length of each element and varying only in the thickness of it. Therefore, in order to calculate the local effective parameters from expressions (5),(6), it would be necessary to know the temperature distributions $T_i(s,t^*)$ along the thickness S_i of each wall element. Since the thicknesses of the elements are relatively small, a sufficiently accurate evaluation of the local effective parameters can be performed asssuming that each $T_i(s,t^*)$ is parabolic along the correspondent S_i and imposing to $T_i(s,t^*)$ to assume just the experimental values at the three points of S_i where the thermistors were located.

Under these assumptions, if T_{1i}, T_{3i} are the measured temperatures at the outer surfaces and T_{2i} is the measured temperature at middle thickness of every i^{th} wall element at a generic t^* instant, it is easy to obtain the instantaneous, approximate expressions of the local effective parameters:

8) Local mean temperature

$$T_{m_i} \approx \frac{T_{1i} + 4T_{2i} + T_{3i}}{6}.$$

9) Local linear gradient

$$DT_i \approx \frac{T_{1i} - T_{3i}}{S_i},$$

The self-compensated non-linear part of the local temperature distribution becomes:

10)

$$T_{a_i} \approx \left(\frac{T_{1i} - 2T_{2i} + T_{3i}}{6} \right) \left(\frac{12s^2}{S_i^2} - 1 \right) = B_i \left(\frac{12s^2}{S_i^2} - 1 \right), \quad \text{with:} \quad (-S_i/2 \le s \le + S_i/2)$$

The time-histories of each T_{mi}, DT_i and B_i quantity has then calculated from the measured temperatures according to expressions (8),(9),(10) and plotted all over the three years of monitoring time.

In figure 3 are reported the time variations of the effective mean temperatures and of the linear gradients, within the wall elements of the cross section, calculated during a typical summer period where a great amount of direct solar radiation occurs and where the most severe transversal efforts, according to **M.N.Elbadry, A.Ghali** [5] and **M.Ramezankhani, P.Waldron** [6], should occur.

It can first of all be observed that the thermal rensponses of the two lateral sloping webs are almost coincident as well as that of the vertical internal webs. This is due to the broad lateral overhanging cantilevers and to the great inclination of the lateral webs which produce almost a total sheltering of these wall elements from the direct solar radiations. Now, since also the thermal rensponses of the lateral upper slabs are almost the same, it follows that the global horizontal gradient must be aspected to be practically zero as it is indeed (see ref. [8]) thus confirming the good thermal behaviour of trapezoidal sections theoretically already predicted in [6].

The number of variables that occur in the evaluation of transversal thermal effects still remains quite large, in spite of the already introduced simplified calculation of the local effective parameters, making it difficult to formulate simple design rules but, in the present case and in similar other cases, it may be reduced without significantly affecting the level of accuracy requested for structural design calculations. We can indeed notice that the mean temperatures of the three upper slabs differ from each other not more than about 3°C during only a few hours per day. For this reason they can be unified with good approximation in their mean value:

11)

$$T_s = \frac{T_{m1} + T_{m2} + T_{m3}}{3}.$$

For the same reason this operation can be performed also on the mean temperatures of the sloping webs and of the bottom slab, thus obtaining:

12)

$$T_i = \frac{T_{m4} + T_{m5} + T_{m6}}{3}.$$

The mean temperatures of the central webs are not only almost coincident but also almost constant troughout this time interval; let us indicate with T_0 their average value:

13)
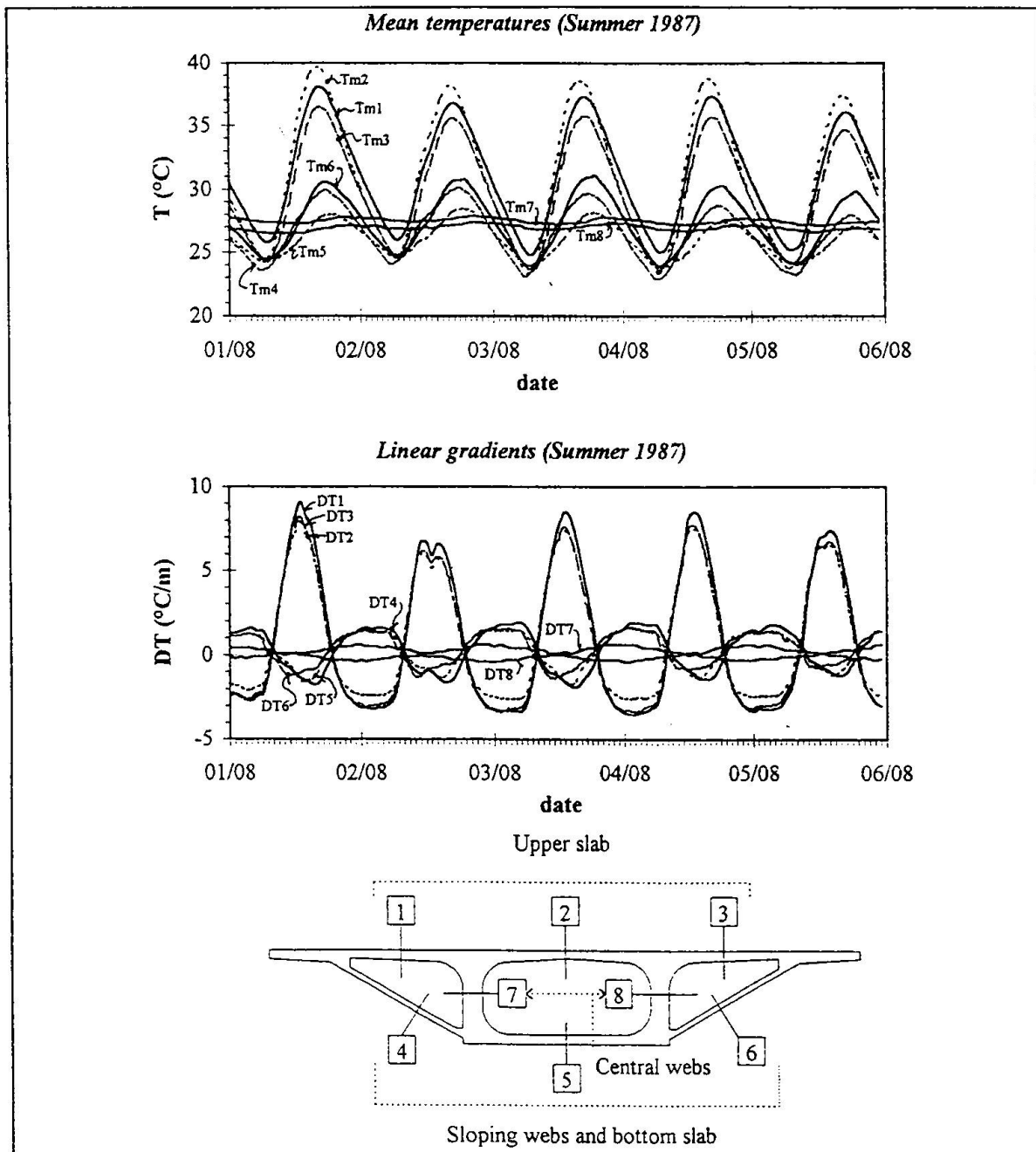
$$T_0 = \frac{T_{m7} + T_{m8}}{2}.$$

Fig. 3. Tipical summer daily distributions of the effective parameters mean and linear gradients within the wall elements of the cross section.

Similar considerations may be applied to the linear gradients thus obtaining the mean quantities DT_S, DT_I, DT_O.

It has been already said that the recording of the temperatures during the erection of the bridge allowed a reasonable evaluation of the absolute value and of the sign of the global thermal actions that the Casilina bridge experienced during the monitoring period and which are reported in reference [11].

This recording cannot be performed with respect to transversal thermal actions because no temperature measurement has been carried on during the concreting.

Nevertheless it is known that, even if the temperature field would change with time but remaining uniform at any instant all over the cross section, there would be a uniform expansion or contraction without any transversal effort. Transversal stresses occur at the generic instant t^* only when mean temperatures T_{mi} of the wall elements are different from each other and when the linear gradients DT_i and the quantities B_i are different from zero.
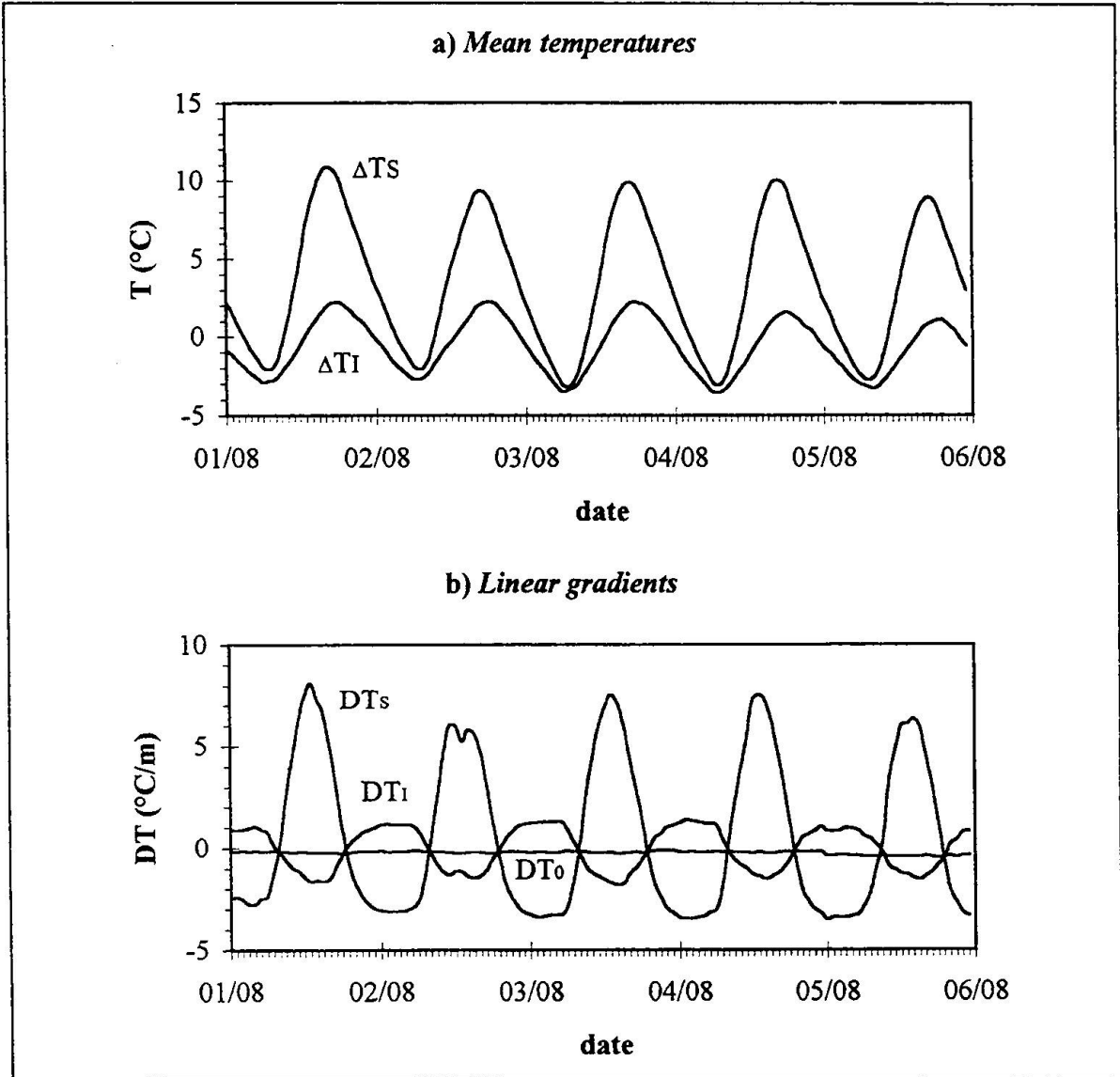

Fig. 4. *Hourly distributions of the daily variations of transverse thermal actions.*

Therefore, it is evident that in the present case, within the performed simplifications, the daily variations of the transversal efforts induced by mean temperature differences depend only on the following two quantities:

$$14) \qquad \Delta T_S = T_S - T_0 \qquad \Delta T_I = T_I - T_0 .$$

that may be than regarded as the daily variations of the local thermal actions "mean temperatures".

The daily variations of the thermal actions "linear gradients" can be calculated from DT_S, DT_I, DT_0 taking as reference those values at a certain time of the day when the gradients are all almost zero. This temporal reference is usually taken early in the morning when the temperature field is normally almost uniform [5], [6] as confirmed in figure 3 too.

Figure 4 collects two typical summer hourly distributions of the daily variations of transversal actions mean temperature and linear gradients.

In an attempt to evaluate also the absolute value and sign of transversal thermal actions, let us notice that precast segments have been placed in a sheltered, shadowed shed to assure a good curing. In the period subsequent to the early phase of the hardening process, where the temperature fields are greatly affected by the production of hydratation heat and are therefore strongly non-linear, it may be reasonably supposed that the temperature field was almost uniform over the cross section.

If this hypothesis is accepted, the daily distributions of the mean temperatures of figure 4 and of the linear gradients of figure 3 are to be regarded as very close to the absolute transversal thermal actions.

3. Transversal thermal efforts and stresses

The problem of the calculation of the stresses induced by assigned time dependent thermal actions in a concrete structure is very delicate because of the interactive relaxation effects of cracking and creep [12],[13].

Nevertheless, many authors have calculated the level of thermal stresses under the simple assumption of linear elastic behaviour of the reinforced concrete (see, for example ref.[5],[6],[14]).
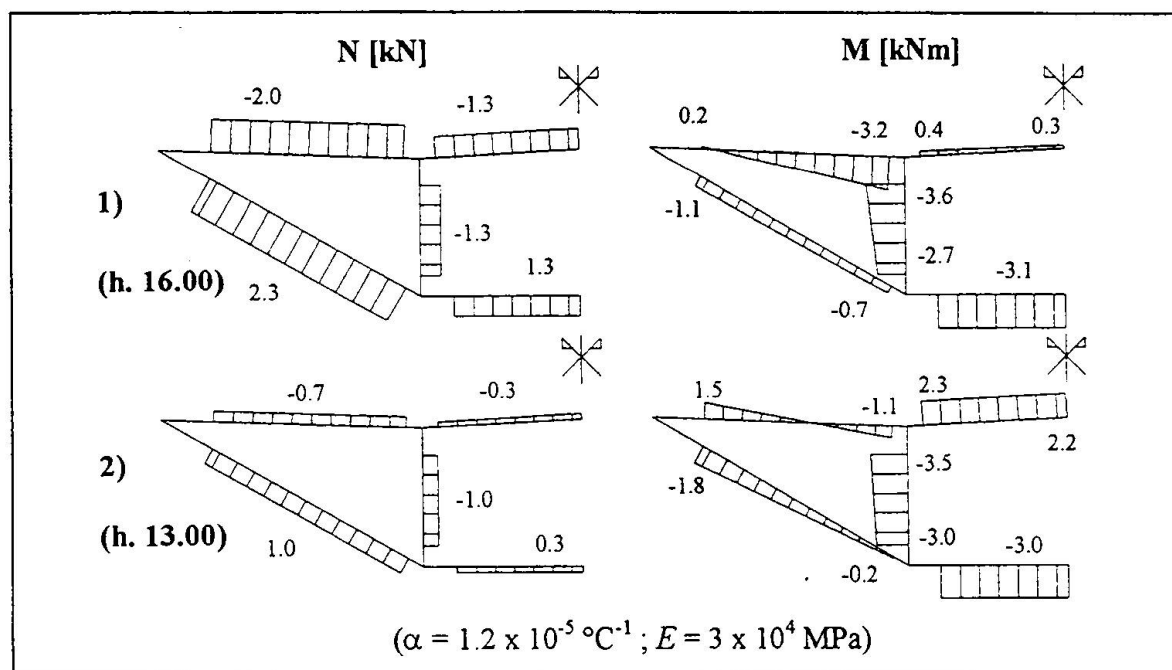

Fig.5. Elastic axial forces and bending moments due to thermal loading.

For this reason, in order that direct comparisons with other studies be made possible, some elastic calculations of transversal stresses have been executed schematizing the cross section as

a closed frame composed by wall elements of constant height and unit width rectangular cross section.

Two combinations of transversal thermal actions have been applied:

1) maximum daily variation of the mean temperatures with associated linear gradients and self-compensated, non-linear temperature distribution,

2) maximum daily variation of linear gradients with associated mean temperatures and self-compensated, non-linear temperature distribution.

Figure 5 illustrates the obtained results.

Table I indicates the primary and secondary elastic thermal stresses calculated at the outer surfaces of each wall element for both load conditions. Negative signs indicate compression.

	Load condition (1) 1/8/87, h16.00 ΔT_S= +7.5°C ; ΔT_I= 0°C ; DT_S= 8°C/m ; DT_I= -1.7°C/m [MPa]			Load condition (2) 1/8/87, h13.00 ΔT_S= 11°C ; ΔT_I= 2°C ; DT_S= 5°C/m ; DT_I= -1.5°C/m [MPa]		
(i)	σ'_c	σ''_c	$\sigma'_c + \sigma''_c$	σ'_c	σ''_c	$\sigma'_c + \sigma''_c$
1;3	-0.65	+0.30	-0.35	-1.30	-0.15	-1.45
		-0.32	-0.97		+0.14	-1.16
2	-0.07	+0.03	-0.04	-0.50	-0.22	-0.72
		-0.04	-0.11		0.22	-0.28,
4;6	-0.14	-0.32	-0.46	-0.14	+0.56	+0.42
		+0.35	+0.21		-0.54	-0.68
5	-0.36	-0.30	-0.66	-0.29	+0.29	0.00
		+0.31	-0.05		-0.29	-0.58
7;8	-0.07	+0.08	+0.01	+0.07	-0.09	-0.02
		-0.10	-0.17		+0.08	+0.15

Table I: Elastic primary (σ'_c) and secondary (σ''_c) transversal thermal stresses in the wall elements.

4. Conclusions

The daily changes of the transversal temperature actions have been obtained by a simple processing procedure of the in-situ collected temperature measurements performed on a concrete box girder bridge near Rome during three years of continuous monitoring.

A typical set of summer days with clear sky and a great amount of solar radiation has been considered as a significant climatic condition where the maximum daily variations of the transversal thermal actions and of the related elastic primary and secondary transversal thermal stresses are likely to be expected.

The resulting low magnitude of the thermal actions and of the calculated elastic thermal stresses, confirms the favourable transversal thermal behaviour of closed trapezoidal cross-sections where broad lateral cantilevers and a relevant slope of the lateral webs minimize the harmful effects of direct lateral solar radiation.

It has also confirmed the relative greater importance of primary transversal stresses in comparison with secondary transversal stresses.

Further research work is in course to assess the statistical meaning of these results. In deep box girder bridges with vertical webs, it has been found on the contrary that transversal thermal actions can reach a high intensity. Therefore, more research work was judged necessary within the Project Team on Part 2.6 of Eurocode 1 to assess reliable rules on this topic.

References

[1] B.PRITCHARD (Editor): "Continuous and Integral Bridges", Proc. of the Henderson Colloquium "Towards Joint-Free Bridges", organized by the British Group of I.A.B.S.E., Pembroke College, Cambridge, 20-21 July 1993, E&FN SPON, London 1994.

[2] F.LEONHARDT, G.KOLBE, J.PETER :"Temperaturunterschiede gefährden Spannbeton-brücke", Beton und Stahlbetonbau, H7, 1957.

[3] M.J.N.PRIESTLEY: "Model Study of a Prestressed Concrete Box Girder Bridge under Thermal Loading", Proc. I.A.B.S.E. 9th Congress, Amsterdam, 1972.

[4] F.FALTUS, M.SKAULOD: "Su alcuni insegnamenti da trarsi da alcuni dissesti di travate da ponte in lamiera irrigidita di acciaio", Costruzioni Metalliche, n.2, 1975.

[5] M.N.ELBADRY, A.GHALI: "Non linear Temperature Distribution and its Effects on Bridges", IABSE Proceedings P-66/83, International Association for Bridge and Structural Engineering, 1983.

[6] M.RAMEZANKHANI, P.WALDRON: "Segmental Construction of Bridges: Differential Temperature Effects in the Cogan Spur Viaduct", Report n° UBCE/C/91/10, University of Bristol, November 1991.

[7] E.MIRAMBELL, A.AGUADO, P.A.MENDES, F.A.BRANCO: "Design Temperature differences for Concrete Bridges", Structural Engineering International, n° 3, 1991.

[8] M.FROLI, N.HARIGA, G.NATI, M.ORLANDINI: "Indagine teorica e sperimentale sul comportamento termico del viadotto in c.a.p. Casilina: effetti longitudinali", Giornale A.I.C.A.P., Industria Italiana del Cemento, n°3, n°4, n°5, 1995.

[9] M.J.N.PRIESTLEY, S.J.THURSTON, N.COOKE: "Thermal analysis of Thick Concrete Sections", A.C.I. Journal, Sept.-Oct.1980.

[10] G.NATI: "Evaluation of Creep and Shrinkage Effects at Casilina Viaduct: Instrumentation used", I.A.B.S.E. Colloquium: "Monitoring of Large Structures and Assessment of Their Safety", Bergamo, October 1987.

[11] M.FROLI, N.HARIGA, G.NATI, M.ORLANDINI: "Longitudinal Thermal Behaviour of a Concrete Box Girder Bridge in Italy", in course of publication on Structural Engineering International.

[12] M.N.ELBADRY, A.GHALI: "Thermal Stresses and Cracking of Concrete Bridges", A.C.I.Journal, Nov.-Dec. 1986.

[13] J.WALRAVEN: "Temperature Stresses in Concrete Bridges", Proc. of the 3rd International Workshop on Bridge Rehabilitation, Technische Hochschule Darmstadt and University of Michigan, Ernst & Sohn , June14-17 1992.

[14] J.HEJNIC: "Thermal Stresses in Concrete Bridges", Proc. I.A.B.S.E. 13th Congress, Helsinky, 1988.

Leere Seite

Blank page

Page vide

Traffic Loads in EC-1. How do they suit to highway bridges in Spain?

César CRESPO-MINGUILLÓN
Civil Engineer, Research Assistant
School of Civil Engineering
Barcelona
Spain

César Crespo Minguillón, born 1969, got his civil engineering degree form the Technical University of Catalonia (UPC) in 1992. Since 1993 he has been a doctoral student at the UPC. His research field is the reliability of partially prestressed concrete bridges.

Juan R. CASAS
Dr. Civil Engineer, Associate Professor
School of Civil Engineering
Barcelona
Spain

Juan R. Casas, born in 1960, received his civil engineering degree from the Technical University of Catalonia (UPC) in 1984 where he completed his doctorate in 1988. Since then, he has been professor of bridge engineering at UPC. His research includes dynamic analysis and field testing of bridges as well as bridge reliability.

Summary

When the definitive draft of the EC-1 Part 3 appeared in Spain, there were several comments on the differences and difficulties that the new proposal presented with respect to the current Spanish National Standard for Traffic Actions on bridges. In this paper, the results of a simulation process of real Spanish traffic flow over several bridges, are shown and compared to the predictions of EC-1 for the same cases. At the end, some conclusions regarding the feasibility of EC-1 to represent Spanish Traffic Loads are drawn.

1. Introduction

The current Spanish National Standard for Traffic Actions over Bridges, recommends a traffic model for the design of new structures formed by a three-axles truck with a total weight of 600 KN, and a uniform distributed load of 4.0 KN/m². Since no failure has been related because of an excess over the capacity of any bridge in the Spanish roadways' net, it was thought that the new EC-1 proposal could lead to highly conservative predictions. Given the difference between what has been the common practice till now and the new proposal, and the absence of an objective calibration of the present National Standard, a research project was planned to study real traffic actions over Spanish bridges, at the School of Civil Engineering in Barcelona [1]. One conclusion of this study will be a proposal for the set of adjusting factors α_i that EC-1 includes for each relevant authority to adapt EC-1 model to every specific traffic.

In this paper, the first results and conclusions of this research are shown. They are presented as a comparison between the results of a simulation of real flows of Spanish traffic over four representative bridges, and the results that EC-1 model predicts for these same cases. The values to compare, will be those obtained for different return periods. These specific return periods are: one week, (what EC-1 calls the frequent value), one year, (the infrequent value in EC-1), and one thousand years, (which corresponds to the value that has a probability of 10 per cent of being exceeded in one hundred years and is called the characteristic value by EC-

1). To quantify the differences, one bridge will be designed with the frequent values predicted by the simulation and EC-1 model, for the verification of the SLS of decompression. The total amount of postensioning steel area in both cases, will be compared, as well as their reliability in front of the ULS of bending.

2.   Traffic model and simulation conditions

The simulation traffic model used, was originally created for the analysis of the fatigue performance of bridges [2]. So, it is a simulation model of real traffic flow. It is composed by two algorithms. First one, creates a fictitious traffic record and the second manages the pass of the vehicles of this record over the length of the bridge. The structure is taken into account as a surface of influence of the studied effect.

To include all the uncertainties inherent to the traffic phenomenon, a statistical treatment is given to the main variables that characterizes traffic action, e.g. type of each vehicle arriving, its gross weight, its distribution between the axles, the total length, its distribution to each pair of axles, its velocity, time of arrival, etc. [2]. To define all these variables, real Spanish traffic records have been used. Another important trait of the traffic model, is that different operations such us: to brake, to accelerate, to pass other vehicles, etc. are permitted to account for the interrelation between vehicles of different lanes.

Given that EC-1 tries to represent very heavy traffic conditions in Europe, the simulation of Spanish traffic is based on the heaviest conditions encountered in Spanish highways. These conditions can be found in the industrial zones of the Metropolitan Area of Barcelona, and have been translated into an average daily traffic of 20000 vehicles per day, with a 30 per cent of trucks in a roadway with two lanes in the same direction. It has been considered that one week traffic could be taken as the representative time [3], and two hundred weeks of traffic have been simulated for each case.

3.   Examples and results

In fig. 1, the longitudinal layouts of the analysed structures, and their cross-sections are shown. They are: a continuous box girder bridge (CB), a continuous slab bridge (CS), a simply supported bridge formed by precast beams with an in-situs cast slab (SB) and a simply supported slab bridge (SS). In the continuous bridges both, the section over support and the one at midspan of the main span, were studied. In the simply supported, only midspan sections were analysed.

Once the simulation processes had been run, two hundred values corresponding to maximum weekly effects were available. These data were used to extrapolate to the values of the studied effect that corresponded to the different return periods. The methodology used for this extrapolation, is based on the study of tail probabilities through the analysis of extreme order statistics with Generalized Pareto Distributions [4], [5]. The final results are presented in table 1. Always, the calculated bending moments include the specific bridge's coefficient of eccentricity, (relation between the maximum and mean stresses in the whole cross-section).
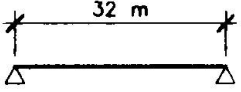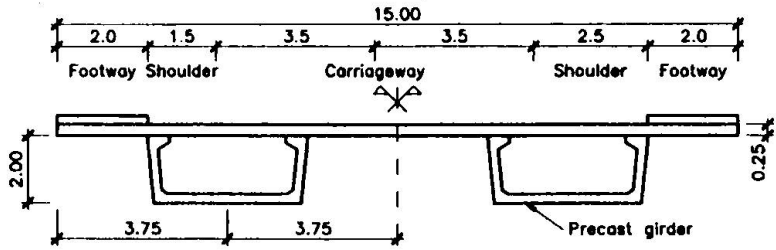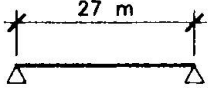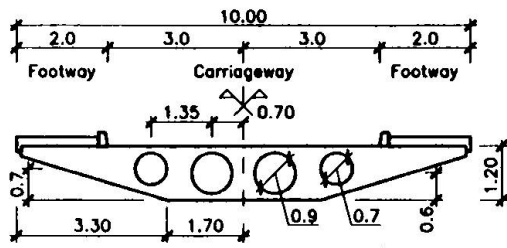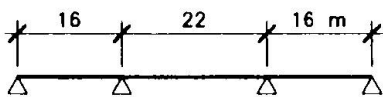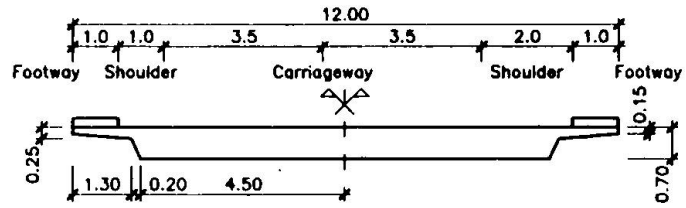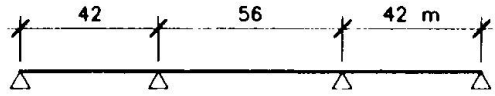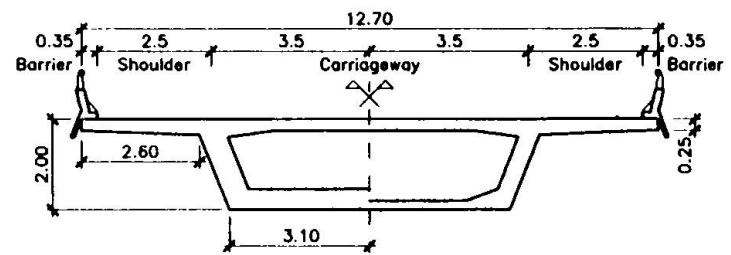
Bridge	Longitudinal profile	Cross—section
SB	32 m	15.00 — 2.0 Footway / 1.5 Shoulder / 3.5 Carriageway / 3.5 / 2.5 Shoulder / 2.0 Footway; 2.00; 0.25; 3.75 / 3.75; Precast girder
SS	27 m	10.00 — 2.0 Footway / 3.0 Carriageway / 3.0 / 2.0 Footway; 1.35 / 0.70; 0.7; 1.20; 3.30 / 1.70; 0.9 / 0.7; 0.6
CS	16 / 22 / 16 m	12.00 — 1.0 / 1.0 Footway Shoulder / 3.5 Carriageway / 3.5 / 2.0 Shoulder / 1.0 Footway; 0.15; 0.25; 0.70; 1.30 / 0.20 / 4.50
CB	42 / 56 / 42 m	12.70 — 0.35 Barrier / 2.5 Shoulder / 3.5 Carriageway / 3.5 / 2.5 Shoulder / 0.35 Barrier; 2.00; 0.25; 2.60; 3.10

Figure 1. Layout and cross-sections of the studied bridges.

Bridge	Method	Return Period			
		1 week	2 weeks	1 year	1000 years
CBM	Simulation	7655.	9798.	11926.	18428.
	EC-1	13994.		19145.	23931.
CBS	Simulation	6507.	7639.	9782.	14258.
	EC-1	12134.		19006.	23758.
CSM	Simulation	2157.	2785.	3687.	5520.
	EC-1	4257.		5168.	6460.
CSS	Simulation	1757.	2294.	2792.	4565.
	EC-1	3200.		4368.	5460.
SB	Simulation	6748.	9621.	11861.	18273.
	EC-1	11039.		14294.	17867.
SS	Simulation	5130.	6937.	8499.	13709.
	EC-1	7064.		9202.	11503.

Table 1. Comparison of results from EC-1 and simulation (in KNxm).

Suffixes M and S added to the continuous bridges' notation, mean the sections at midspan of main span and over intermediate support, respectively.

As it was explained above, the result of the extrapolation to one thousand years corresponds to the value with 0.10 probabilities of being exceeded by the maximum effect in 100 years. To get this result, the parameters of the assumed Gumbel distribution of the maximum effect in 100 years were first calculated. These parameters were obtained through a simulation based on a wide, but particular, set of data. Because of this, and to account for possible not-considered conditions, it was decided to assume the calculated mean of the distribution as a true value but its coefficient of variation, (which was around the 7 per cent in all cases), was increased to the 12 per cent.

From the results of simply supported bridges, it can be seen that, although the predictions for the characteristic maximum value in 100 years from simulation are greater than those calculated with EC-1, the predictions for shorter return periods are lower. This shows that the methodology and the set of coefficients proposed to get the frequent and infrequent values of the traffic action, do not apply to the Spanish traffic particularities.

In continuous bridges, it can be seen that the results predicted by EC-1 for a return period of one week, are, in average, 85 per cent higher than those resulting from simulation. The results for a return period of one year are around 60 per cent higher and those corresponding to the return period of one thousand years, are 25 per cent greater. These excesses are more

important in the sections over support than in midspan.

In the simply supported bridges, the differences are lower and, for the return period of one thousand years they are even negative. One reason that contributes to have a higher value predicted by simulation than by EC-1, in the beams' bridge (SB), is the coefficient of eccentricity. It is significantly greater for the case of a single lorry (as in the simulation), than for the set of three tandems proposed by Eurocode, placed side by side (the difference was 1.40 to 1.20). In the simply supported slab (SS), one of the reasons for having lower results from EC-1 than from simulation is its narrow traffic section (only 6.0 metres). The first consideration that could be made is about if it is acceptable that a bridge over which are expected to cross 6000 trucks per day has no shoulders. The second could be about if it is acceptable that 20000 vehicles with a 30 per cent of heavy vehicles crossed over an urban bridge as this seems to be. This example was chosen to show a possible case of a bridge that suffers very heavy traffic conditions when it was not originally thought for them. Could this bridge be assessed using the EC-1 traffic model to define the external action? The conclusion is clearly negative. This example also shows that EC-1 predictions depend on the width of the roadway platform, no matter how many real lanes are defined on the structure.

The analysis of the line of influence of the positive bending moment at midspan of the continuous box girder bridge (CB), of spans' lengths 42, 56, 42 metres respectively, shows a maximum of value around 9.0, at the centre of the main span. This value would also correspond to the maximum of the influence's line of a single span bridge of 36 metres length. So, in both cases, the maximum positive bending moment caused by an axial load would be the same. With a uniformly distributed load, it would not have happened like this. Because of the main continuous span is longer than the simply supported one, the contribution of the distributed load to the maximum positive bending moment would be more important in the continuous bridge that in the other. Given that 1) the results predicted by EC-1 in the case of this continuous bridge are greater than those resulting from simulation, 2) in the case of the simply supported bridge of 32. metres long it happens the contrary and 3) the effect of the tandems of EC-1 to its final predictions can be assumed to be similar in both cases, it can be concluded that the relative contribution of the distributed load seems to be too large in the continuous bridge.

To quantify the differences between the EC-1 predictions and the results of the simulation of the heaviest traffic conditions in Spain, the continuous slab bridge, (CS), was designed using both, the frequent value proposed by EC-1 and that corresponding to a return period of one week from the simulation. The representative values of the variable actions to use in the frequent combination to verify the SLS of Decompression, were calculated following the EC-2 recommendations, and are shown in table 2. The total amounts of postensioned steel area are shown in table 2, as well as the reliability indexes in front of the ultimate limit state of bending for both cases. The external traffic action adopted for both evaluations, corresponds to the results of the simulation of real traffic in Spain, considering two lanes.

Method	M_{sw}	M_{dl}	M_{temp}	M_{traf}	$A_s(cm2)$	$F_\infty(KN)$	M_{prest}	β_u
Simulation	4219.	529.	902.	2157.	201.6	24122.	1165.	6.34
EC-1	4219.	529.	902.	4257.	252.0	29015.	1404.	7.11

(sw = self weight, dl = dead load)

Table 2. Design of the continous slab with traffic results of EC-1 and simulation, (in KNxm)

The results show that the security in front of the ultimate limit state of bending of these postensioned concrete bridges designed with a SLS verification criteria, is higher than what can be assumed as the minimum necessary, $\beta_u = 4.5$. So, the worldwide common practice of imposing SLS verifications for the design of new postensioned concrete bridges, leads to an excess of postensioning steel area. Therefore, it appears to be necessary to analyse the reasons why this practice is maintained. This study should reflect in quantitative terms, what negative effects for the security or for the functional service of the bridge, does this extended practice prevent the structures from. It has been the object of a parallel research [2],[6].

4.   Conclussions

From the comparison of the results derived from the simulation of Spanish traffic and those predicted by EC-1 part 3, the following conclussions derive:

- Predictions of values of traffic effects for short return periods, using EC-1 are much higher that those from simulation, even in the case of simulating very heavy traffic conditions in Spain. Given their importance when designing a new structure, it is the authors opinion that further research should be carried in Spain to analyse a possible modification of the coefficients ψ_i proposed by Eurocode for the combinations of variable actions leading to these short time return periods (frequent and infrequent values). This modification should be based on quantifiable criteria instead of the subjective and qualitative current criteria, [6]. On the other hand, there is no justification for the placement of fictitious tandems or vehicles in all physically-possible lanes when calculating short terms representative values.

- Further research is needed in order to set definitive conclussions for a proposal for the adjusting factors (α_i) to apply to the representative magnitudes of the traffic load systems in EC-1, to addapt them to Spanish traffic conditions. The simulation presented in this paper, reflects very heavy traffic conditions. Since 70 per cent of bridges in Spain are placed in roadways with much lighter conditions, it could be interesting to study the possibility of defining those adjusting factors as a function of the roadway's traffic characteristics. This research is now in progress [1].

- It should be deeper studied if it is appropiate to divide the real platform into notional lanes for the calculation of representative values of the effects of traffic action. This practice leads to unsafe results in the assesstment of the bearing capacity of old narrow bridges. This consideration illustrates again the need for specific live load models (or correction coefficients) for the assessment of existing bridges. It also can result in unsafe predictions for bridges with

high coefficients of eccentricity, e.g. precast girders, double T sections, etc.

- The relative contribution of the distributed load has been found to be too large for continous bridges in Spain. So, it seems that the relative weight that the uniformly distributed load system has in the EC-1 model for traffic actions, should be decreased. This decrease would lead to very significant drops in the predictions for maximum negative bending moments over supports, closing them to the results from simulation.

5. Acknowledgements

6. References

1. Casas, J.R. and Crespo-Minguillón, C.. *On the definition of a Traffic Model for Spanish Highway Bridges. Comparison to EC-1.* Research Project PB-1199 in progress at the Technical University of Catalonia.

2. Crespo-Minguillón, C.. *A reliability based methodology to define the Limit State of Decompression in prestressed concrete bridges.* Ph. D. Thesis. Dept. of Construction Engineering. Technical University of Catalonia. To be published in 1996.

3. Jacob, B. and Jiang, L.. *Probability Fatigue Reliability.* ICOSSAR 93. 6th Int. Conf. on Structural Safety and Reliability, pp. 1075-1081. Innsbrück. August 1993.

4. Maes, M.A. *Tail Heaviness in Structural Reliability.* Proceedings Applications of Statistics and Probability. ICASP, pp. 997-1002. Paris. 1995.

5. Dargahi-Noubary, G.R. *New Method for Prediction of Extreme Wind Speeds.* Journal of Engineering Mechanics. Vol 114. No. 4. Pp. 859-866. April, 1989.

6. Crespo-Minguillón, C., Casas, J.R. *Reliability Criteria for the SLS of Cracking in Prestressed Concrete Bridges.* 15th IABSE Congress. Copenhagen. June 1996.

Leere Seite

Blank page

Page vide

NAD for Traffic Load on Bridges

**Charlotte Togsværd v
SCHOLTEN**
Civil Engineer, M.Sc.
Road Directorate
Copenhagen
Denmark

Charlotte Togsværd v Scholten, born in 1961, obtained her M.Sc. Degree in Civil and Structural Engineering from the Technical University of Denmark in 1987. From 1987 to 1994 employed by RAMBØLL, Bridge Department engaged with the Great Belt Bridge, motorway bridges, Eurocodes, etc. From 1994 employed with the Road Directorate, Bridge Department.

Summary

The first draft of a Danish National Application Document for ENV 1991-3:"Eurocode 1 - Basis of design and actions on structures - part 3 : Traffic load on bridges" was issued in September 1995 for the road and footbridge part. The ENV 1991-3 with the NAD will when published replace the existing Danish requirements. Some modifications of the loading models have been introduced in the NAD and the load safety factors have been adjusted in order to be consistent with the material safety factors defined in the Danish codes. The Eurocode safety level is kept unchanged. The set of models of special vehicles is considered in relation to the classification of existing bridges. Simple calculations have been made to clarify the consequences of introducing the Eurocodes for the design of bridges in Denmark. Only insignificant changes in cost and safety are involved.

1. Introduction

A National Application Document for ENV 1991-3 :"Eurocode 1 - Basis of design and actions on structures - part 3 : Traffic load on bridges" is in preparation by the Road Directorate in Denmark for the road and footbridge part. The first draft was issued in September 1995 and the final version is expected to be completed in the autumn of 1996.

It is the intention that the final NAD shall cover railway as well as road and footbridge loadings. Railway bridges are not included in this paper because the responsibility for preparation of the NAD is divided between the Road Directorate and the Danish Railways, each authority covering its own field. Before publication, the contributions from the Danish Railways and the Road Directorate will be adjusted in order to avoid inconsistencies in the final document.

In this paper the implementation of the Eurocode with the corresponding NAD is discussed. Some of the main subjects to be decided on in the NAD are discussed and the adjustments described.

2.   Objective

The objective of the NAD is to adjust the ENV 1991-3 to the design of small and medium size bridges in Denmark. The aim is to limit the additions and changes to ENV 1991-3 as far as possible, as this will make the full transition to a uniform Eurocode system easier.

3.   Implementation

It is the policy of the Road Directorate in Denmark to implement the Eurocodes for design and execution of structures and other works related to roads as soon as possible after publication. The argument is that bridges and roads are influenced by developments in other European countries, especially the neighbouring countries Sweden and Germany. Since the traffic crosses the borders more or less freely it is obvious that the loadings and the safety requirements should be equalized. Furthermore, it is preferable to spend time and money in adjusting the Eurocodes to Danish requirements rather than preparing new Danish documents.

It is the intention to implement the ENV 1991-3 together with the Danish NAD as soon as these documents are ready for use. This shall of course be seen in relation to other codes in use at the time of issue. For example, it would be advantageous if the Eurocodes for Design of Concrete and Steel Bridges were to be implemented simultaneously with the Eurocode for Loadings on Bridges.

A Road Regulation is a collection of requirements and/or instructions for the design of a specific bridge/road item, prepared and issued by the Danish Road Directorate. In the future Road Regulation for design of bridges it will be stated which codes are to be used and, if necessary, supplementary instructions will be given. In this way we hope to be able to make the use of ENV 1991-3 together with ENV 1991-2 : "Eurocode 2 part 2 : Design of Concrete Bridges" obligatory in 1996. The Road Regulation will thereafter be updated in accordance with the development of the relevant Eurocodes.

4.   Safety

As stated above it has been the intention to limit the NAD adjustments of the Eurocode as far as possible. Due to this as well as consequence evaluations it was therefore decided to maintain the Eurocode safety level in the Danish application. In order to do so, the partial safety factors and the reduction factors as well as the different loading combinations are in principle kept unchanged.

It is crucial that the system of partial safety factors in ENV 1991-3 be compatible with the other Eurocodes and NADs to be used in the design of bridges. In the preparation of Danish NADs for ENV 1992-1 and ENV 1993-1 it was decided to convert the values of the material partial safety factors into the present Danish values. This is expected also to be done for Part 2 concerning bridge structures. In order to keep the safety level unchanged an adjustment factor is introduced. By multiplying this factor on the load partial

safety factors as specified in the Eurocode safety system, these safety factors will be more or less consistent with the material safety factors defined in the Danish system and transferred to the Danish NADs.

The value of the adjustment factor is obtained as the ratio between the material partial safety factors given in the Eurocode and the corresponding values given in the Danish code. Since the these ratios vary from material to material, an average value has been selected. This will result in some variation in safety between the different materials. This variation is assessed to be insignificant. It should be noted that the use of this adjustment factor is strictly valid only for linear limit states.

A framework with all load combinations to be considered has been set up in order to facilitate the engineers' work and to avoid errors and misunderstandings. An example of such a framework is given in Figure 4.1.

EC Safety System

Ultimate Limit State (ULS):

Load Combinations for In-service situations: $\sum \gamma_{Gj} G_{kj} + \gamma_P P_k + \gamma_{Q1} Q_{k1} + \sum \gamma_{Qi} \Psi_{0i} Q_{ki}$

Load Combination	a	b	c	d	e	f	g	h	i	j	k
Permanent Loads											
Dead Load	1.00/1.35	1.00/1.35	1.00/1.35	1.00/1.35	1.00/1.35	1.00/1.35	1.00/1.35	1.00/1.35	1.00/1.35	1.00/1.35	1.00/1.35
Superimposed Dead Load	1.00/1.35	1.00/1.35	1.00/1.35	1.00/1.35	1.00/1.35	1.00/1.35	1.00/1.35	1.00/1.35	1.00/1.35	1.00/1.35	1.00/1.35
Earth Pressure	1.00/1.35	1.00/1.35	1.00/1.35	1.00/1.35	1.00/1.35	1.00/1.35	1.00/1.35	1.00/1.35	1.00/1.35	1.00/1.35	1.00/1.35
Prestressing	1.00	1.00	1.00	1.00	1.00	1.00	1.00	1.00	1.00	1.00	1.00
Settlements of supports	1.00	1.00	1.00	1.00	1.00	1.00	1.00	1.00	1.00	1.00	1.00
Variable Loads											
Traffic Load											
g1: LM1: TS	1.35	0.75x1.35=1.01			1.01		(1.01)	1.01	1.01	1.01	1.01
UDL	1.35	0.40x1.35=0.54			0.54		(0.54)	0.54	0.54	0.54	0.54
Footway/Cycle tracks	1.35										
g2: Braking and Acceleration Forces, Centrifugal Forces	0.40x1.35=0.54	1.35									
g3: Footway/Cycle tracks			1.35								
g4: LM4: Crowd Loading Footway/cycle tracks				1.35 1.35							
g5: LM3: Special vehicles						1.35					
g6: LM2: Single Axle Load							1.35				
Wind Load: F_w	0.35x1.90=0.67	0.67	0.67	0.67	0.67		1.90	0.67		0.67	0.7x1.9=1.33
(F_w)	(1.0x1.9=1.90)	(1.90)	(1.90)	(1.90)	(1.90)			(1.90)		(1.90)	(1.90)
Temperature Effects										1.50	
Horizontal Mass Load									1.50		
Ice Load										1.50	
Wave and Current Loads							0.7x1.5=1.05				1.50

Figure 4.1

In order to be able to compare the Eurocode load combinations, safety factors and reduction factors inclusive, with the Danish load combinations, a second adjustment factor is introduced. This adjustment factor has arisen from the difference in the return periods on which the characteristic load values are based. ENV 1991-3 has based its definition of the road traffic loads on 1000-year return periods (90% fractile, reference period 100 years), whereas the Danish code uses a 50-year return period (98% fractile, reference period 1 year). An adjustment factor has been estimated from calculations based on assumptions concerning the traffic load distribution.

5.   Loading models

The present Danish load models are in principle very similar to those given in ENV 1991-3.

The main loading system in the Danish model consists of two three-axled vehicles, one with a total load of 780 kN and the other with a total load of 390 kN. The heavy vehicle is defined in order to take heavy vehicles moving with the normal traffic into consideration. The uniformly distributed load in lane 1 is somewhat larger in ENV 1991-3 than in the Danish rules but the positioning is the same. The difference between the Danish rules and the Eurocode is significant only for small bridges and for local effects.

The Danish rules include a single load of 260 KN for local effects, similar to that of ENV 1991-3 load model 2.

A set of models of special vehicles forms the basis of the classification of existing bridges in Denmark. This classification system is a very important tool for the administration of heavy vehicles moving with the normal traffic (see below). The present Danish classification system is described in a Road Regulation, separate from the bridge design Road Regulation.

In order to evaluate and adjust the load models given in ENV 1991-3, bridge classes were defined similar to the bridge classes in the Danish regulations. Three classes are defined in the NAD :

Bridge class 1 :   Road bridges for public roads with normal traffic and for privately-owned common roads with equivalent traffic.

Bridge class 2 :   Road bridges for privately-owned common roads and public roads with light traffic only.

Bridge class 3 :   Footbridges with only pedestrian and cycle traffic.

Considering the main loading system (load model 1), the first approach in the NAD is to apply the following α-values :

Bridge class 1 : $\alpha_{Q_i} = 1.0$ and $\alpha_{q_l} = 1.0$

Bridge class 2 : $\alpha_{Q_i} = 0.8$ and $\alpha_{q_l} = 3.0/9.0$

For bridge class 1 it is under consideration to set $\alpha_{q_l} = 6.0/9.0$ and in addition to require design for special vehicle class 900/150 (load model 3). This is believed to be more in agreement with future traffic intensities in Denmark and with the Danish tradition of designing for a heavy special vehicle moving freely around in the traffic.

For the single axle load (load model 2) located in the most adverse position on the carriageway, $\beta_Q = 0.8$.

The set of special vehicles (load model 3) has not been evaluated in detail so far, because it is of little relevance for the present design of bridges. In the long term it may become relevant for heavy vehicles (see below).

Amendments to centrifugal forces are under consideration and a lateral force such as side-impact will probably be included in the NAD.

When looking upon fatigue load models generally, the traffic intensity given in ENV 1991-3 Table 4.5 has to be decreased considerably for the design of Danish bridges. As a first approach, values from the Great Belt Bridge Basis of Design, and the values given in the present Road Regulations are applied, but further investigations may be carried out in the near future.

The fatigue load models 2 and 3 are considered not applicable, and the number of lorries to be investigated in load model 4 is reduced from five to two, as can be seen in Figure 5.1. The Table shown has to replace Table 4.7 in ENV 1991-3.

Only the first lorry (axle loads 70 and 130 kN) and the third lorry (axle loads 70, 150, 90, 90 and 90 kN) should be considered.

The percentage of the two standard lorries in the traffic flow should be taken as :

Lorry (axle loads)	Long Distance	Medium Distance	Local traffic
	Lorry Percentage	Lorry Percentage	Lorry Percentage
70 and 130 kN	20	50	80
70, 150, 90, 90 and 90 kN	80	50	20

Figure 5.1

6.   Classification of existing bridges

A bridge classification system is in use for handling heavy transports in Denmark.

The Basis of Design for Bridges has changed significantly through the years, from no design basis at all to the detailed rules we have today. The existing bridges in Denmark therefore have different capacities for the passage of heavy vehicles. In order to administer applications for permission to pass with vehicles that exceed the limits given in the traffic regulations it is necessary to have a consistent and unambiguous classification system covering both bridges and vehicles.

Because of international road traffic this is an important European matter; we would therefore like to have a European classification system. Whether it is possible to convert the series of standard vehicles into the series of ENV 1991-3 load model 3, and thus to take the first step towards a common European system, is to be investigated.

7.   Evaluation of consequences

A preliminar comparison between bridge design according to Eurocodes and bridge design according to the present Danish rules was made in spring/summer of 1994. NAD amendments were not taken into consideration.

The consequences were determined from the static loadings only. Dynamic loading and fatigue were not taken into consideration. Normally dynamic loading and fatigue have no effects on reinforced concrete bridges, but they have considerable effects on steel bridges.

The following conclusions were derived from the investigation:

-       There is no significant difference in the safety level obtained by design according to Eurocode and Danish requirements/codes.

-       The above applies to both dead load-dominated cases and live load-dominated cases.

-       There is no significant change in the quantity of construction material.

-       There is no change in the relative competitiveness of concrete and steel bridges.

When comparing design of prestressed bridges according to Eurocodes and Danish codes the conclusions derived above still apply.

Since the adjustments of ENV 1991-3 in the Danish NAD do not have any influence on the safety level, the consequences when considering the NAD are more or less the same as those for the Eurocode itself.

More detailed calculations and comparisons have to be made before it is possible to clarify the full consequences of designing Danish bridges according to Eurocodes. Since most of the Danish small to medium-size bridges are of reinforced concrete, interest is primarily focused on this bridge type, but it is of course important also to clarify the consequences for steel bridges. It will be of great interest to see whether the bridge class (heavy vehicles) according to the Danish classification system changes with the change from Danish design regulations to Eurocodes.

The detailed investigations will be carried out after the entire set of Eurocodes for the design of bridges, including the corresponding NADs, has been issued.

New Generation of U.S. Bridge Design Codes

Andrzej S. NOWAK
Professor of Civil Engineering
University of Michigan
Ann Arbor, MI
USA

John M. KULICKI
Senior Vice-President
Modjeski & Masters
Harrisburg, PA
USA

Andrzej S. Nowak received his PhD from Warsaw University of Technology, Poland, and has been at University of Michigan since 1979. He has been involved in reliability-based development of the LRFD bridge design codes in the United States and Canada.

John M. Kulicki received his PhD from Lehigh University in 1974. He has over 25 years of bridge design experience. He was selected to lead a 50-member team of experts to develop a new LRFD bridge design specification which was adoped by AASHTO in 1993.

Summary

The paper presents the development of a new load and resistance factor design (LRFD) bridge code in the United States. It is based on a probability-based approach. Structural performance is measured in terms of the reliability index. The major steps include selection of representative structures, calculation of reliability for the selected bridges, selection of the target reliability index and calculation of load and resistance factors. Load and resistance factors are derived so that the reliability of bridges designed using the proposed provisions will be at the predefined target level.

1.   Introduction

The need for a new bridge design code in the United States was formulated as a result of an earlier NCHRP Project 20-7/31. The objectives in the development of this new specification may be summarized as:

- To develop a technically state-of-art specification which would put U.S. practice at or near the leading edge of bridge design.

- To make the specfication as comprehensive as possible and include new developments in structural forms, methods of analysis and models of resistance.

- To the extent consistant with the thoughts above, keep the specfication readable and easy to use, bearing in mind that there is a broad spectrum of people and organizations involved in designs.

- To keep specification-type wording.

- To encourage a multi-disciplinary approach to bridge design, particularly in the area of hydraulics and scour, foundation design and bridge siting.

- To place increasing importance on the redundancy and ductility of structures.

Many changes had to be made in the content and appearance of the AASHTO Standard Specifcication (1992) to achieve the objectives outlines above. The major changes are identified below:

- The introduction of a new philosophy of safety.
- The identification of four limit states.
- The development of new load factors.
- The development of new resistance factors.
- The relationship of the chosen reliability level, the load and resistance factors, and load models through the process of calibration.
- The development of improved load models necessary to achieve adequate calibration, including a new live load model.
- Revised techniques for analysis and the calculation of load distribution.
- A combined presentation of plain, reinforced and prestressed concrete.
- The introduction of limit state-based provisions for foundation design and soil mechanics.
- Expanded coverage on hydraulics and scour.
- Changes to the earthquake provisions to eliminate the seismic performance category concept by making the method of analysis a functions of the importance of the structure.
- Inclusion of large portions of the Guide Specification for Segmental Concrete Bridge Design.
- Inclusion of large portions of the FHWA Specfication for ship collision.
- Expanded coverage of bridge rails based on crash testing, with the inclusion of methods of analysis for designing the crash specimen.
- The introduction of the isotropic deck design process.
- The development of a parallel commentary.

The objective of this paper is to present the calibration procedure, in particular calculation of load and resistance factors for the ultimate limit states. The resistance factors are considered for slab on girder bridges including non-composite and composite steel girders, reinforced concrete T-beams and prestressed concrete AASHTO type girders.

2. Calibration Procedure

The calibration procedure was developed as a part of the project FHWA/RD-87/069 (Nowak et al. 1987). In this project, the work on the new bridge design code was formulated including the following steps:

(a) Selection of representative bridges

About 200 structures are selected from various geographical regions of the United States. These structures cover materials, types and spans which are characteristic for the region. Emphasis is placed on current and future trends, rather than very old bridges. For each selected bridge, load effects (moments, shears, tensions and compressions) are calculated for various components. Load carrying capacities are also evaluated.

(b) Establishing the statistical data base for load and resistance parameters.

The available data on load components, including results of surveys and other measurements, is gathered. Truck survey and weigh-in-motion (WIM) data are used for modeling live load. There is little field data available for dynamic load therefore a numerical procedure is developed for simulation of the dynamic bridge behavior. Statistical data for resistance include material tests,

component tests and field measurements. Numerical procedures are developed for simulation of behavior of large structural components and systems.

(c) Development of load and resistance models.

Loads and resistance are treated as random variables. Their variation is described by cumulative distribution functions (CDF) and correlations. For loads, the CDF's are derived using the available statistical data base (Step b). Live load model includes multiple presence of trucks in one lane and in adjacent lanes. Multilane reduction factors are calculated for wider bridges. Dynamic load is modeled for single trucks and two trucks side-by-side. Resistance models are developed for girder bridges. The variation of the ultimate strength is determined by simulations. System reliability methods are used to quantify the degree of redundancy.

(d) Development of the reliability analysis procedure.

Structural performance is measured in terms of the reliability, or probability of failure. Limit states are defined as mathematical formulas describing the state (safe or failure). Reliability is measured in terms of the reliability index, β. Reliability index is calculated using an iterative procedure. The developed load and resistance models (Step c) are part of the reliability analysis procedure.

(e) Selection of the target reliability index.

Reliability indices are calculated for a wide spectrum of bridges designed according to the current AASHTO (1992). The performance of existing bridges is evaluated to determine whether their reliability level is adequate. The target reliability index, β_T, is selected to provide a consistent and uniform safety margin for all structures.

(f) Calculation of load and resistance factors.

Load factors, γ, are calculated so that the factored load has a predetermined probability of being exceeded. Resistance factors, ϕ, are calculated so that the structural reliability is close to the target value, β_T.

3. Load and Resistance Models

Load and resistance parameters are random variables. For prestressed concrete bridges the statistical models of resistance were developed by Nowak, Yamani and Tabsh (1994), Tabsh and Nowak (1991) and Nowak and Yamani (1995). Bridge load models were developed by Nowak (1995), Nowak and Hong (1991), and Hwang and Nowak (1991).

It was determined, that the bias factor (ratio of mean to nominal) for dead load is $\lambda = 1.03\text{-}1.05$, and coefficient of variation is $V = 0.08\text{-}0.10$. For live load, $\lambda = 1.6\text{-}2.1$ (depending on span length) and $V = 0.12$. The nominal live load is represented by HS-20 truck (AASHTO 1992). HS20 loading consists of either three axles: 35kN, 142kN and 142kN, spaced at 4.3m, or a uniformly distributed lane load of 9.3kN/m with a moving concentrated force of 80kN. In the new LRFD AASHTO Code (1994), live load is a combination of HS-20 truck and a uniformly distributed load of 9.3 kN/m. Therefore, the bias factor for live load is $\lambda = 1.25\text{-}1.35$. Dynamic load associated with an extreme value of truck load is about 0.10-0.15 of the static portion of live load, with $V = 0.80$. For a combined static and dynamic live load $V = 0.18$.

The basic random variables considered in development of resistance models are dimensions, concrete compressive strength, and properties of structural steel, prestressing and non-

prestressing strands. The parameters for moment carrying capacity are $\lambda = 1.12$ and $V = 0.10$, for non-composite and composite steel girders, $\lambda = 1.14$ and $V = 0.13$, for reinforced concrete T-beams, and $\lambda = 1.05$ and $V = 0.075$, for prestressed concrete AASHTO-type girders. For shear capacity the parameters are $\lambda = 1.14$ and $V = 0.105$ for steel girders, $\lambda = 1.20$ and $V = 0.155$ for reinforced concrete T-beams, and $\lambda = 1.15$ and $V = 0.14$ for prestressed concrete AASHTO-type girders.

4. Reliability Analysis Procedure

Reliability indices, β, are calculated using a specially developed computer procedure based on the first order reliability method. The available reliability methods are reviewed in several textbooks (Thoft-Christensen and Baker 1982). The methods vary with regard to accuracy, required input data, computational effort and special features (time-variance). In some cases, a considerable advantage can be gained by use of the system reliability methods. The structure is considered as a system of components. In the traditional reliability analysis, the analysis is performed for individual components. Systems approach allows to quantify the redundancy and complexity of the structure. The new LRFD code is based on element reliability. However, system reliability methods are used to verify the selection of redundancy factors.

Structural performance is measured in terms of the reliability index, β (Thoft-Christensen and Baker 1982). Reliability index is defined as a function of the probability of failure, P_F,

$$\beta = - \Phi^{-1}(P_F) \tag{1}$$

where Φ^{-1} = inverse standard normal distribution function.

It is assumed that the total load, Q, is a normal random variable. The resistance, R, is considered as a lognormal random variable. The formula for reliability index can be expressed in terms of the given data $(R_n, l_R, V_R, m_Q, s_Q)$ and parameter k as follows (Nowak 1995),

$$\beta = \frac{R_n \lambda_R (1 - kV_R)[1 - \ln(1 - kV_R)] - m_Q}{\sqrt{[R_n V_R \lambda_R (1 - kV_R)]^2 + \sigma_Q^2}} \tag{2}$$

where R_n = nominal (design) value of resistance; λ_R = bias factor of R; V_R = coefficient of variation of R; m_Q = mean load; σ_Q = standard deviation of load. Value of parameter k depends on location of the design point. In practice, k is about 2.

5. Reliability Analysis for AASHTO (1992)

Reliability indices, β, are calculated for girders designed using the AASHTO Specifications (1992). The basic design requirement is expressed in terms of moments or shears (Load Factor Design),

$$1.3 D + 2.17 (L + I) < \phi R \tag{3}$$

where D, L and I are moments (or shears) due to dead load, live load and impact, R is the moment (or shear) carrying capacity, and ϕ is the resistance factor. Values of the resistance factor

are ϕ = 1.00 for moment and shear in steel girders, ϕ = 0.90 and 0.85 for moment and shear in reinforced concrete T-beams, respectively, ϕ = 1.00 and 0.90 for moment and shear in prestressed concrete AASHTO-type girders, respectively.

The results of calculations show a considerable variation in reliability indices depending on limit state and span length, from about 2 for short span (10m) and short girder spacing (1.2m) to over 4 for larger spans and girder spacing. The target reliability index was selected β_T = 3.5.

6.   New Load and Resistance Factors

The results of the reliability analysis for the current AASHTO Specifications (1992) served as a basis for the development of more rational design criteria for the considered girders. The load factors developed for the LRFD AASHTO Code (1994) are

$$1.25 \, D + 1.50 \, D_A + 1.75 \, (L + I) < \phi \, R_n \tag{4}$$

where D = deal load, D_A = dead load due to asphalt wearing surface, L = live load (static), I = dynamic load, R_n = resistance (load carrying capacity), and ϕ = resistance factor.

In the selection of resistance factors, the acceptance criterion is closeness to the target value of the reliability index, β_T. The recommended resistance factors are ϕ = 1.00 for moment and shear in steel girders, ϕ = 0.90 for moment and shear in reinforced concrete T-beams, ϕ = 1.00 and 0.90 for moment and shear in prestressed concrete AASHTO-type girders, respectively.

Reliability indices calculated for bridges designed using the new LRFD AASHTO code (1994) are close to the target value of 3.5 for all materials and spans. The calculated load and resistance factors produce a uniform spectrum of reliability indices.

For comparison, the ratio of the required load carrying capacity by the new LRFD AASHTO code (1994) and the AASHTO 1992 varies from 0.9 to 1.2.

Conclusions

The calculated load and resistance factors provide a rational basis for the design of bridges. They also provide a basis for comparison of different materials and structural types.

The study has several important implications. The calculated load and resistance factors for the new LRFD code provide a uniform safety level for various bridges. The statistical analysis of load and resistance models served as a basis for the development of more rational design criteria.

Bridge components designed using the proposed LRFD Code have reliability index from 3.5 to 4.0.

Acknowledgements

or implied in the paper are those of the writers and are not necessarily those of the sponsoring organizations.

References

AASHTO, 1992, "Standard Specifications for Highway Bridges", American Association of State Highway and Transportation Officials, Washington, DC.

AASHTO, 1994, "LRFD Bridge Design Specifications", American Association of State Highway and Transportation Officials, Washington, DC.

Ellingwood, B. Galambos, T.V., MacGregor, J.G. and Cornell C.A., "Development of a Probability Based Load Criterion for American National Standard A58", National Bureau of Standards, NBS Special Publication 577, Washington, D.C. (1980).

Hwang, E-S. and Nowak, A.S., 1991, "Simulation of Dynamic Load for Bridges," ASCE Journal of Structural Engineering, Vol. 117, No. 5, pp. 1413-1434.

Kulicki, J.M. and Mertz, D.R., "Development of Comprehensive Bridge Specifications and Commentary", Final Report submitted to NCHRP, December 1993.

Nowak, A. S., Czernecki, J., Zhou, J. and Kayser, R., "Design Loads for Future Bridges," Report UMCE 87-1, University of Michigan, Ann Arbor, MI (1987).

Nowak, A.S., 1993, "Live Load Model for Highway Bridges", Journal of Structural Safety, Vol. 13, Nos. 1+2, December, pp. 53-66.

Nowak, A.S., 1995, "Calibration of LRFD Bridge Code", ASCE Journal of Structural Engineering, Vol. 121, No. 8, pp. 1245-1251.

Nowak, A.S. and Yamani, A.S., 1995, "Reliability Analysis for Girder Bridges", Structural Engineering Review, Vol. 7, No. 3, Aug. 1995, pp. 251-256.

Nowak, A.S., Yamani, A.S. and Tabsh, S.W., 1994, "Probabilistic Models for Resistance of Concrete Bridge Girders", ACI Structural Journal, Vol. 91, No. 3, pp. 269-276.

Nowak, A.S. and Hong, Y-K., 1991, "Bridge Live Load Models," ASCE Journal of Structural Engineering, Vol. 117, No. 9, pp. 2757-2767.

Tabsh, S.W. and Nowak, A.S., "Reliability of Highway Girder Bridges," ASCE Journal of Structural Engineering, Vol. 117, No. 8, (1991), pp. 2373-2388.

Thoft-Christensen, P. and Baker, M.J., 1982, "Structural Reliability Theory and Its Application", Springer-Verlag, p. 267.

Traffic Actions for the Design of Long and Medium Span Road Bridges. A Comparison of International Codes.

Mourad M. BAKHOUM
Lecturer
Structural Eng. Dept.,
Cairo University, Egypt

Mourad Michel BAKHOUM, born 1959,
B. Sc., M.Sc. Civil Eng. (Cairo Uni., Egypt),
Ph. D. (MIT-USA). Works at Structural Eng.
Department-Cairo Uni.,and Arab Consulting
Engineers (Moharram-Bakhoum)

Summary

Highway Bridge Design Codes & Suggested Provisions from USA, UK, Japan, Egypt, and Eurocode are considered. Comparisons of Action effects due to Traffic actions only, & Traffic actions combined with Permanent actions are carried out. ULS & SLS are considered. It is noted that comparing Traffic actions alone, a large difference is observed between codes (about 60%). When combined with Permanent actions (assuming concrete bridges), this difference reduces considerably (to about 15%). A brief comparison of Resistance of R.C. sections at ULS is also carried out.

1. Introduction

Traffic Actions (Live loads) given in Bridge Design Codes are models of actual traffic running on the bridges. It is recognized that traffic patterns in different countries are different to some extent, however, this does not justify the huge differences between traffic action models (LL) specified in the codes. Several studies have been carried out to compare LL in different bridge codes for short/medium span bridges [1,5] & few studies for long span bridges [3]. These studies give useful information, however, more studies are needed because: *i)*Introduction of new codes and new traffic action models such as Eurocode, *ii)* Previous studies focused on comparing Live Loads only. This is not sufficient, and might even be misleading. *iii)* New comparison between codes should include different load types (Live load, Dead Loads, other loads) and their load combinations, moreover, *iv)* not only loads, but also Resistance of sections should also be considered. An attempt to make such a study is given in this paper.

2. Selection of Parameters

The parameters considered in the study, are presented in the following:
--*Bridge Codes:* Five Codes from different countries are considered to investigate practices in different parts of the world. i) AASHTO & ASCE [USA], ii) BD 37/88 & BS5400:Part4 (UK), iii) EGCPL & EGCPC (Egypt), iv) JRA (Japan), and v) EC1:Part3 & EC2 (Eurocodes).
--*Actions Considered & Combination of Actions:* Actions considered in the study are: Traffic actions, Impact or Dynamic allowance for traffic actions (where applicable), Permanent actions due to self-weight of Structural elements & Non-Structural elements. The following terms & abbreviations are used interchangeably with the above mentioned actions: Live loads (*LL*), Impact (*IM*), Dead Loads (*DL*), Superimposed Dead Loads (*SDL*). Concerning combination

of actions, it is noted that for the design of bridge superstructures, the combination including above mentioned actions is --in many instances-- the most critical load combination. Hence, it is the only load combination considered in this study.

--*Load factors*: taken from AASHTO (both for ASCE & AASHTO loads), BD 37/88, EC1. Concerning EGCPL, no values for load factors are given in this code. Hence, load factors of EGCPC are assumed, for the sake of this comparative study, to be applicable to bridges at ULS. Load factors at ULS are given in Fig. 5 (top three rows). JRA is not considered in this study at ULS. Load factors for SLS or ASM are taken equal to 1 for all codes, except for BD 37/88 which uses 1.2 for HA loading, and 1.2 for SDL(deck surfacing).

--*Live Loads*: Figures 4a, 4b show a brief description of the LL considered in this study, & the application of the LL to a 4-lane bridge. It is noted that the AASHTO code is applicable only to spans up to 150 m. Hence, the LL suggested by ASCE for long span bridges are used in this study instead of AASHTO for spans >=125m. Also, EC1:Part3 is applicable up to 200m only. But, it is extended up to 1000m in this study. Pedestrian loads (sidewalk) not considered.

--*Live Load Classes*: Live loads considered here are heaviest loads specified in the codes for First class (Federal, Interstate) highways, e.g. for AASHTO use HS20-44.

--*Live Load Levels*: Some codes (e.g. JRA, ASCE) specify different LL intensities depending on percentage of heavy or large vehicles on bridge. LL levels considered are shown in Fig. 4.

--*Live Load Models*: Some codes (EGCPC/DIN & ASCE) specify one live load model only. In other codes, several LL models are given. For example BD 37/88 specifies: HA load, HB, & combination of HA,HB. Also, AASHTO specifies(HS20 truck, HS20 lane load, Military load). In this study, the live load models believed to produce largest load effects (in the longitudinal direction) in main girders of medium & long span bridges are considered.(see Fig. 4).

--*Traffic Lanes, Bridge Deck Width, and Geometrical Design Issues*: Bridges with 2-lanes, 4-lanes, and 6-lanes are considered in the study. Total bridge deck widths (B) are 12.30m, 19.80m, 28.40m, respectively (Fig. 4 shows a drawing of 4-lane bridge). These are derived as follows: Lane width assumed to be 3.65m. Values for Median, Median clearance, Shoulder (side clearance), Side walk (for maintenance purposes) and space for Handrail are given in the table below. Most of these values conform to AASHTO Geometric Design requirements.

	Total Width	LaneWidth	Side Clr.	Side Walk	Handrail	Median	Median Clr.
2-lanes	12.30m	3.65m	1.25m	0.75m	0.50m	---	---
4-Lanes	19.80m	3.65m	0.60m	0.75m	0.50m	1.0m	0.25m
6-Lanes	28.40m	3.65m	1.25m	0.75m	0.50m	1.0m	0.25m

--*Bridge Spans*: Medium & long span bridges are considered. Medium span bridges are defined as 30m, 60m, 90m, 120m. Long span bridges are defined as 125m, 250m, 500m, 1000m. It is noted that bridges with span of about 125m could be considered as Medium/Long bridges.

--*Bridge Systems*: For spans 30m to 120m, structural system assumed to be Concrete "Box Girder Beam" Bridges (*BGB*). For spans 125m to 1000m, structural system assumed to be Concrete "Cable-Stayed" Bridges (*CSB*). It is noted that 1000m is probably too long for a Concrete CSB, however, it is considered here just for comparison purposes.

--*Estimation of Dead Load Intensity of Structural elements*: DL=(25kN/m3)*(B)*(tav.) kN/m where B is the bridge width as described above, tav is the average or equivalent thickness of bridge in transversal direction. tav. could be estimated as follows: for spans 30m to 120m, following formulas (for BGB) could be useful: tav.=0.35+0.0045L [6], or tav.=0.4+0.0035L. For spans 125m to1000m (Concrete CSB), use tav=0.50m. Walther (Ref. 7,Table 3.30)

observed that for CSB road bridges, with spans ranging from 97m to 440m, including both One-plane & Two-plane CSB, tav. is about 0.50m. Values of tav. considered in the study are:

Span	30m	60m	90m	120m	125m	250m	500m	1000m
tav.	0.512m	0.64m	0.745m	0.85m	0.50m	0.50m	0.50m	0.50m

-- *SDL, Weight of Non-Structural elements:* Deck surfacing (22 kN/m3)*(B*0.08m), Handrails (2*5kN/m), Traffic Barriers (n*3kN/m/barrier, n=2 for 2-lanes, n=4 otherwise).

--*Resistance of Sections at Ultimate:* Figure 5 gives some of the relevant data.

3. Presentation and Discussions of Results

Figure 1 shows four different comparisons between the loads of the bridge codes considered in this study, for a 2-lane bridge. In Fig. 1a, only traffic actions and impact are considered. All loads are multiplied by 1. In Fig.1b, above values are multiplied by load factors for ULS (see Fig.5). Fig. 1c shows combination of Traffic actions (LL, IM) with permanent actions (DL, SDL) at SLS. Finally, Fig. 1d shows loads at ULS. The vertical axis in the figures gives EUDL. For a given bridge code & span, *EUDL* is a uniformly distributed load, which produces the same maximum moment in a simply supported beam subjected to the live loads given in the bridge code considered. The horizontal axis in the figures comprises two parts. Left part for spans 30m to120m (considered as med. span bridges in this study). Right part for spans 125m to 1000m (long span). Refer to Section 2, for discussions on Bridge systems. *Tables next to the Figs. 1a to 1d,* give relative values of EUDL for a certain code, with respect to EUDL for Eurocode. For example,for Fig. 1a, EUDL(AASHTO) / EUDL (EC1)=0.40. (considering unfactored LL only). Also, for Fig. 1d, considering all loads factored for ULS, EUDL(AASHTO) / EUDL (EC1)=0.89. Discussions above apply to Fig. 2,3 as well.

Figure 4 gives some information concerning the Road traffic actions considered in this study. Note large differences in the Topology of the load models.

Figure 5: Safety requirements in all codes requires that action effects at a section must be ≤ Resistance (Strength,Capacity) of the section. Parameters on both sides of this design equation are selected & calibrated so as to lead to safe structures. Work reported up till now focused on left side of the design equation (action side). In order to complement this comparative study, it would be useful to consider also Resistance considerations in the different codes. In Fig. 5, rows 1,4,5,7 give some of the code provisions for resistance & actions. Rows 6,8 present some calculations concerning resistance. Rows 2, 3 give values related to action effects as previously reported in Fig. 2. Now, a comparison is made between Actions (row 3) & Resistance (row 6) for flexure design. It could be said that EC, BS5400, EGCP would give similar dimensions (EGCP slightly bigger), while AASHTO would be less conservative than EC. Now, another comparison is made between Resistance of Sections in Flexure (row 6), & in Axial Load (row 8). It could be observed that i)there are larger differences between codes in row 8 than in row 6, ii) AASHTO is the least conservative in flexural resistance, & one of the most conservative in axial resistance. It is noted that axial strength of Columns in EC2 (given in row 8) is based on the following equation: Nud = 0.57 .fck .Ac + 0.87. fyk. As [Ref. 2].

From results reported in the study, an observation is made relating live loads levels specified in AASHTO (Fig. 1 to 3), and the performance of bridges in USA. It is well known that LL in AASHTO are lower than other codes, even lower than actual loads on bridges in USA[8].

Based on the results reported in this paper, and comparing AASHTO to other bridge codes (take Eurocode for example), Tables 1c, 1d show relative values of EUDL for a 2-lane bridges (both permanent actions and traffic actions are considered at SLS and ULS). The ratio of EUDL in AASHTO with respect to Eurocode is 0.86(SLS), and 0.89 (ULS). i.e. the difference between codes is smaller at ULS than at SLS. This might be one of the explanations why many bridges in the USA suffer serviceability problems (more than in other countries, partly due to low values of live loads in AASHTO), but bridges do not suffer from complete failure (high value of live load factor at ULS, =2.17, contribute to a large value of ultimate action effect).

4. Conclusions

For the cases considered in this paper, some conclusions are given: (1) Concerning traffic actions on bridges, large differences are observed between actions intensities given in the codes (Fig. 1a,2a,3a). (2) Same applies to load factors (Fig.5). (3)When variable actions are combined with permanent actions, the difference is still observed. However, it decreases, especially at ULS (Fig. 1d,2d,3d). (4) Differences between Action effects are more than differences between Resistance of sections in Flexure. (5) Considering both Action effects and Resistance at ULS, AASHTO is less conservative than EC in flexure, and much more conservative in Axial Loads.

5. Bibliography

1.Bakhoum M.M., *A Comparative Study of Highway Bridge Loading*, M.Sc., Cairo Uni.,1984.
2.Beckett D. et al., *Intr. to Eurocode 2: Design of Concr. Str.*, Uni. Greenwich, 93,. page 247.
3.Buckland P.G., "North American & BritishLong-Span Bridge Laods," *JSD*, ASCE,Oct.91.
4.Calgaro J., & Sedlacek G., "EC1:Traffic Loads on Road Bridges," *IABSE Conf.*, Davos, 92.
5.Chatterjee S., "*The Design of Modern Steel Bridges*," BSP Prof. Books, London, 1991.
6.Schlaich J., & Scheef J., "*Concrete Box Girder Bridges*," Struct. Eng. Doc., IABSE, 1982.
7.Walther R. et al., "*Cable-Stayed Bridges*," Thomas Telford, London, 1988.
8.Nowak A.S., "Calibration of LRFD Bridge Code," *JSD*, ASCE, August, 1995.

6. Acknowledgment

7. Selected Notation

AASHTO: Standard Specifications for Highway Bridges, USA, 15th Edition, 1992.
ASCE: American Soc. of Civil Eng., USA, Recommendations for Bridge Loading, 1981
BD 37/88: Ministry of Transport, UK. Departmental Standard: Loads for Highway Bridges.
BS5400: Code of Practice & Specs. for Design of Brides (Part 4: Concrete), BSI,UK.
EC1, EC2: Eurocode 1-Part3:Traffic loads on bridges & EC2: Design of Concrete Structures.
EGCPL: Egyptian Code of Practice for Loads, 1993. Highway Loads same as DIN.
EGCPC: Egyptian Code of Practice for Design and Execution of Concrete Struc., 1989.
SLS, ASM: Serviceability Limit State, Allowable Stress Method or Working Stress Method
ULS: Ultimate Limit State for EC, UK, Egypt. In this paper, ULS is used also to denote also factored loads at Ultimate in the AASHTO code.
JRA: Japan Road Association, Japan

Fig.1a: LL+IM unfactored
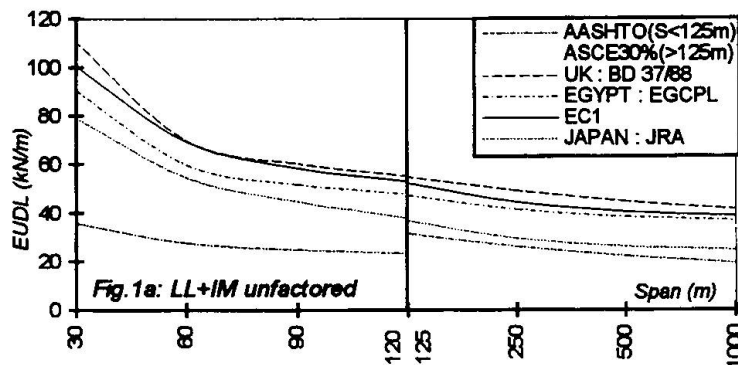
Rel.load w.r.t.(EC1)		
Code	Span (m)	
	60m	250m
AASHTO	0.40	0.59
BD 37/88	1.01	1.11
EGCPL	0.87	0.93
EC1	1.	1.
JAPAN	0.79	0.67

Fig.1b: LL+IM factored for ULS
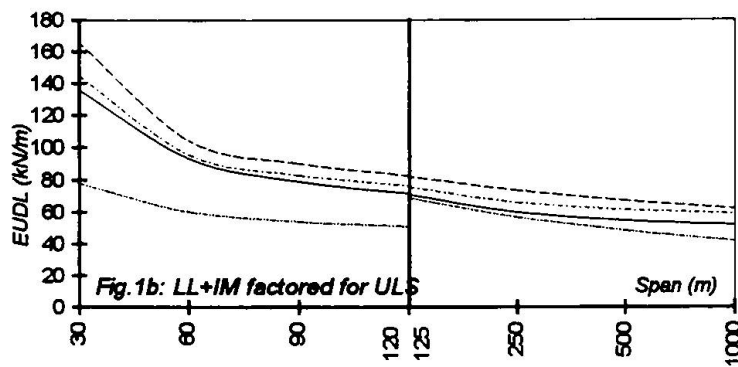
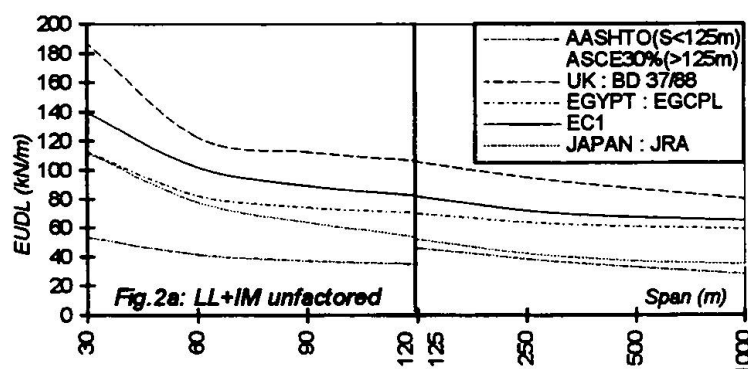| Rel.load w.r.t.(EC1)		
Code	Span (m)	
	60m	250m
AASHTO	0.64	0.95
BD 37/88	1.12	1.23
EGCPL	1.03	1.10
EC1	1.	1.
JAPAN	-	-

Fig.1c: DL+SDL+LL+IM for SLS (or ASM)
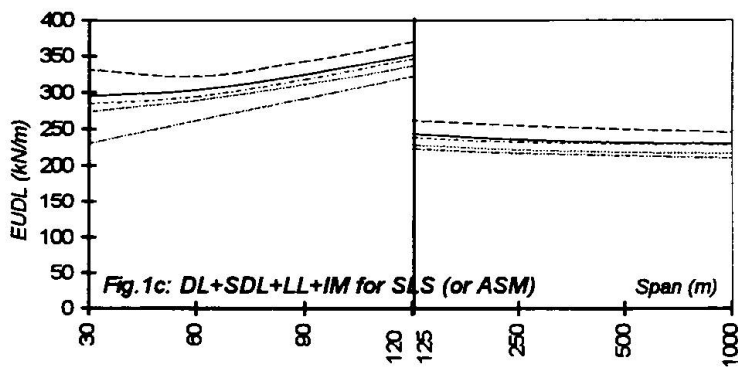
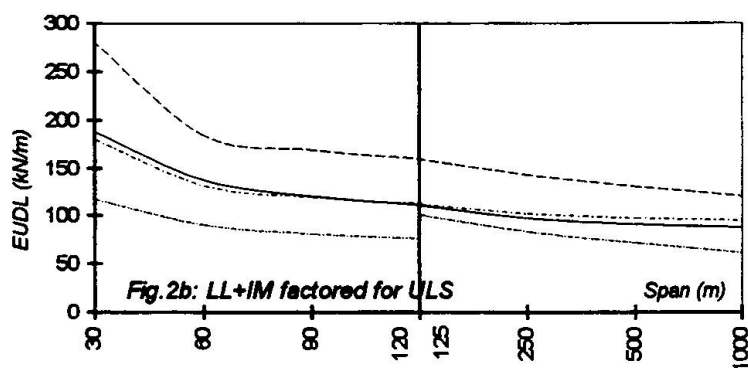| Rel.load w.r.t.(EC1)		
Code	Span (m)	
	60m	250m
AASHTO	0.86	0.92
BD 37/88	1.06	1.08
EGCPL	0.97	0.99
EC1	1.	1.
JAPAN	0.95	0.94

Fig.1d: DL+SDL+LL+IM factored for ULS
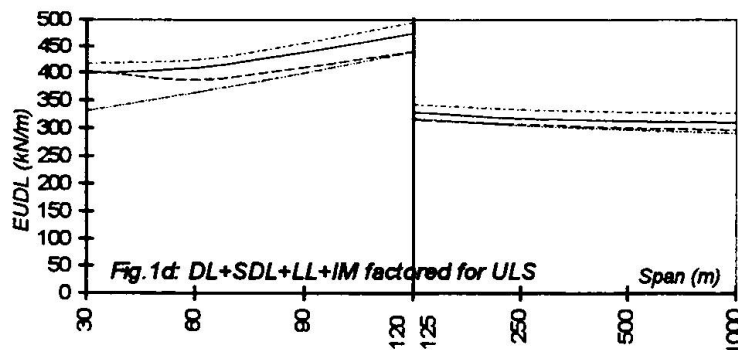
Rel.load w.r.t.(EC1)		
Code	Span (m)	
	60m	250m
AASHTO	0.89	0.96
BD 37/88	0.95	0.97
EGCPL	1.03	1.05
EC1	1.	1.
JAPAN	-	-

Notes: 1)EUDL:Equivalent Unif. Dist. Load,gives same max. moment as in simply supported bridge
2) Fig.1a,b: Traffic Actions only (LL,IM) — Fig.1c,d: combined with Permanent Actions (DL,SDL)
3) DL Intesity:Assume Conc.Br., B=12.3m, $t_{av.}$=0.51m to 0.85m & 0.50m(span <125m & >=125m)

Fig.1: Comparison of Traffic Actions (Live Loads) on 2-Lane Bridges

Fig.2a: LL+IM unfactored — legend: AASHTO(S<125m), ASCE30%(>125m), UK : BD 37/88, EGYPT : EGCPL, EC1, JAPAN : JRA

Rel.load w.r.t.(EC1)		
Code	Span (m)	
	60m	250m
AASHTO	0.41	0.53
BD 37/88	1.20	1.32
EGCPL	0.81	0.88
EC1	1.	1.
JAPAN	0.76	0.59

Fig.2b: LL+IM factored for ULS

Rel.load w.r.t.(EC1)		
Code	Span (m)	
	60m	250m
AASHTO	0.66	0.86
BD 37/88	1.34	1.46
EGCPL	0.96	1.05
EC1	1.	1.
JAPAN	-	-

Fig.2c: DL+SDL+LL+IM for SLS (or ASM)
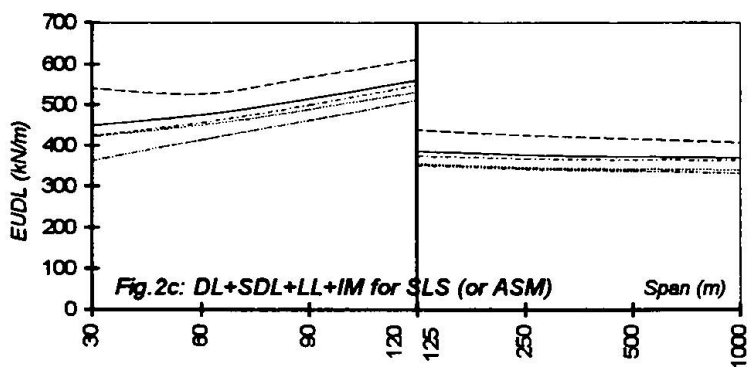
Rel.load w.r.t.(EC1)		
Code	Span (m)	
	60m	250m
AASHTO	0.87	0.91
BD 37/88	1.11	1.13
EGCPL	0.96	0.98
EC1	1.	1.
JAPAN	0.95	0.92

Fig.2d: DL+SDL+LL+IM factored for ULS

Rel.load w.r.t.(EC1)		
Code	Span (m)	
	60m	250m
AASHTO	0.90	0.94
BD 37/88	0.99	1.01
EGCPL	1.02	1.04
EC1	1.	1.
JAPAN	-	-

Notes:1)EUDL:Equivalent Unif. Dist. Load,gives same max. moment as in simply supported bridge
2) Fig.2a,b: Traffic Actions only (LL,IM) — Fig.2c,d: combined with Permanent Actions (DL,SDL)
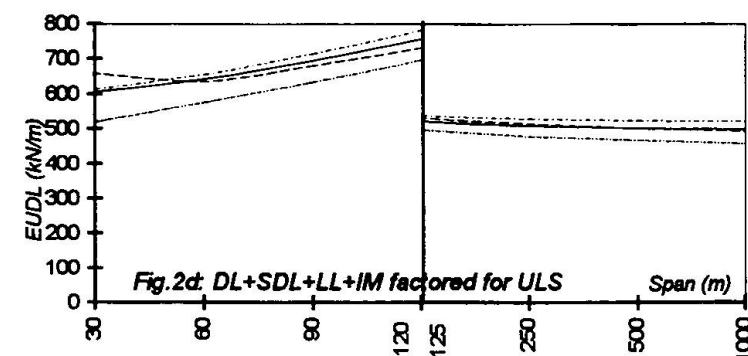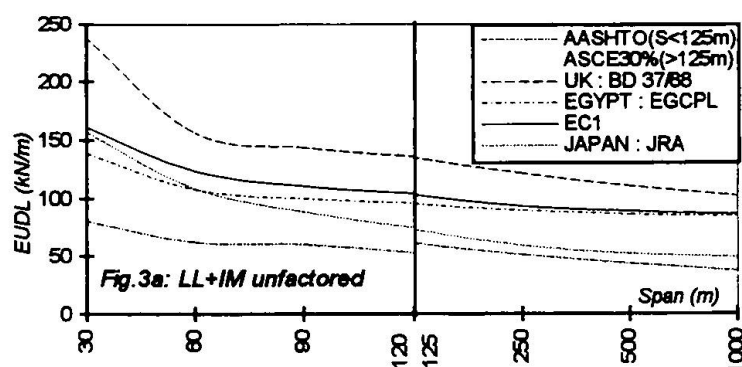3) DL Intesity:Assume Conc.Br., B=19.8m, $t_{av.}$=0.51m to 0.85m & 0.50m(span <125m & >=125m)

Fig.2: Comparison of Traffic Actions (Live Loads) on 4-Lane Bridges

Fig.3a: LL+IM unfactored

Rel.load w.r.t.(EC1)		
Code	Span (m)	
	60m	250m
AASHTO	0.51	0.54
BD 37/88	1.27	1.29
EGCPL	0.88	0.96
EC1	1.	1.
JAPAN	0.88	0.63

Fig.3b: LL+IM factored for ULS

Rel.load w.r.t.(EC1)		
Code	Span (m)	
	60m	250m
AASHTO	0.81	0.87
BD 37/88	1.41	1.44
EGCPL	1.04	1.13
EC1	1.	1.
JAPAN	-	-

Fig.3c: DL+SDL+LL+IM for SLS (or ASM)

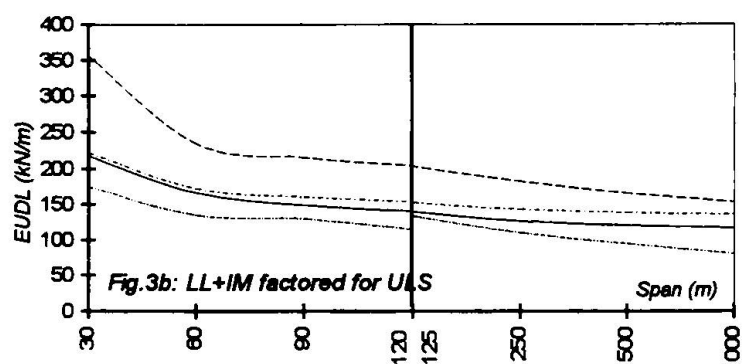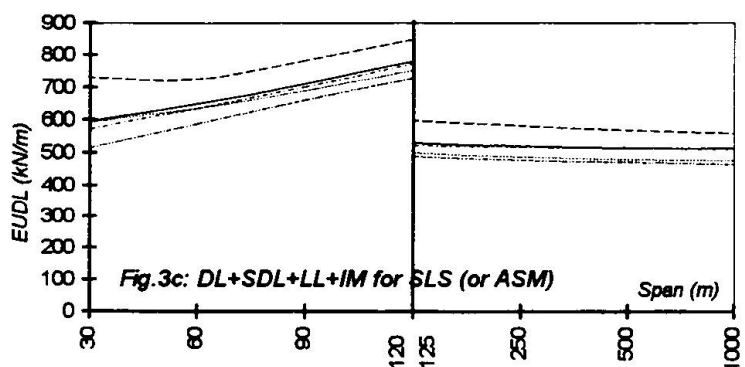| Rel.load w.r.t.(EC1)		
Code	Span (m)	
	60m	250m
AASHTO	0.91	0.92
BD 37/88	1.11	1.12
EGCPL	0.98	0.99
EC1	1.	1.
JAPAN	0.98	0.93

Fig.3d: DL+SDL+LL+IM factored for ULS
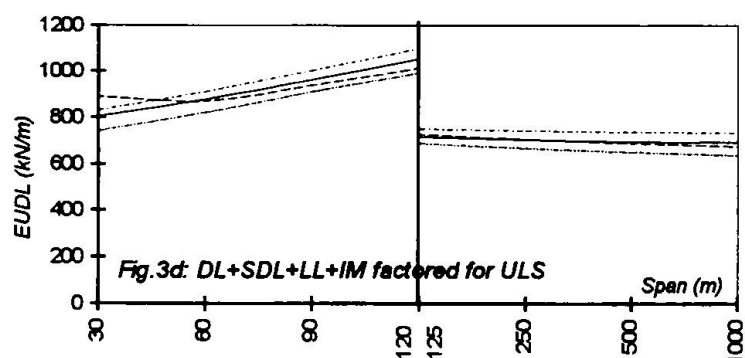
Rel.load w.r.t.(EC1)		
Code	Span (m)	
	60m	250m
AASHTO	0.93	0.95
BD 37/88	0.99	1.00
EGCPL	1.04	1.05
EC1	1.	1.
JAPAN	-	-

Notes:1)EUDL:Equivalent Unif. Dist. Load,gives same max. moment as in simply supported bridge
2) Fig.3a,b: Traffic Actions only (LL,IM) — Fig.3c,d: combined with Permanent Actions (DL,SDL)
3) DL Intesity:Assume Conc.Br., B=28.4m, $t_{av.}$=0.51m to 0.85m & 0.50m(span <125m & >=125m)

Fig.3: Comparison of Traffic Actions (Live Loads) on 6-Lane Bridges

4-LANES BRIDGE

Dimensions: 19.80 / 17.30 / 8.15 / 1.00 / 8.15 / 0.75 / 0.50 / 0.60 / 3.65 / 3.65 / 0.25 / 1.00 / 0.25 / 3.65 / 3.65 / 0.60 / 0.75 / 0.50

- Lane width = 3.65m
- Side clearance/Shoulder = 0.60m
- Side walk (Maintenance) = 0.75m
- Barrier/Handrail = 0.50m
- Median clearance = 0.25m
- Raised Median = 1.00m

EGYPT: EGCPL

- Similar to DIN (German) Bridge Loads
- No length limit
- Impact: $I = 1.4 - 0.008L \geqslant 1$
  Impact applied to 600kN, 5kN/m² only
- $W1 = 3(17.3-6)$ kN/m
  $W2 = 5(3)+3(17.3-3)$ kN/m

5 kN/m² / 3 kN/m² / 600 kN / 300 kN / 3.0 kN/m² / 5 kN/m² / 3 kN/m²
1.50,1.50,1.50 / 300 300 300 kN / 3.0 / 3.0 / 11.30

5kN/m² / 3kN/m²
300 300 / 150 150

U.K.: BD 37/88

- See also BS5400
- Length limit 1600m
- Impact is included in the loading
- Two load models : HA & HB
- HA model :
  P = 120 kN/lane
  $w = 336(1/L)^{0.67}$ kN/m/lane (L<50m)
  $= 36(1/L)^{0.10}$ kN/m/lane (L>50m)
- Multi lane loading: See figure & below
  4 Traffic lanes
  6 Loading Notional lanes
- $F = 4.07$ (L>112m), 4.40 (L≤50m)

Fx(120 kN) / FxW / 120 kN / q depends on span / 2.72 / 2.72 / 2.72 / 2.72 / 2.72 / 2.72

For 20<L≤50: 1.0 1.0 0.6 0.6 0.6 0.6
For 50<L≤112: 1.0 (7.1/√L) 0.6 0.6 0.6 0.6
For L>112: 1.0 0.67 0.6 0.6 0.6 0.6

EUROCODE: EC1

- Length limit 200m
- Impact is included in load models
- Four load models
- Main loading system (Load model 1)
  See figure
- $W = 9(3)+2.5(17.3-3)$ kN/m

800 kN 800 kN / 800 kN / 800 kN / W / 1.20 / 600 kN / 400 kN / 200 kN / 9.0 kN/m² / 2.5 kN/m² / 2.5 kN/m² / 2.5 kN/m² / 3.0 / 3.0 / 3.0 / 8.30
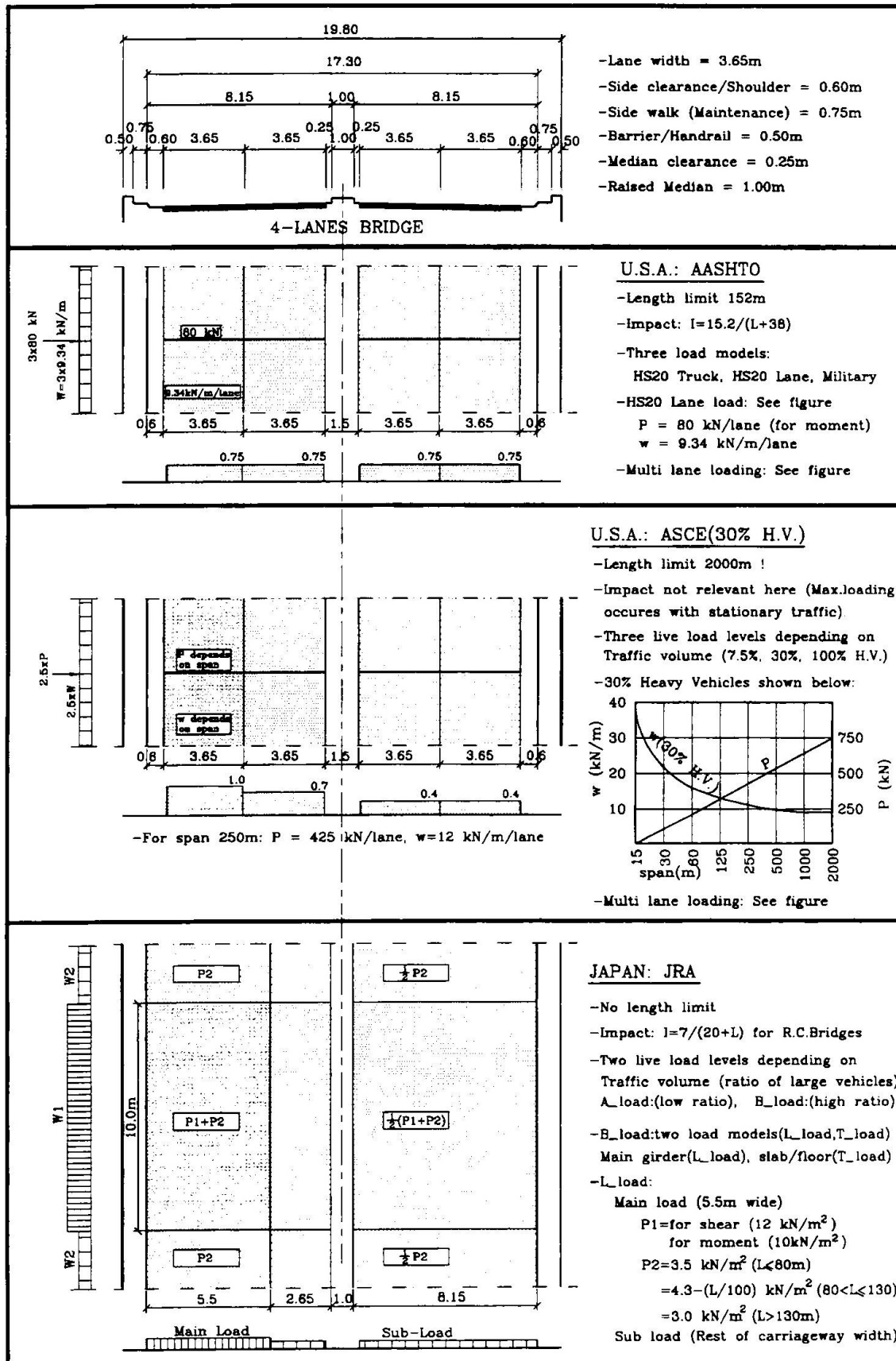
9 kN/m² / 2.5 kN/m²
2x300 kN / 2x200 kN / 2x100 kN

Fig.4a: Traffic Actions (Live Loads) Applied to 4-lane Bridge

Top section — 4-LANES BRIDGE:

19.80
17.30
8.15   1.00   8.15
0.75 0.60 3.65   3.65 0.25 0.25 3.65   3.65 0.60 0.75
0.50   1.00   0.50

4-LANES BRIDGE

-Lane width = 3.65m
-Side clearance/Shoulder = 0.60m
-Side walk (Maintenance) = 0.75m
-Barrier/Handrail = 0.50m
-Median clearance = 0.25m
-Raised Median = 1.00m

U.S.A.: AASHTO

3x80 kN   w=3x9.34 kN/m
80 kN
9.34kN/m/lane
0.6 3.65   3.65 1.5 3.65   3.65 0.6
0.75 0.75   0.75 0.75

-Length limit 152m
-Impact: $I=15.2/(L+38)$
-Three load models:
   HS20 Truck, HS20 Lane, Military
-HS20 Lane load: See figure
   $P = 80$ kN/lane (for moment)
   $w = 9.34$ kN/m/lane
-Multi lane loading: See figure

U.S.A.: ASCE(30% H.V.)

2.5xP   2.5xW
P depends on span
w depends on span
0.6 3.65   3.65 1.5 3.65   3.65 0.6
1.0   0.7   0.4   0.4

-For span 250m: P = 425 kN/lane, w=12 kN/m/lane

-Length limit 2000m !
-Impact not relevant here (Max.loading occures with stationary traffic)
-Three live load levels depending on Traffic volume (7.5%, 30%, 100% H.V.)
-30% Heavy Vehicles shown below:

w (kN/m)   40 30 20 10   P (kN) 750 500 250
30% H.V.   P
span(m) 15 30 60 125 250 500 1000 2000

-Multi lane loading: See figure

JAPAN: JRA

W2   W1   W2   10.0m
P2   P2
P1+P2   (P1+P2)
P2   P2
5.5   2.65 1.0   8.15
Main Load   Sub-Load

-No length limit
-Impact: $I=7/(20+L)$ for R.C.Bridges
-Two live load levels depending on Traffic volume (ratio of large vehicles) A_load:(low ratio), B_load:(high ratio)
-B_load:two load models(L_load,T_load) Main girder(L_load), slab/floor(T_load)
-L_load:
   Main load (5.5m wide)
      P1=for shear (12 kN/m²)
         for moment (10kN/m²)
      P2=3.5 kN/m² (L≤80m)
         =4.3-(L/100) kN/m² (80<L≤130)
         =3.0 kN/m² (L>130m)
   Sub load (Rest of carriageway width)

Fig.4b: Traffic Actions (Live Loads) Applied to 4-lane Bridge

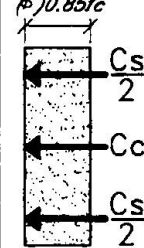|		AASHTO	EC	BS 5400	EGCP
Action Side	**1– Load factors at ULS** Dead load Super imposed Dead Load Live Load	1.3 1.3 2.17	1.35 1.35 1.35*	1.15 1.75⊕ 1.5	1.4 1.4 1.6
	2–Factored Action at ULS EUDL in kN/m,4 lanes Br., see fig. 2d ●Span 60m ●Span 250m	575.9 479.2	642.1 508.5	635.8 515.0	654.9 528.3
	3– Relative action values w.r.t. EC1: ●Span 60m ●Span 250m	90% 94%	100% 100%	99% 101%	102% 104%
Resistance Side in Flexure	**4– Material factors for R.C.** section in flexure Concrete Steel	ϕ=0.90	1/1.50** 1/1.15**	1/1.50 1/1.50	1/1.50 1/1.15
	5– Equilibrium of under **reinforced sections in** **flexure at failure** 	$C=0.85f_c \bullet a \bullet b$ $T=f_y \bullet A_s$ 	$C=0.567f_{ck} \bullet a \bullet b$ $T=\frac{f_{yk}}{1.15} \bullet A_s$ 	$C=0.4f_{cu} \bullet a \bullet b$ $T=\frac{f_y}{1.15} \bullet A_s$ 	$C=0.45f_{cu} \bullet a \bullet b$ $T=\frac{f_y}{1.15} \bullet A_s$
	6– Ult. Moment of Resistance of under singly rft. section (fck=40N/mm², fy=500N/mm², P=1.0%)	106%	100%	98.7%	100%
Resistance Side in Axial Load	**7– Resistance of Axially** **loaded sections at Ultimate** **Limit State (Theoretical case** **of pure axial load)** 	$C_c=0.85f_c \bullet b \bullet t$ $\frac{C_s}{2}=f_y \bullet A_s/2$ *** 	$C_c=0.567f_{ck} \bullet b \bullet t$ $\frac{C_s}{2}=\frac{f_{yk}}{1.15} \bullet \frac{A_s}{2}$ 	$C_c=0.4f_{cu} \bullet b \bullet t$ $\frac{C_s}{2}=\frac{f_y}{1.15} \bullet \frac{A_s}{2}$ 	$C_c=0.45f_{cu} \bullet b \bullet t$ $\frac{C_s}{2}=\frac{f_y}{1.15} \bullet \frac{A_s}{2}$
	8– Ult. capacity of short columns (fck=40N/mm², fy=500N/mm², P=1.0%)	80%***	100%	87%	77%
Notes	Assume: fcu(BS 5400)=fcu(EGCPC)=1.25fck(EC2)=1.25f'c(AASHTO) * Traffic action ** For fundemental combination only ⊕ 1.75 for deck surfacing, 1.2 for other SDL ***80% from 0.8[ϕ 0.85f'c] to account for accidental moments in tied columns				

Fig.5 Comparison of Action Effects & Resistances in Bridge Design Codes at ULS

Effectiveness of User-Load-Control on Reinforced Concrete Bridges

Joseph J.A. MSAMBICHAKA
Civil Engineer
University of Dortmund
Dortmund Germany

Joseph Msambichaka, born 1958, B.Sc. and M.Sc. degrees from Mysore University, India and University of Dar-es-Salaam, Tanzania respectively. Worked as Engineer with the Ministry of Communications and Works, later as Lecturer, University of Dar-es-Salaam. Now doing doctorate research studies at the University of Dortmund, Germany.

Summary

The paper discusses the effectiveness of weighing bridges which were constructed as user-load-control points so as to limit the truck axle loading on a 900 km long TanZam highway road in Tanzania to those intended in the design. A number of reinforced concrete bridges have shown signs of distress which are typical to overloading and at least one ultimately collapsed. It is important, in design stage, to forecast effectiveness of measures used to control vehicle weights on a road.

1. Introduction

A site investigation was conducted to assess the condition of the superstructure of 66 RC (Reinforced Concrete) bridges located between two weighing bridge stations 600 km apart on the TanZam highway which are utilised as user-load-control points for trucks using the highway in Tanzania. The two lane 900 km road connects the port of Dar es Salaam with the southern part of the country and neighbouring countries namely north of Zambia, north of Malawi and south of Zaire. The user-load-control points were constructed at certain intervals so as to limit the truck axle loading on the TanZam highway road in Tanzania to those intended in the design. A number of RC bridges have shown indications which are characteristic to overloading and at least one bridge collapsed. It has been observed that RC bridges on the TanZam highway designed according to AASHTO [1] to carry trucks of up to about 40 tons 25 years ago [2] have been in the cause of time supporting trucks of up to 90 tons. It should be noted that bridge designing in the southern countries, outside europe, in the moment is done based on various european or north american structural design codes directly or indirectly through local structural design codes of practice.

2.   Axle Loading of Trucks Plying on TanZam Highway

The RC bridges on TanZam highway were designed 25 years ago on the basis of the three-axle trucks with axle loading distribution of 36 kN--144 kN--144 kN and width 1.83 m. This truck has a maximum axle loading of 144 kN within a 4.27 m of road length. In comparison, the survey in 1995 shows that there are diverse configurations and capacities of truck axle loading plying on the TanZam highway as summarised in Fig. 1. These have axle loadings capacity of up to 480 kN within 2.6 m of road length. The total truck loading capacity now reaches 960 kN whereas the total load of the design truck was 324 kN. The truck axle load configuration keeps on changing with time as transporters strive as much as possible to acquire higher load carrying capacity per truck.
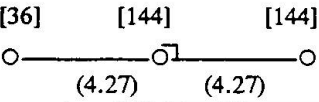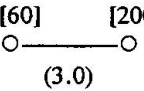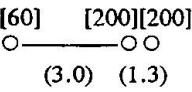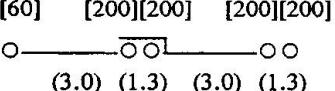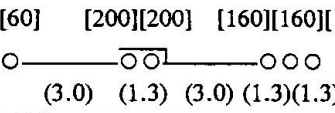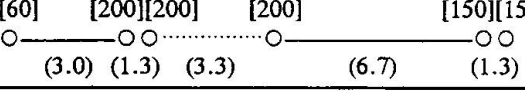
Configuration of Axle Loading Capacity of Trucks on TanZam Highway		Total Truck Load Capacity	Minimum Axle Spacing	Load on Minimum Axle Spacing	Effective Burden Increment Factor
[36] [144] [144] O————O̅————O (4.27) (4.27)	[kN] (m)	324 kN	4.27 m	288 kN	1
[60] [200] O————O (3.0)	[kN] (m)	260 kN	3.0 m	260 kN	1.3
[60] [200][200] O————OO (3.0) (1.3)	[kN] (m)	460 kN	1.3 m	400 kN	4.67
[60] [200][200] [200][200] O————O̅O̅————OO (3.0) (1.3) (3.0) (1.3)	[kN] (m)	860 kN	1.3 m	400 kN	4.67
[60] [200][200] [160][160][160] O————O̅O̅————OOO (3.0) (1.3) (3.0) (1.3)(1.3)	[kN] (m)	940 kN	1.3 m 2.6 m	320 kN 480 kN	2.8 3.7
[60] [200][200] [200] [150][150] O————OO···········O————OO (3.0) (1.3) (3.3) (6.7) (1.3)	[kN] (m)	960 kN	1.3 m	300 kN	1.04

Fig. 1. Axle loading configuration of trucks plying on TanZam highway.

The effective burden increment has been determined by considering increment of axle load on minimum axle spacing and decrease of minimum axle spacing of a truck in comparison to the design truck. In comparison, the main loading system (load model 1) with a tandem system of characteristic axle load of 600 kN within 1.2 m of road length and a uniformly distributed load of 9 kN/m^2 are specified for design in Eurocode 1: part 3 [3].

3. Investigation of RC Bridges Between Two User-Load-Control Points on TanZam Highway

User-load-control points are weighing bridges which were constructed at certain intervals along the TanZam highway so as to limit the truck axle loading on a 900 km long TanZam highway road in Tanzania to those intended in the design. Between the two selected user-load-control points 600 km apart there are a total of 72 bridges. These are steel deck-steel beam, steel truss-steel deck, RC slab-steel beam, RC slab and RC slab-RC beam bridges. The number of each is as summarised in the table shown in Fig. 2.

No.	Type of bridge superstructure	Total number	Total length	Number of spans	Maximum span
	steel deck-steel beam	4	14 - 24 m	1	13 - 23 m
	steel truss-steel deck	1	104 m	3	50 m
	RC slab-steel beam	1	123 m	4	30 m
	RC slab	46	4 - 20 m	1-3	3 -10 m
	RC slab-RC beam	20	10 - 77 m	1-5	9 - 20 m

Fig. 2 Table showing the number of bridges between the two user-load-control points.

In this investigation only RC slab and RC slab-RC beam bridges lying between the two user-load-control points were considered. The RC bridges have a transverse curb to curb width of 7 m to 9.5 m. The total transverse bridge width varies from 9 m to 10.5 m. The RC bridges have clear spans ranging from 3 m to 20 m and total lengths ranging from 4 m to 120 m each.

4. Results Showing the Condition of the Superstructure of RC Bridges on TanZam Highway

4.1 Large Cracks on RC Beams and RC Slabs

Some 5 RC bridges on the TanZam highway showed large cracks on the RC beams and slabs which was an indication of the bridges being subjected to overloading. One other bridge eventually collapsed after its RC slab deck failed due to overloading. A typical case of a bridge beam on the TanZam highway with 2 mm wide cracks is shown in Fig. 3.

4.2   Damages Due to Accidental Impacts by Vehicles

Most of the RC bridges on the TanZam highway have damages on the top part of their superstructure namely on railing and apron. The damages are mostly due to accidental impact by vehicles on the bridge superstructure. The shock due to impact has short term reverberations on the load carrying structural part of the bridge and adds up to the existing overload due to normal daily traffic loads.
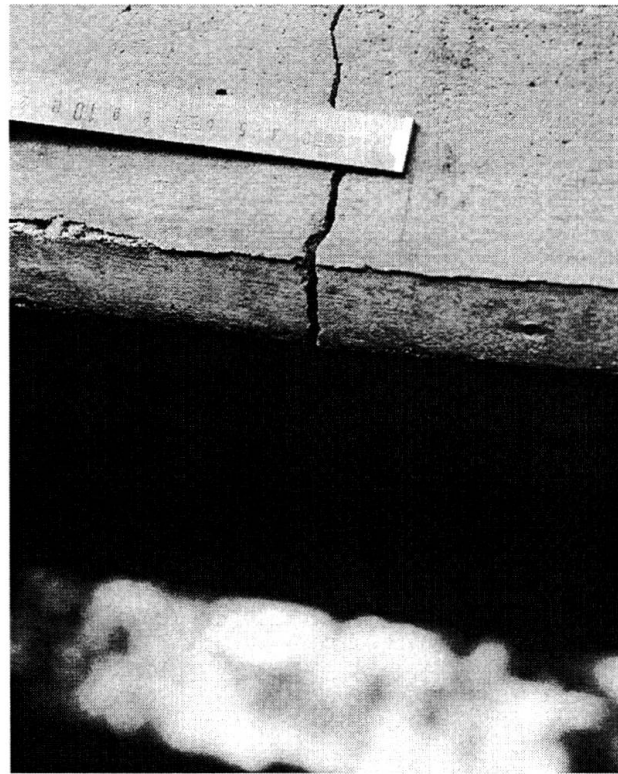
Fig. 3. A Photo showing typical large cracks in RC beam of a bridge on TanZam highway.

4.3   Classification of the Condition of the RC Bridges on TanZam Highway

The condition of the RC bridges between the two user-load-control points were ranked as follows:

- RC bridges without any damages.
- RC bridges with damages on the top auxiliary parts of the bridge.

- RC bridges with small cracks on the RC beams and/or RC slabs in addition to damages on top auxiliary parts.
- RC bridges with large cracks on the RC beams and/or RC slabs in addition to damages on the top auxiliary parts of the bridge.

The Table in Fig. 4. shows a summary of the condition of RC bridges on the TanZam highway according to the above ranking.

Category	Proportion in Percent of RC Bridges on TanZam Highway in Each Damage Classification				
	Good Condition	Damages on Top Auxiliary Parts Only	Small Cracks on Beams and Slab	Large Cracks on Beams or Slabs	Sum
According to Type of Bridge					
RC Slab Bridges	31	60	7	2	100
RC Slab-RC Beam Bridges	0	43	38	19	100
According to Maximum Free Span of Bridge					
3 m to 10 m	29	63	8	0	100
11 m to 20 m	0	33	39	28	100
According to the Distance from User Load Control Points					
0 to 200 km	33	67	0	0	100
200 to 400 km	18	51	22	10	100

Fig. 4. Table summarising the condition of the RC bridges on TanZam highway.

4.4 Type of RC Bridges Showing Higher Distress Condition

The results in Fig. 4 have shown that large cracks appeared on bridges with comparatively large clear spans. Also, large cracks were mostly present on RC slab-RC beam bridges in comparison to RC slab bridges. But most of the RC slab-RC beam bridges had large spans which is the main reason that they showed higher degree of deterioration compared to the slab bridges. In addition, RC bridges located between 200 and 400 km showed higher distress conditions than those located within 200 km from both ends.

5. Discussion

5.1 Estimation of Design Loading

It is usually economical to use local data on trends of vehicle loading to estimate future loading for design purposes. But the 900 km long TanZam highway was an upgrading of an existing unpaved road to a paved road. Hence it was expected that by estimating future traffic loads based on evaluation of traffic loads of the then existing unpaved road and extrapolation of local vehicle trends at that time could lead to underestimation because the user's response to changes in such an extreme road upgrading is a sharp increase in the utilisation of the road due to the availability of a much better road and bridges. The relation of design loading, user response and load control is shown in Fig. 5.
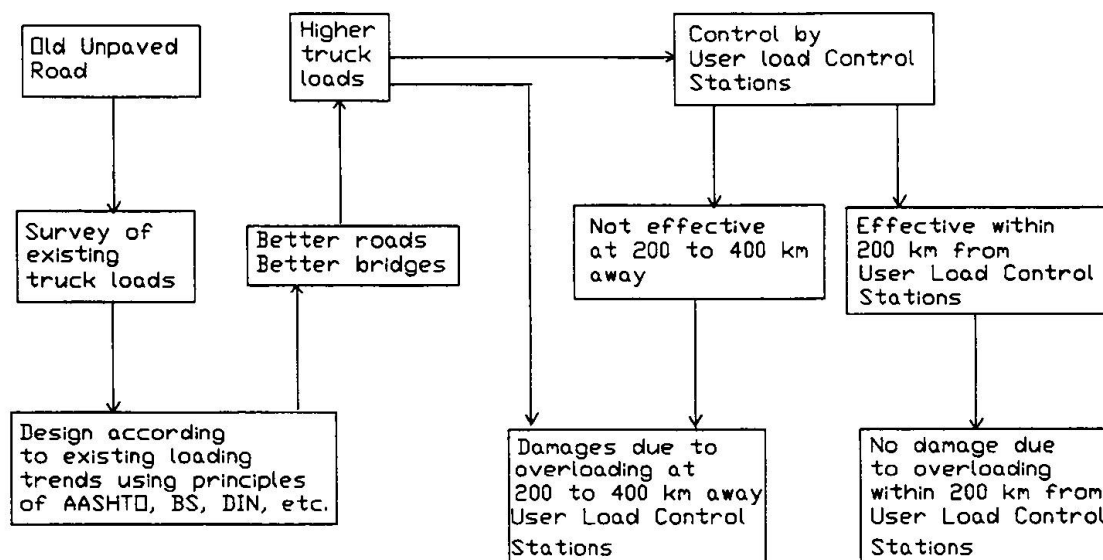
Fig. 5. Chart summarising the relation of design loading, user response and load control.

In this particular case, the increase was from a maximum of 40 ton truck loads expected during the upgrading to more than 90 ton truck loads at present in the normal daily traffic. The solution to the expected increase of truck axle loading capacity was to install user-load-control points.

5.2 Effectiveness of User-Load-Control Points

It is seen from the results in Fig. 4 that bridges with large cracks are concentrated at a distance of between 200 to 400 km from the two user-load-control weighing bridges. This shows that the control of truck axle loads at the user-load-control points benefits structures of up to a distance of 200 km on TanZam highway. For distances further than 200 km, there is not much influence of the truck axle load control done at the user-load-control

points. The influence of user-load-control points is also illustrated by the graph shown in Fig. 6 below.

The concentration of damages on bridges located at a distance between 200 and 400 km along the TanZam highway is attributed to the intermediate truck traffic whose axle loading could not be controlled. This intermediate traffic is confirmed by the fact that trucks with high axle load capacity shown on the table in Fig. 1 move on this highway and road users naturally tend to move as much load as the truck can carry when there is no control.

Therefore risk of overloading the bridges increases in proportion to the distances of bridges from the user-load-control points, especially in the region beyond the influence of the user-load-control points.
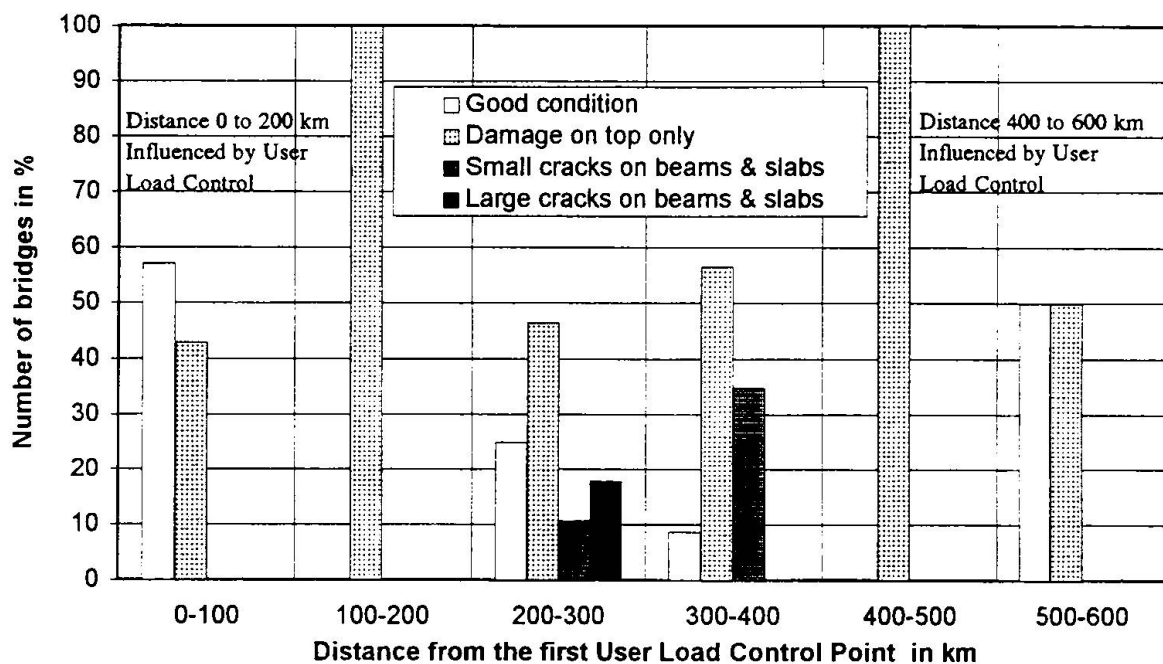
Fig. 6. Distribution of bridge damages on the 600 km road length.

5.3 Eurocode 1 on Bridges for Restricted Weight of Vehicles

Eurocode 1 part 3 [3] specifies in section 4.1 that, "for bridges to be equipped by appropriate road signs intended to limit strictly the weight of any vehicle, specific models may be defined or authorised by relevant authority". But the specific load models will tend to assume reduced design loads for all bridges on the entire road with restricted

vehicle weights. Therefore, it is suggested from the results of this investigation that it is essential to add a statement to section 4.1 of Eurocode 1: Part 3 that the specific models have also to consider the effectiveness, to each bridge, of the control measures taken to limit the vehicle weights on the road and to appropriately increase the design loading for bridges which might be beyond the influence of the load control measures.

6.   Conclusions

The results of the investigation indicate that overloading on RC bridges was apparently severe the further the RC bridges were away from the user-load-control points intended for the purpose of limiting the traffic load. This was due to intermediate traffic which could not be controlled by the weighing bridges.

The results show also that availability of better roads and bridges increased the utilisation from expected 40 ton truck loads during design to more than 90 tons at present. In addition, RC bridges with larger spans tended to show greater deterioration due to overloading than those of smaller spans.

Therefore, the aspects of traffic loads listed above should be considered in future design of bridges on roads under similar circumstances. That means safety factors should therefore be increased in proportion to the risk of overloading instead of applying a uniform reduced value to all bridges on the specific road. For example, in this particular case, the safety factors values could be increased in proportion to the distances of bridges from the user-load-control points.

Acknowledgement

References

[1]   American Association of State Highway and Transport Officials (AASHTO), *Standard Specifications for Highway Bridges*, Washington D.C., 1977.

[2]   Ministry of Communications and Works, *Engineering Design of Bridges*, Dar es Salaam, 1990.

[3]   Eurocode 1, *Basis of Design and Actions on Structures - Part 3: Traffic Loads on Bridges*, CEN, Brussels, 1993.

DUCTILITY REQUIREMENTS OF A BRIDGE PIER SUBJECT TO IMPACT

Enzo CARTAPATI
Senior Researcher
Structural and Geotechn.
Engineering Dept.
University "La Sapienza"
Rome, ITALY

Enzo Cartapati, born in 1946,
got his civil engineering degree
in 1971 at the University "La
Sapienza", Rome, Italy. He has
been researcher and encharged
professor of Strength of
Materials and Construction
Technics at the same University.

Summary

The behaviour of a beam, fixed at its ends and axially stressed, subject to the impact of a mass at a given speed is considered. The scope of the paper is to stress the role of ductility in structural elements subject to the impact of deviating vehicles as, e.g., the piers of an overbridge. The behaviour of the pier has been studied through three or four successive phases, taking into account the shear, flexural and axial ultimate stresses. The displacement of impact section is determined as well as the maximum strain at plastic hinges.

1. Introduction

1.1 Foreword

Within a research program on the behaviour of fiber-reinforced concrete structural elements, carried out at the Department of Structural and Geotechnical Engineering of the Rome University "La Sapienza", mono- and bi-dimensional elements subject to repeated dynamic loads and impact have been considered. Experimental tests have been performed on plain and f.r. concrete slabs subject to impact, and on plain and f.r. concrete beams subject to static loads in order to characterize the behaviour of f.r. concrete with respect to plain concrete [1,2]. The present paper follows a recent study [3] on the theoretical aspects of the case of a beam fixed, hinged or simply supported at its ends subject to heavy impact loads. The aim is to underline the ductility requirements of such structures, that, for usual design static equivalent loads, undertake values much beyond those normally accepted for statically loaded structures.

The study of effects of impulsive actions requires the knowledge of physical and mechanical behaviour of materials beyond the elastic field; the structure is studied in the non-linear field of large displacement taking into account the interaction among shear, bending moment and axial stress at ultimate state.

1.2 The materials

The behaviour of materials under impulsive loading beyond elastic limit is very complex.

It depends on several parameters as loading rate, strain rate, instant temperature and steel hardening. Such parameters sometimes are also intercorrelated. Several laws based on theoretical or experimental studies have been proposed for impact loading problems [4,5].

The use of such expressions makes very complex the detailed representation of the behaviour of a structure subject to impact loads. Therefore the influence of the above said parameters is often neglected and rigid-plastic or elasto-plastic laws are considered. Taking into account that, due to the large displacements occurring, the elastically dissipated energy results to be absolutely negligible with respect to the energy dissipated in plastic field, the use of a rigid-plastic model appears quite acceptable and allows a great simplification for the study.

1.3 Structural behaviour and interaction laws

The behaviour of a structure subject to impact loads is characterized by its response in terms of stress distribution and strain development. The collapse mechanism and the variable plasticized sections must be found, depending on the structure shape, load type and materials behaviour. The main aspects to be considered are: the dynamic loads much greater than the static ultimate ones and the large displacements undertaken by the structure. In the first case shear deformations may become not negligible [6,7], in the second one large axial stresses may arise. It turns necessary the account of plastic interaction among bending moment, axial stress and shear stress, that is, the assumption of a suitable plasticization law [8].

Several proposal are at hand in reference [9,10], mainly for steel sections, based on theoretical and experimental studies and related to section and structural shape. For a general steel section or for a reinforced concrete section the following expression has been assumed in [3]:

$$f = \left[\left| \frac{M}{M^*} \right| + \left(\frac{N - N^*}{N_0 - N^*} \right)^2 - 1 \right] \left(\left| \frac{Q}{Q_0} \right| - 1 \right) = 0 \qquad (1)$$

in that N_0 and Q_0 are the ultimate values of tensile stress and shear; M^* is the maximum ultimate bending moment of the section that acts together with the axial stress N^*. For a r.c. section equation (1) approximates with a parabole arch the ductile plastic interaction curve of the section (Fig. 1):
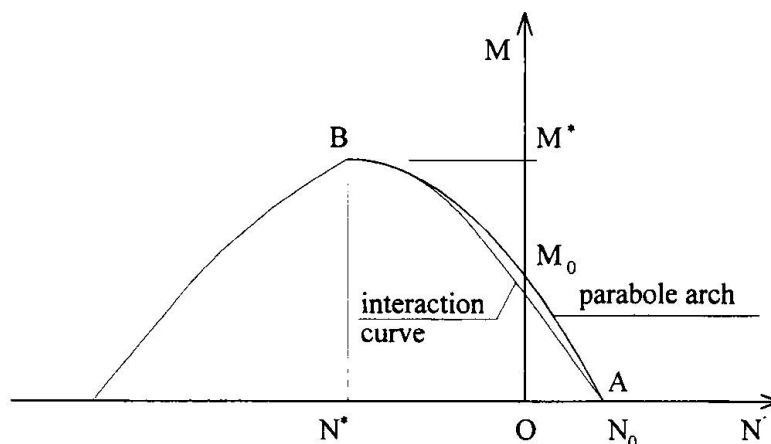

Fig. 1. Interaction curve of reinforced concrete sections.

1.4 The local missile-structure interaction

A further uncertainty contribution, besides those already mentioned, comes from the unknown part of the striking mass energy that is dissipated at impact under damping, friction, sound waves and, mainly, missile deformation. The last contribution is particularly important in the case of impact of deviating vehicles against structures placed close to carriageways. In such case data from experimental tests are quite necessary. In the following it is assumed that the kinetic energy transmitted by the missile to the structure is net from local dissipation and missile deformation. Therefore the impact speed v_0 shall be considered as a reduced speed in order to take into account such dissipated energy. However normatives and constructive recommendations usually propose values of impact forces of deviating vehicles specifying that the whole kinetic energy must be transferred to the impacted structure.

2. Beam dynamic equilibrium

2.1 Assumptions

The development of the structure collapse mechanism is analyzed taking into account the interaction among bending moment, shear and axial stress accordingly with plasticization law (1). In order to reduce the complexity of the problem, the material behaviour is assumed as rigid-plastic and the effect of strain rate and impulse duration is neglected. The analytical results are summarized from [3] and are based on the studies of T. Nonaka [10], but have been extended to different beam end conditions and to a more generic plasticization surface.

2.2 The beam with fixed ends

In this paper, due to synthesis reasons, only the results relative to a beam with fixed ends are reported, allowing for an extension, as limit case, for a hinged beam. The beam, according to the scheme in fig. 2, is impacted at midspan section by a mass m_0 having v_0 velocity.

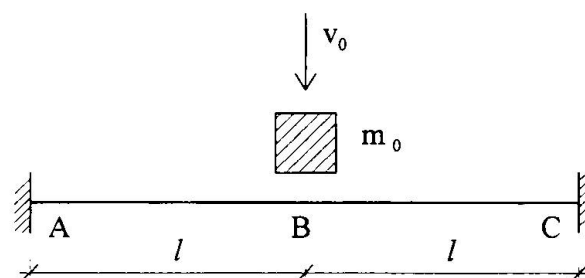*Fig. 2. Scheme of the clamped beam subject to impact.*

Referring to above figure: - m is the mass per unit length of the beam; - M_{01} and $M_{02} = M_{01}/K$ the ultimate plastic moments of sections B and C rispectively (with N = 0); - N_{01} and N_{02} the maximum tensile stresses that brings sections B and C to plasticization; - Q_0 the ultimate plastic shear of section B.

2.2.1   First phase

In the first phase, following immediately the impact, the beam, close to the impact area, is subject to a strong shear stress such as to reach the ultimate shear strength and to force the stroken part of the beam to slide with respect to the remaining parts. The half beam limited by the stroken section and the restrained end is subject to the ultimate shear at midspan and to the inertial forces. It begins to rotate producing a plastic hinge at midspan and at its fixed end. The hypothesis is assumed that another plastic hinge takes place at an intermediate position, where inertial forces equilibrate the ultimate shear acting at midspan (Fig. 3).

By means of the impulse theorem and the dynamic equilibrium of the two parts of the half beam, it is possible to determine the end of the relative sliding between the stroken part of the beam and the remaining parts. The speed and the displacement of the stroken part at such instant are determined. Being the displacements very small in this phase, the contribution of axial force is neglected. Assuming $N \cong 0$, it results $M_C \cong M_{02}$ and $M_B \cong M_{01}$.
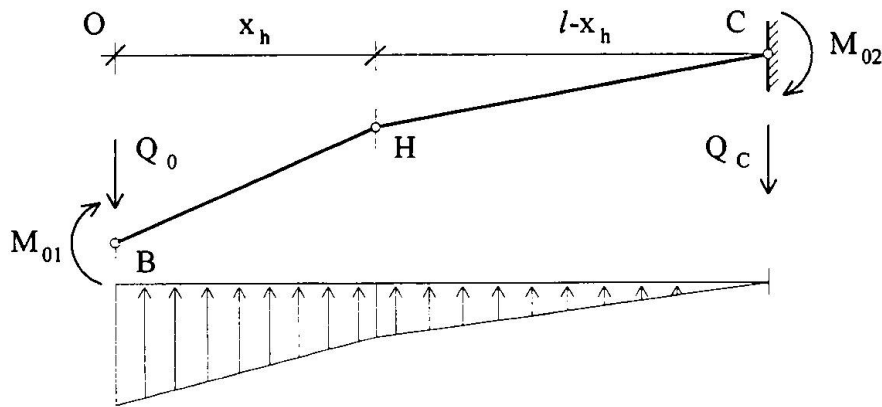
Fig. 3. Scheme of the impacted beam during first phase.

By means of the impulse theorem applied to the striking mass, the speed of the mass is:

$$\dot{y}_0 = \frac{I}{m_0} - \frac{2Q_0 t}{m_0} \tag{2}$$

If $\dot{y}_B$ and $\dot{y}_H$ are the speeds of points B and H, the theorem of the impulse for the part BH

gives:
$$Q_0 t = \int_0^{x_h} \left[\dot{y}_B + \frac{\dot{y}_H - \dot{y}_B}{x_h} x \right] m\, dx \tag{3}$$

From the theorem of angular momentum with respect to O, it results:

$$\int_0^{x_h} \left[\dot{y}_B + \frac{\dot{y}_H - \dot{y}_B}{x_h} x \right] x\, m\, dx = 2 M_{01} t \tag{4}$$

Applying the same theorem to part HC with respect to point C, considering x_h costant versus

time, it follows:
$$\int_{x_h}^{l} \dot{y}_H \frac{l-x}{l-x_h}(l-x)m\,dx = (M_{01}-M_{02})t \qquad (5)$$

From equations (3), (4) and (5) the expressions of $\dot{y}_B$, $\dot{y}_H$ and x_h can be obtained.
The first phase ends when the relative sliding between the stroken part and the remaining part
stops; that is if $\dot{y}_B = \dot{y}_0$. From such condition, it results (2):

$$t^{\bullet} = \frac{I/m_0}{\alpha_1 + 2Q_0/m_0} \qquad (6) \qquad \text{with} \quad \alpha_1 = \frac{2Q_0}{mx_h} - \frac{3\Delta M_0}{m(l-x_h)^2}$$

Equation (6) gives the speed and displacement of midspan section at end of the first phase:

$$\dot{y}_B^{\bullet} = \alpha_1 t^{\bullet} \qquad ; \qquad y_B^{\bullet} = \frac{\alpha_1}{2}t^{\bullet 2}$$

and $\qquad \dot{y}_H^{\bullet} = \alpha_2 t^{\bullet} \qquad$ with $\qquad \alpha_2 = \frac{3\Delta M_0}{m(l-x_h)^2}$

At the end of this phase it is possible to check the hypothesis of the formation of the

intermediate plastic hinge: it happens if the angular speed $\dot{y}_B/l$ is greater than $\dot{y}_H/(l-x_h)$,

that is: $\qquad \frac{\alpha_1(l-x_h)}{\alpha_2 l} > 1 \qquad (7)$

If inequality (7) is not true, only the plastic hinges in B and C take place; the theorems of
impulse and angular momentum applied to the whole half beam give the following
expressions:

$$(Q_0 - q)t = \frac{\dot{y}_B ml}{2} \qquad ; \qquad \frac{m\dot{y}_B l^2}{6} = \left(M_{01} + \frac{M_{01}}{K} - ql\right)t$$

from which we can obtain:

$$\dot{y}_B = \alpha_3 t \qquad \text{with} \qquad \alpha_3 = 3\frac{Q_0 l - M_{01}(1 + 1/K)}{ml^2}$$

In analogy with the preceeding case, it results:

$$t^{\bullet} = \frac{I/m_0}{\alpha_3 + 2Q_0/m_0} \qquad ; \qquad \dot{y}_B^{\bullet} = \alpha_3 t^{\bullet} \qquad ; \qquad y_B^{\bullet} = \frac{\alpha_3}{2}t^{\bullet 2}$$

2.2.2 Second phase

In the second phase, that is present only if the intermediate plastic hinge takes place, such
hinge moves rapidly towards the restrained end of the beam, because of the reduced shear
force and the increase of axial force effect. This phase develops very quickly and can be
examined by means of the conservation of kinetic energy through the end of phase one and the

end of phase two. The speed and the displacement of midspan section at the end of this phase are determined:

$$E = \frac{m(l-x_h)\ddot{y}_H^2}{6} + \frac{1}{4}m_0\ddot{y}_B^2 + \frac{1}{2}m\int_0^{x_h}\left(\dot{y}_B^* + \frac{\dot{y}_H^* - \dot{y}_B^*}{x_h}x\right)^2 dx = \frac{1}{4}m_0\dot{y}_x^2 + \frac{1}{6}ml\dot{y}_x^2$$

$$y_x = \sqrt{\frac{m\dot{y}_H^*\left(\dot{y}_H^*l + \dot{y}_B^*x_h\right) + \dot{y}_B^{*2}\left(\frac{3}{2}m_0 + mx_h\right)}{\frac{3}{2}m_0 + ml}}$$

2.2.3 Third phase

The third phase is the most important one, due to the presence of axial stress which gives its contribution to dissipate, together with the plastic hinges, the residual kinetic energy. The axial force must be considered in this phase because the displacements become not negligible; therefore the interaction N - M will be taken into account..
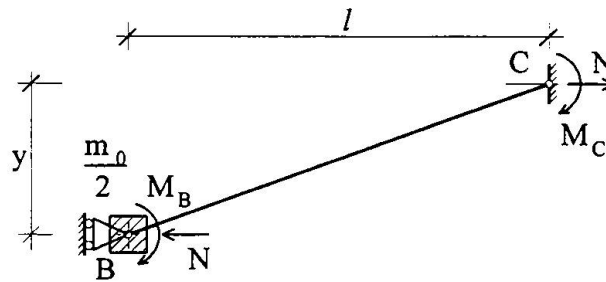

Fig. 4. Scheme of the impacted beam during third phase.

At plastic hinges B and C, whose equivalent lengths can be assumed as d_1 and d_2, the strain rate vector has components:

$$\dot{\varepsilon}_1, \dot{K}_1, 0 \quad \text{in B}$$
$$\dot{\varepsilon}_2, \dot{K}_2, 0 \quad \text{in C}$$

being ε and K the axial strain and the curvature. The axial strain rate of the beam is:

$$\dot{\Delta l} = \frac{\partial(l'-l)}{\partial t} = \frac{\partial}{\partial t}\left(\sqrt{y^2 + l^2}\right) = \frac{y\dot{y}}{\sqrt{y^2 + l^2}} \cong \frac{y\dot{y}}{l}$$

If the axial strain is localized in B and C according to the quantities s and 1-s, it follows:

$$\dot{\varepsilon}_1 = \frac{sy\dot{y}}{d_1l} \quad ; \quad \dot{\varepsilon}_2 = \frac{(1-s)y\dot{y}}{d_2l} \quad ; \quad \dot{K}_1 = \frac{\dot{y}}{d_1l} \quad ; \quad \dot{K}_2 = \frac{\dot{y}}{d_2l}$$

Furthermore the strain rate vector is constrained to be tangent to the yield surface; therefore:

$$\frac{\dot{\varepsilon}}{\dot{K}} = \frac{\partial f}{\partial N}\bigg/\frac{\partial f}{\partial M} = \frac{2(N-N^*)}{(N_0-N^*)^2}M^*$$

From the preceeding expressions it follows:

$$N = \frac{(N_{01} - N_1^*)^2}{2M_1^*} sy \qquad ; \qquad N = \frac{(N_{02} - N_2^*)^2}{2M_2^*}(1-s)y \qquad (8)$$

Those expressions allow the determination of s; being:

$$K^* = \frac{M_1^*}{M_2^*} \quad \text{and} \quad H = \frac{(N_{02} - N_2^*)^2}{(N_{01} - N_1^*)^2} \quad , \qquad s = \frac{K^* H}{1 + K^* H} \qquad (9)$$

Referring to fig. 4, by means of the dynamic equilibrium of moments acting on the halfbeam with respect to point C, it results:

$$\frac{1}{2} l m_0 \ddot{y} + \int_0^l \frac{\ddot{y}}{l} x^2 m \, dx + M_B + M_C + Ny = 0 \qquad (10)$$

Using the interaction law (1), substituting the expression of N (8) and s (9); multiplying by $\dot{y}$, integrating and introducing the following constants:

$$\alpha = \frac{l m_0}{4 M_1^*} + \frac{l^2 m}{6 M_1^*} \qquad ; \qquad \beta = \frac{K^*(N_{02} - N_2^*)^2}{12 M_1^{*2}(1 + K^* H)}$$

$$\gamma = \frac{N_1^* K^* H + N_2^*}{2 M_1^*(1 + K^* H)} \qquad ; \qquad \delta = \left(1 + \frac{1}{K^*}\right) - \frac{N_1^{*2} K^* H + N_2^{*2}}{K^*(N_{02} - N_2^*)^2}$$

equation (10) becomes:

$$\alpha \dot{y}^2 + \beta y^3 + \gamma y^2 + \delta y = \text{cost}$$

The motion stops when $\dot{y} = 0$; it results then:

$$\beta y_u^3 + \gamma y_u^2 + \delta y_u = \alpha \dot{y}^{*2} + \beta y^{*3} + \gamma y^{*2} + \delta y^*$$

where $\dot{y}^*$ and y^* are known from preceeding phases. This equation allows to obtain the final displacement y_u of midspan section B.

The value of N from equation (8) must be compared with the maximum value at point A of fig. 1, that is with N_{02}. When N reaches such value, it results from (8):

$$y_M = \frac{2 N_{02} M_1^*}{s(N_{01} - N_1^*)^2}$$

If y_u is lower than y_M, the motion effectively stops; otherwise, if $y_u > y_M$, N reaches the value of N_{02} and keeps constant. In this case it is necessary to consider a further phase.

2.2.4 Fourth phase

In the fourth phase the axial stress is kept constant at its maximum value and no bending moment is taken into account in the weakest hinge for the dynamic equilibrium. According to
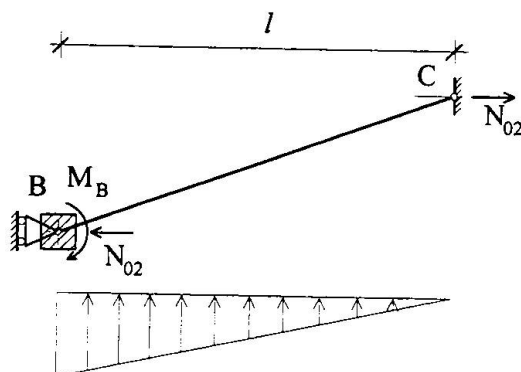
Fig. 5. Scheme of the impacted beam during fourth phase.

the static scheme of fig. 5, equation (10) becomes:

$$2\alpha \, \ddot{y} + \frac{M_B}{M_1^*} + \frac{N_{02}}{M_1^*} y = 0$$

Following the same steps as for phase three, for:

$$b = \frac{N_{02}}{2M_1^*} \qquad ; \qquad c = 1 - \left(\frac{N_{02} - N_1^*}{N_{01} - N_1^*}\right)^2$$

it results:

$$by_u^2 + cy_u = \alpha \, \dot{y}_M^2 + by_M^2 + cy_M = cost - \beta \, y_M^3 - \gamma \, y_M^2 - \delta \, y_M + by_M^2 + cy_M$$

from which it is possible to obtain the final displacement y_u of midspan section.

3. The case of an overbridge pier

The results just obtained have been applied to the case of an overbridge pier subject to the impact of a deviating truck. The reinforced concrete pier of an overbridge is 8.0 m high and the deviating truck, coming from a road on embankment, strikes the pier at halfheight at the velocity of 50 km/h. The mass of the truck is 30000 kg (see [11], par 4.3, table 4.3.1, urban area). The static equivalent impact load is 2000 KN. Static calculations and ultimate moments and forces evaluation have been carried out with reference to Eurocode 2 [12]. Two different square sections have been considered: 1.00x1.00 m and 1.20x1.20 m. Variable percentages of bending reinforcement have been taken into account and variable strength ratios between midspan and fixed end sections, in order to study different restraint condition from the perfectly clamped beam with constant strength to the end-hinged beam. For each section two different shear reinforcements have been considered: the lower reinforcement designed with reference to the static equivalent impact force, the higher nearly twice the first one. The results of dynamic calculations of displacements for impact velocity of 10 m/s have been reported in figures from 6 to 9. In the diagrams the plastic strains of bending reinforcement are represented versus reinforcement percentage for different ultimate moment ratios of midspan and fixed end sections. Plastic strain of bending reinforcement has been calculated from final displacement of midspan section considering the localized rotations at plastic
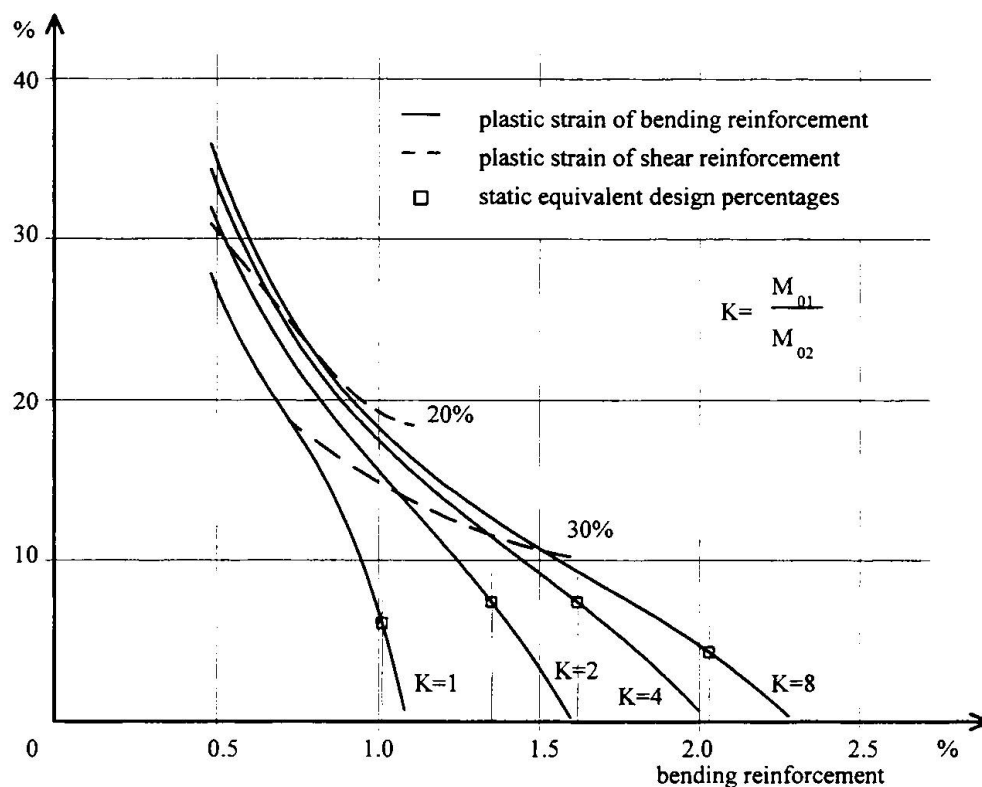
Fig. 6. Bending and shear reinforcement strains.
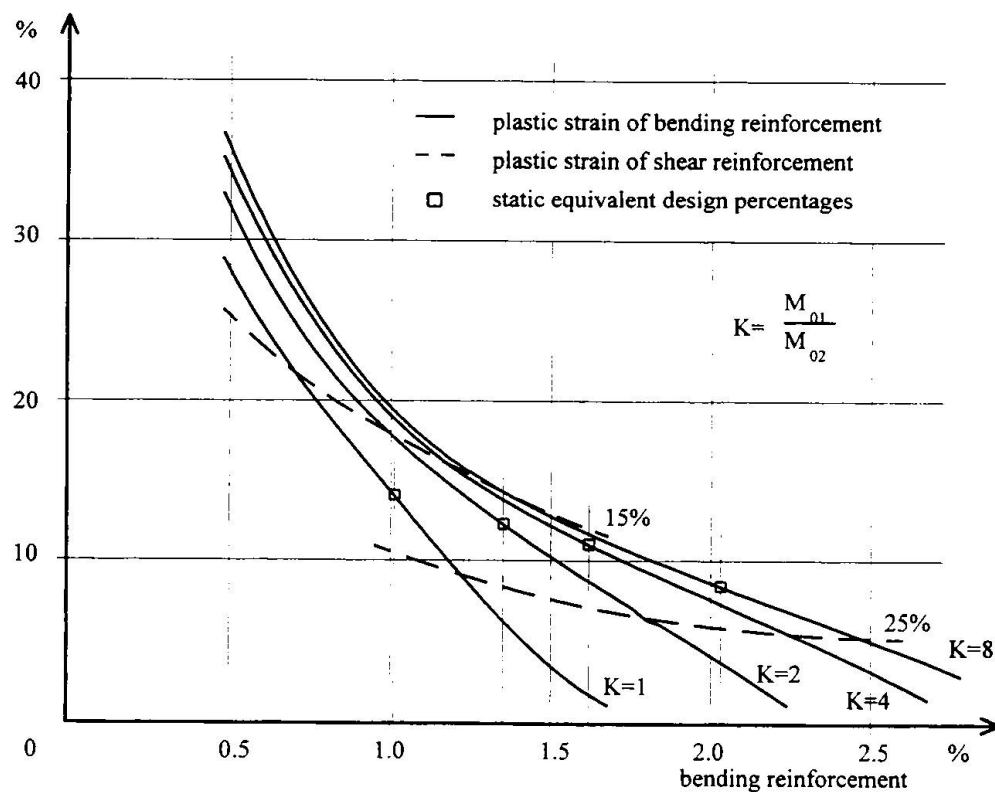
Section 1.00x1.00 m, stirrups 4φ12mm/250mm.

Fig. 7. Bending and shear reinforcement strains.
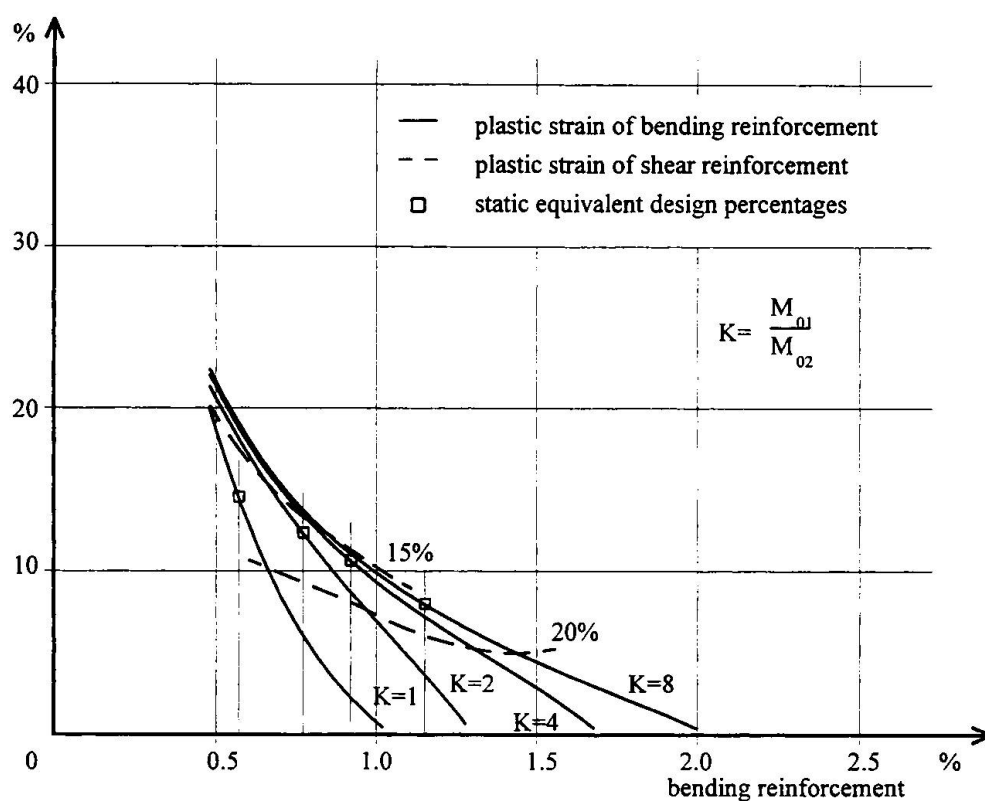
Section 1.00x1.00 m, stirrups 4φ14mm/200mm.

Fig. 8. Bending and shear reinforcement strains.

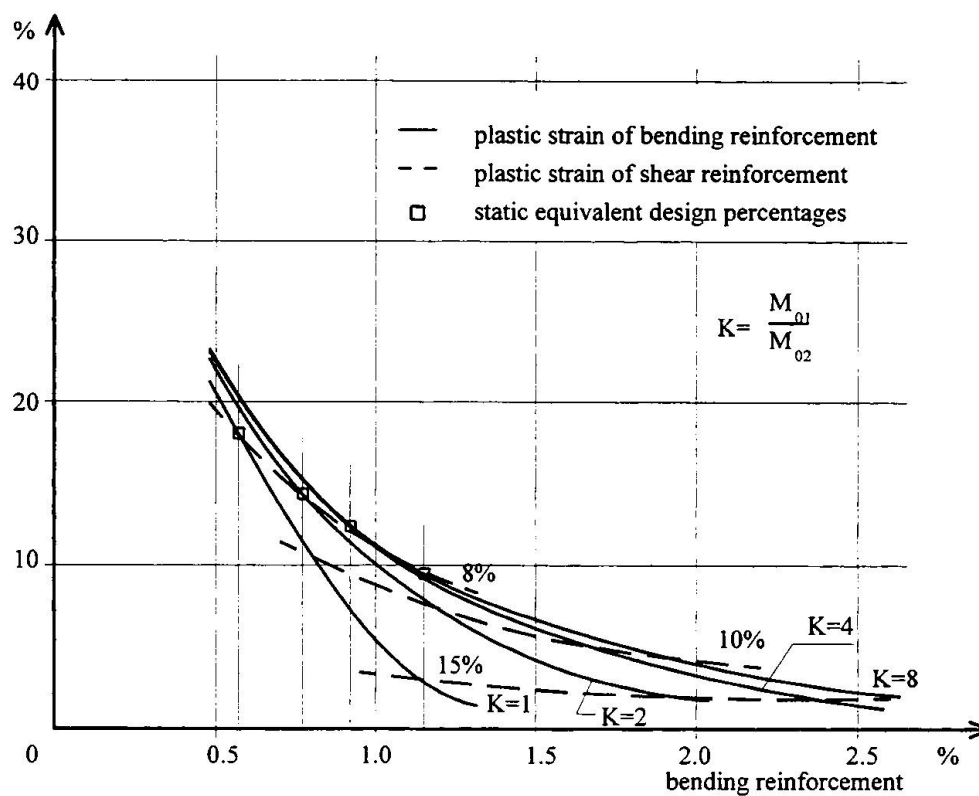*Section 1.20x1.20 m, stirrups 4ϕ12mm/200mm.*

Fig. 9. Bending and shear reinforcement strains.

Section 1.20x1.20 m, stirrups 6ϕ14mm/200mm.

hinges and the length of strained reinforcement as twice the equivalent length of plastic hinge [13], that is about 1.2 times the effective depth of cross section. Diagrams are given also for the plastic strain of shear reinforcement, that varies with the bending reinforcement percentage. Stirrups strain, considered constant along the full depth of the section, has been calculated from the relative displacement due to the sliding that occurs during the first phase.

The mechanical characteristics of materials are:
- characteristic strength of concrete: $f_{ck} = 25$ N/mm^2
- characteristic yield strength of reinforcing steel: $f_{yk} = 440$ N/mm^2

4.   Concluding remarks

Although the data reported in fig. 6-9 refer to a particular case, it seems very clear that the results of dynamic calculations leed to values of reinforcement strain much greater than static calculations. Moreover close to impact section the ultimate shear strength is reached immediately after impact and causes a remarkable localized sliding of the part directly in contact with the missile with respect to the remaining part of the beam, until relative speed vanishes. Such localized sliding produces very high strain in shear reinforcement. On the other side, increasing shear strength reduces inversely shear reinforcement strain but increases bending reinforcement strain, because less kinetic energy is dissipated at impact zone and plastic hinges undergo an increase of localized rotation.

Furthermore it must be noted that dynamic calculations have been carried out for a reduced impact velocity (10 m/s instead of 13.89 m/s = 50 km/h) in contrast respect to the application rule given in [11] at par. 4.2, where it is suggested that " all available energy of the colliding object is fully transferred into elastic or plastic deformation energy of the structure".

With reference to restraints conditions it seems more favourable the choice of a hinged beam with a higher bending reinforcement percentage, because for the same bending reinforcement strain the shear reinforcement strain is reduced. On the contrary, small increases of bending reinforcement in fixed end beam with uniform strength leed quickly to a condition in which the greater part of kinetic energy of the impacting body is dissipated by shear reinforcement with too high strain levels.

Finally, it seems necessary that designing with respect to an accidental action like impact be performed by means of a dynamic analysis of the structure; otherwise the analysis for a static equivalent load model must be accompanied by specific recommendations that take into account the inertia effects in order to limit reinforcement strains.

The account of strain rate and strain hardening effects reduces the strains evaluated and reported in above diagrams, but the reduction is small compared with the absolute value of computed strains. Further investigation on the topic is in program. Anyway introducing iterative procedures at intermediate stages of preceding calculations may improve the reliability of results, but doesn't change the mutual interdependence of main parameters.

5.   References

1.   Calamani S., Cartapati E., Materazzi A.L.: "Impact behaviour of polypropylene-fiber-reinforced concrete plates", Eight european Conference on Fracture, Fracture Behaviour and Design of Materials and Structures, Torino, 1-5 October 1990, pag. 755-760.

2.   Radogna E.F., Cartapati E., Materazzi A.L.: "Piastre di conglomerato cementizio rinforzato con fibre "morbide" sottoposte ad azioni impulsive: problemi di modellazione e verifiche sperimentali", Giornate A.I.C.A.P. '91, Spoleto, 16-18 may 1991, pag. 409-424.

3.   Cartapati E.: "Indagine teorico-sperimentale sull'effetto di azioni impulsive su elementi strutturali lineari", Studi e Ricerche, Dipartimento di Ingegneria Strutturale e Geotecnica, Università di Roma "La Sapienza", gennaio 1996.

4.   Jones N.: "Influence of strain hardening and strain rate sensitivity on the permanent deformation of beams", International Journal of Mechanical Science, Vol. 9, 1967.

5.   CEN: Bulletin d'information n°187: "Concrete structures under impact and impulsive loading", August 1988.

6.   Bleich H.H., Shaw R.: "Dominance of shear stresses in early stages of impulsive motion of beams", Journal of Applied Mechanics, Vol. 27, March 1960.

7.   Karunes B., Onat E.T.: "On the effect of shear on plastic deformation of beams under transverse impact loading", Journal of Applied Mechanics, Vol. 27, March 1960.

8.   Neal B.G.: "The effect of shear and normal forces on the fully plastic moment of a beam of a rectangular cross section", Transactions ASME, Vol. 83, Series E, June 1961, pag.269-274.

9.   Hodge P.G.: "Interaction curves for shear and bending of plastic beams", Transactions ASME, Vol. 79, September 1957, pag. 453-456.

10.   Nonaka T.: "Some interaction effects in problem of plastic beam dynamics - Parts 1,2,3", Journal of Applied Mechanics, Vol. 34, September 1967, pag.623-643.

11.   CEN: EUROCODE 1: Basis of design and actions on structures. Part 2-7: Accidental actions. Draft, June 1995.

12.   CEN: EUROCODE 2: Design of concrete structures. Part 1: General rules and rules for buildings. Final Draft, 31 october 1990.

13.   Park R., Pauley T.: "Reinforced Concrete Structures", John Wiley & Sons, New York, 1975.